2013

Stilling Basin Scour Remediation Using Air Injection and Flat Plate Extension

Rachael Barlock
Michigan Technological University

STILLING BASIN SCOUR REMEDIATION USING AIR INJECTION AND FLAT PLATE EXTENSION

By

Rachael R. Barlock

A THESIS

Submitted in partial fulfillment of the requirements for the degree of

MASTER OF SCIENCE

In Civil Engineering

MICHIGAN TECHNOLOGICAL UNIVERSITY

2013

This thesis has been approved in partial fulfillment of the requirements for the Degree of MASTER OF SCIENCE in Civil Engineering.

Department of Civil and Environmental Engineering

Thesis Advisor: *Dr. Brian Barkdoll*

Committee Member: *Dr. Veronica Griffis*

Committee Member: *Dr. Casey Huckins*

Department Chair: *Dr. David Hand*

Table of Contents

LIST OF FIGURES

LIST OF TABLES

PREFACE

The information collected and reported regarding the air diffusers in this thesis was collected to satisfy the requests of a client, the South Florida Water Management District (SFWMD). The data collection was conducted by Rachael Barlock, and the findings were presented to SFWMD in report form, written collaboratively by Dr. Brian Barkdoll and Rachael Barlock. Chapter 3 was submitted in part to the South Florida Water Management District in a progress report titled Erosion Reduction by Air Entrainment Phase IV Task 3-Effect of 2D Diffuser Plate.

ACKNOWLEDGEMENTS

I would like to thank my advisor, Dr. Brian Barkdoll for his support throughout this project, as well as his patience, which I surely tested. I would also like to thank Jennie Tyrrell, Megan MacNeill, and many undergraduates for their help in conducting experiments and data collection.

I would like to thank the Civil and Environmental Engineering department for funding my education through graduate teaching assistantships, as well as the students, faculty, and staff of the CEE department for their friendship and support.

I would also like to thank my parents for their continuous support. I would have never achieved this much without them. Finally, I'd like to thank my friends for their understanding of my erratic experimentation schedule which caused my absence at many social events.

ABSTRACT

The South Florida Water Management District (SFWMD) is responsible for managing over 2500 miles of waterways and hundreds of water control structures. Many of these control structures are experiencing erosion, known as scour, of the sediment downstream of the structure. Laboratory experiments were conducted in order to investigate the effectiveness of two-dimensional air diffusers and plate extensions (without air injection) on a 1/30 scale model of one of SFWMD gated spillway structures, the S65E gated spillway. A literature review examining the results of similar studies was conducted. The experimental design for this research was based off of previous work done on the same model. Scour of the riverbed downstream of gated spillway structures has the potential to cause serious damage, as it can expose the foundation of the structure, which can lead to collapse. This type of scour has been studied previously, but it continues to pose a risk to water control structures and needs to be studied further.

The hydraulic scour channel used to conduct experiments contains a head tank, flow straighteners, gated spillway, stilling basin, scour chamber, sediment trap, and tailwater tank. Experiments were performed with two types of air diffusers. The first was a hollow, acrylic, triangular end sill with air injection holes on the upstream face, allowing for air injection upstream. The second diffuser was a hollow, acrylic rectangle that extended from the triangular end sill with air injection holes in the top face, allowing for vertical air injection, perpendicular to flow. Detailed flow and bed measurements were taken for six trials for each diffuser ranging from no air injection to 5 rows of 70 holes of 0.04" diameter. It was found that with both diffusers, the maximum amount of air injection reduced scour the most. Detailed velocity measurements were taken for each case and turbulence statistics were analyzed to determine why air injection reduces scour. It was determined that air injection reduces streamwise velocity and turbulence.

Another set of experiments was performed using an acrylic extension plate with no air injection to minimize energy costs. Ten different plate lengths were tested. It was found that the location of deepest scour moved further downstream with each plate length. The 32-cm plate is recommended here. Detailed velocity measurements were taken after the cases with the 32-cm plate and no plate had reached equilibrium. This was done to better understand the flow patterns in order to determine what causes the scour reduction with the extension plates. The extension plate reduces the volume of scour, but more importantly translates the deepest point of scour downstream from the structure, lessening the risk of damage.

CHAPTER 1: INTRODUCTION AND MOTIVATION

1.1 Introduction

Erosion of sediment, known as scour, downstream of water control structures can expose the foundation of the structures, which can potentially cause the structures to fail. Because of expensive equipment and training that may be needed to measure the depth and volume of the bed scour, scale model experiments are more economically viable. A scale model of a structure suffering from erosion can be constructed, and experiments can be conducted to determine the best approach for minimizing scour. This study explored the effectiveness of air-injection diffusers and structure extensions in reducing scour, as well as the flow patterns associated with those methods.

The South Florida Water Management District (SFWMD), which is responsible for operation and maintenance of over 2500 miles of waterways and 645 water control structures in the southern part of Florida, was concerned about scour downstream of one of their gated weir stilling basins. The S65E gate, which controls the flow from the Kissimmee River into Lake Okeechobee, protects the small residential area nearby from flooding, as well as offers a source of irrigation for the large agricultural industry that surrounds it.

The experiments to follow built off of the work of Ted Champagne (2011), who determined the initial conditions of the scale model and investigated the effects of air injection on scour in various patterns and locations.

1.2 Literature Review

For many years, attempts have been made to understand scour and what causes it (Hager 1998). Several articles have been written about scour; those relevant to air injection as a scour remediation tool are described below.

1.2.1 Air Injection to Scour-Inducing Flow

Mason (1989) conducted laboratory tests in which he varied the percentage of air entrained, discharge, and head drop in a plunge pool in order to understand how it affected scour. He found that scour predictions are dependent upon the amount of air. Mason did not study various angles of air injection, however, and while he did study the amount of air, he also varied discharge and head. His study cannot be directly applied to this study.

Canepa and Hager (2003) conducted laboratory experiments in which they studied scour produced by an angled plunging jet. The variables in their experiments were the amount of air, sediment size, and water velocity. It was found that a relationship exists for maximum scour and maximum aggradation heights. The study found that in certain cases,

depending on jet velocity and sediment size, air injection increased scour depth. "However, if the reference would be the air-water mixture velocity, scour depth decreases significantly by the addition of air to the jet." There are similarities to the present study, such as the use of a Froude number based on the amount of air, which was used by Champagne (2011) when designing the initial experimental setup for his study and the present study.

Pagliara, Hager et al. (2006) varied the shape, velocity, and air concentration in the jet as well as tailwater elevation, granulometry, upstream flow to the scour hole, and the end scour profile in terms of the basic scour features. Scour as a function of densimetric Froude number was not largely affected by jet shape, scour was decreased logarithmically with air injection, and scour was found to be linearly related to densimetric Froude number. Air injection location for this study is different than that of Pagliara, Hager et al. (2006).

Air injection was studied by Xu, Deng et al. (2004) on a jet angled at gravel sediment. Scour for aerated and non-aerated flow was measured. Variables included jet thickness and velocity and concentration of air. It was found that the concentration of air was the main cause of scour, and that the other variables minimally affected the bed. Relationships were found for ratio of scour as a function of air concentration and for scour hole as a function of scour depth. The current study examines air injection at two different angles, but the angle of flow does not change.

Air injection can serve as a solution in wastewater treatment plants as well, as studied by Neto, Zhu et al. (2008). This study was conducted to determine the effect of single- and multiple-hole nozzles. When air was injected from beneath the submerged sediment, it caused suspended sediment. The structure of the bubbles resulting from air injection was studied. While the velocity of the bubbles did not change significantly, the size of the bubbles decreased and the turbulent flow increased when a porous airstone was used instead of nozzles with large openings. Similar results were found when a nozzle with several smaller-diameter openings was used. The present study uses smaller-diameter holes, but injects air at the point where the flow exits the control structure rather than the sediment bed.

1.2.2 Air-Water Multiphase Flow

A two-dimensional air-injection source method was studied (Brevik 1977). The authors studied the theory of the flow over the air injection location. While the study did not include bed sediment, it is still applicable to the current study, as it involves two-dimensional flow and leads to some understanding of why the solution may work. Brevik and Killie (1996) also studied bubble plumes and the theory behind them. Using equations for the conservation of mass, momentum and kinetic energy, they estimated

bubble velocity. This paper, like the previous one, may offer some understanding of why bubble plumes are a solution to scour problems. Another model for two-dimensional air-injection was presented by Brevik and Kristiansen (2002). Again, the research focused on the theory behind the bubble plumes, basing the model off of conservation equations. With this research, they found that the water velocity was of more interest than the velocity of the bubbles, which is what Brevik focused on in previous work. While the effects of these findings on scour were not studied, the information is still applicable to the present study, as water velocity was measured in an attempt to understand the flow patterns that cause scour reduction.

Freire, Miranda et al. (2002) studied bubble plumes flowing next to another bubble plume. The experiments resulted in evidence of a relationship between the angle of the bubble plume and the Weber and Froude numbers. This study applies to the current study in the case of the two-dimensional diffusers, as bubble plumes will be adjacent to one another while exiting the diffuser. However, because several rows of several air-injection holes will be studied, the relationships found by Freire, Miranda et al. may not apply.

More like the current study, Gabillet, Colin et al. (2002) looked at air injection from a channel bed with liquid flowing across the bubble plume. Similar to one of the diffusers tested in the current study, the authors injected air through a porous plate that was on the lower wall of the channel. A fiber-optic probe and hot-film anemometer measured bubble void fraction, bubble velocity and diameter, and velocity and turbulence, respectively. It was found that the average velocity of the liquid decreases where the bubbles exit the plate because of friction, while the turbulent kinetic energy increases.

Martínez-Bazán, Montañés et al. (2002) performed experiments where they injected air into the center of a jet of water. They measured bubble size distribution using a Phase Doppler Particle Analyzer. The current study differs from that of Martínez-Bazán, Montañés et al. because it focuses on air injection in a cross-flow rather than a water jet.

Three-dimensional bubble plumes were studied by Simiano, Zboray et al. (2006). They studied bubble velocity, liquid velocity, void fraction, and bubble size using particle image velocimetry, optical probes, and high speed cameras. However, in this study, air was injected into stagnant water, not cross-flow as in the present study. However, the findings of this study help in the understanding of bubble plume spread and the influence of void fraction.

Particle Image Velocimetry was used by van Hout, Gulitski et al. (2002) to study a single Taylor bubble in still water. These experiments were done to look into fluid flow induced by bubbles. The results of the study show that liquid flows upward in front of the rising

bubble and flows downward on the sides. This study may offer some insight into how the injected air affects the water flow, which in turn causes a reduction of scour.

Schmocker, Pfister et al. (2008) performed experiments on air injection into plunging flow. They found that air injection does have an effect on the concentration of air in the plunging jet. Although this study shows that air injection can be used in plunging flow, it did not study the effect on scour.

1.2.3 Scour Reduction Methods

Studies have been done on scour reduction methods involving air entrainment. Hamid, Farrant et al. (1952) conducted field experiments on aerodissipators and aerobaffles. The devices entrain air in the flow and cause a reduction in scour. The experiments were done to determine the best sizing and spacing of the devices to allow for more air entrainment. These apparatuses offer a solution that is not energy intensive, like that of air injection, but in cases of extreme scour, they may not be the best or only solution.

Dey and Sarkar (2007) injected water vertically upwards over a scoured area in a channel bed. Scour depth and length, water velocity, and turbulence were measured as the velocity of the injected water was varied. The current study focuses on air-injection, but this study is valuable as it is an alternative attempt at reducing scour.

1.2.4 Scour at Hydraulic Structures

Estimating how and where scour will occur is valuable, especially in scenarios where air entrainment or injection is not an option. Expanding on existing equations for scour, Mason and Arumugam (1985) suggested a new formula in which scour is a function of water level changes both up- and downstream, unit flow, and sediment particle size.

Jia, Kitamura et al. (2001) numerically studied flow from an apron to a scour hole. The study identifies how pressure fluctuations affect scour. However, pressure fluctuations were not studied in the present study.

Dey and Westrich (2003) examined the hydraulics and scour in cohesive soil downstream of an apron. They conducted experiments using the natural sediment in a laboratory channel that had a sluice gate and apron upstream. Discharge, velocity and apron lengths were varied. Results of scour and velocity measurements indicated that scour depth is proportional to tailwater depth and variation in flow depths up- and downstream of the sluice gate. Additionally, scour depth was found to be inversely proportional to apron length. This study is similar to the present study, but does not include a stilling basin on the water control structure and air injection was not investigated. Dey and Sarkar (2006)

conducted a similar experiment, but used non-cohesive soil. The results were very similar.

Using dimensional analysis, D'Agostino and Ferro (2004) studied scour downstream of weir structures. They suggest that normalized scour depth is a power law that is a function of head over the weir and a weaker function of normalized weir width.

Liu (2005) related scour depth to tailwater, water head, unit flow, and sediment resisting power. This suggested relationship was applied to a flip bucket spillway site and is comparable to model-study findings.

Stein, Alonso et al. (1993) investigated scour depth using plunging flow. The bed profiles were measured with photographs of a grid superimposed over the viewing sides of the flume. The results of the experiments were compared to theory based on bed shear stress. The results of the study agreed with theory.

Bennett, Alonso et al. (2000) conducted experiments in which packed clay was subjected to rain, then lateral surface flow. Results showed that flow patterns were similar to patterns of scour downstream of hydraulic structures. This study may help gain an understanding of flow patterns and how they can be adjusted to reduce scour.

1.3 Objectives

Air injection as a scour remediation technique, while studied before, is still a unique solution to scour problems. Current solutions are expensive and not always efficient. Additionally, an extension piece on the existing structure is an innovative and inexpensive remediation technique. Both of these solutions would be costly on a large-scale structure, which is why physical modeling on the 1/30 scale structure was used to understand these techniques. Goals of these experiments were to:

1. Understand why air injection reduces bed scour
2. Determine the optimal spatial extent of air injection
3. Determine if a flat plate extension would reduce scour
4. Understand the flow patterns caused by the extension plate

This information could potentially be used in the field to remedy erosion-related problems.

CHAPTER 2: EXPERIMENTAL SETUP

2.1 Hydrodynamics Laboratory

The experiments discussed in this thesis were conducted in the hydrodynamics lab, which is located in room 110 of Dillman Hall at Michigan Technological University. The lab equipment included a flume, which was used for these experiments.

2.2 Flume Setup

2.2.1 Flume Features

The scour flume (Figures 2.1 and 2.2) in the hydrodynamics lab had an inlet, a flow development section, a gated spillway and stilling basin, a scour chamber, a sediment trap, and an outlet. The perimeter of the flume was comprised of concrete blocks, which were attached to the concrete floor. A 1/16-inch thick rubber membrane lined the walls and floor to prevent leaks. Wood was used to build the approach section, the stilling basin, and the sectional walls. The upper and lower gates were made of aluminum. The flow straighteners were a series of PVC pipes in small diameters. The inside width of the flume was 0.92m, the total height of the flume was 1.04m, and the total inside length was 10.18m. The flume was used by Ted Champagne, and detailed information pertaining to the design and construction can be found in chapter two of his thesis (Champagne 2011).

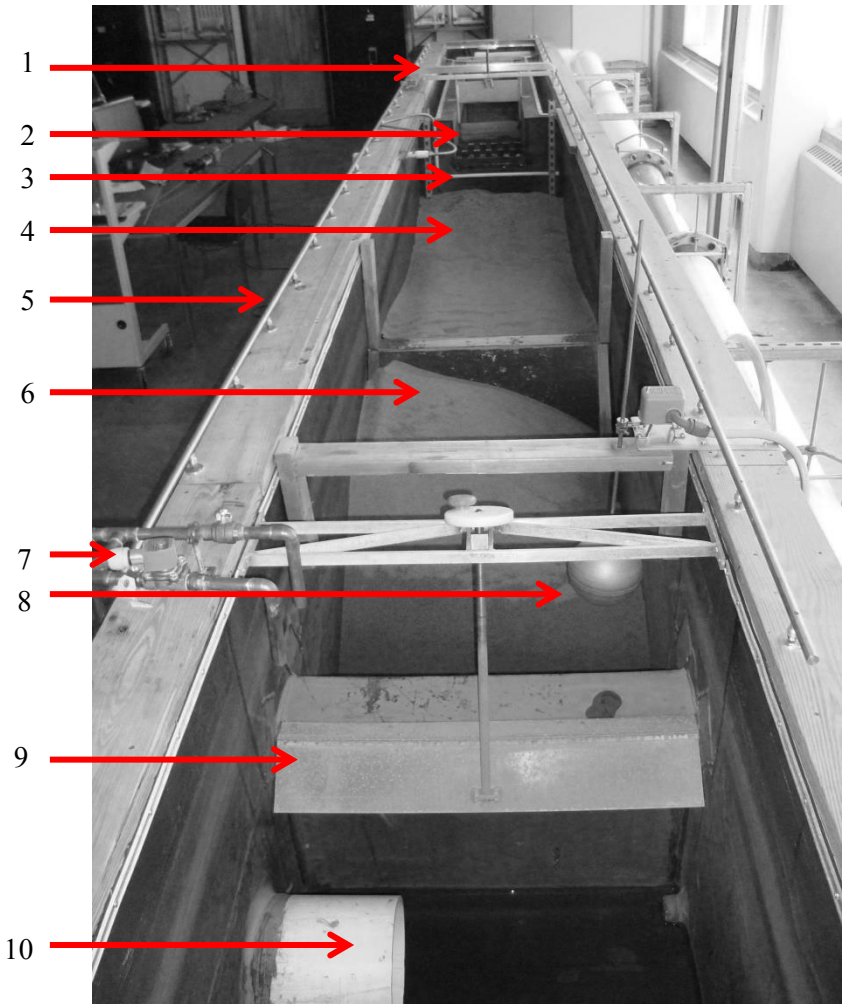

Figure 2.1. *View of flume facing upstream. List below indicates feature details. Figure used with permission from Ted Champagne (Champagne 2011).*

1. Instrument carriage
2. Gated spillway with blocks
3. Injection location for compressed air
4. Sediment scour chamber
5. Guide rails for instrument carriage
6. Sediment trap
7. Water supply
8. Float valve to ensure constant water depth throughout experiments
9. Adjustable tailgate to control tailwater level
10. Outlet to pump for recirculation of water

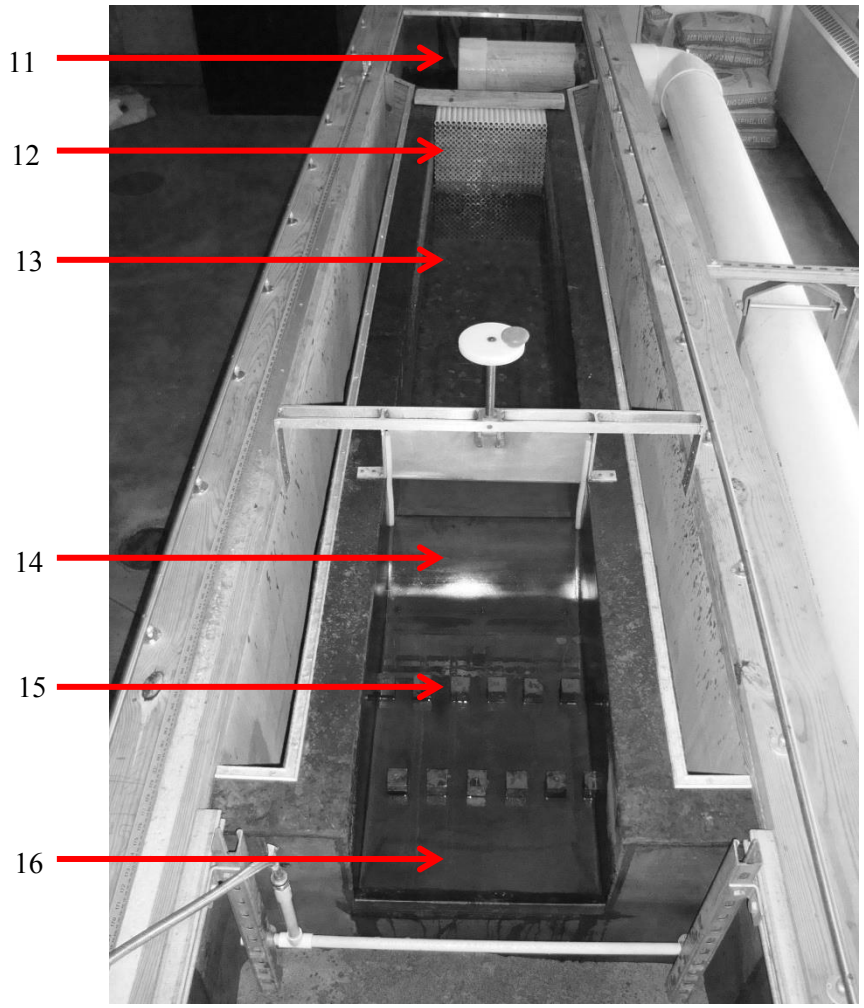

Figure 2.2. *Detailed view of developed flow section and stilling basin. List below indicates features. Figure used with permission from Ted Champagne (Champagne 2011).Note: Air diffusers for this study not shown in the figure.*

11. Inlet from water pump
12. Flow straighteners
13. Developed flow section
14. Gated weir spillway
15. Thrust blocks
16. Stilling basin

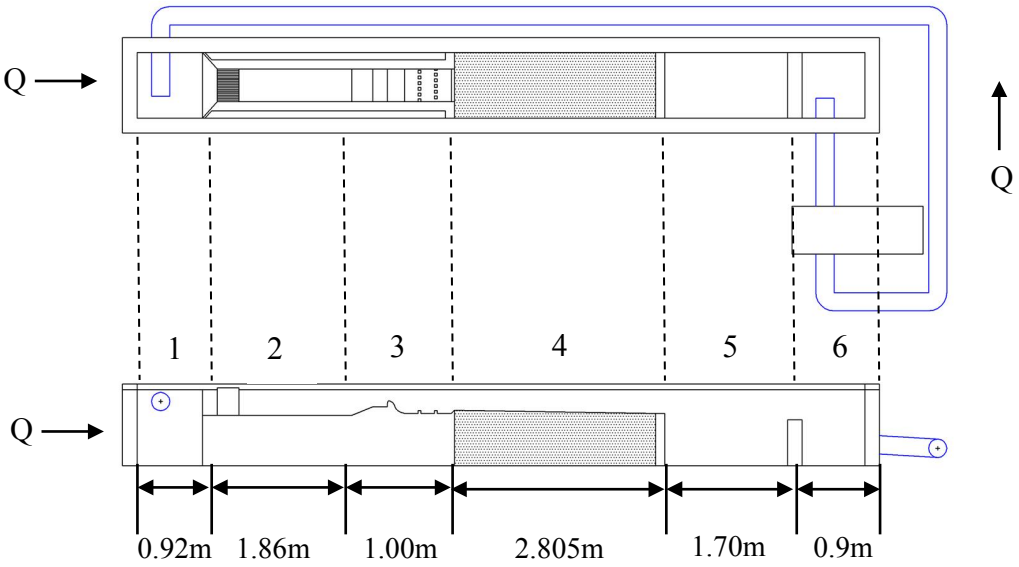

Figure 2.3. *Sections of the scour flume. Sections are numbered and listed below. Figure adapted and used with permission from Ted Champagne (Champagne 2011).*

1. Inlet
2. Flow Developing
3. Spillway/Stilling Basin
4. Scour
5. Sediment Trap
6. Outlet

The plan view is shown in Figure 2.3. The inlet, which is 0.915m, has a 0.254m diameter pipe with 27 1.588mm diameter holes facing downward. Flow enters the flume through these holes. There is an internal wall that separates the inlet and flow-developing sections, which is 0.66m high. The flow-developing section is 1.86m long, with a width of 0.457m. This section has PVC pipes, each with a diameter of 20 mm, stacked parallel to straighten the flow. The bed of the flow-developing section has 12.7mm of gravel to ensure fully-developed flow. To verify that flow in this section was fully developed, velocities were measured using an Acoustic Dippler Velocimeter (ADV) (Champagne 2011).

The scour chamber is 2.805m long and filled to the end sill with fine sand. The sand has a d_{50} of 0.56mm, which is as close as possible to the size needed to be scaled to the model while avoiding cohesion. The sediment size distribution is shown in Figure 2.4. The bottom of the scour chamber is the concrete floor of the laboratory; the scour hole never reached the floor in any of the experiments performed in this study. A 630mm tall partition wall separated the scour chamber from the sediment trap downstream (Champagne 2011).

The sediment trap is where the sand settled out from the flowing water, which prevented it from entering the outlet and recirculating through the pump potentially causing damage. The length of the sediment trap is 1.70 m. No sand was observed flowing over the spillway or stilling basin, proving that the sediment trap effectively settled the sand out of the flow. Sediment was occasionally removed from the gravel in the developed flow section, but was not necessary very often throughout this study (Champagne 2011).

The outlet section is 0.90m long and contained the 0.254m diameter outlet pipe. After the flow entered the piping, it was re-circulated by a centrifugal pump and return piping to the flume inlet (Champagne 2011).

To keep the water level constant throughout the experiment, an adjustable float valve was used. A float was attached to an adjustable rod, which, in the case of a low water level, would activate an electronic valve that was connected to the water supply. This float valve mechanism could sustain a constant water level within 3mm. To protect from the effects of water hammer, surge protectors were also installed on the valves (Champagne 2011).

The compressed air used for air injection during the experiments flowed through a 2.54cm steel pipe. Two different gages were used to measure the air flow rate, dependent upon the desired flow rate. When low air flow rates were desired, the gage offered accuracy within 0.0002cms. Air pressure offered accuracy within 3.448Pa and was measured just downstream of the flow gage (Champagne 2011).

To control water flow rates, a variable-speed electric controller and centrifugal pump were used. The flow rate was measured by a side-contraction manometer with two tubes that was located in the return piping. A 1.829m long, stainless steel, 0.254m diameter pipe was used for the side contraction. The pressure head was measured upstream and downstream of the contraction. The accuracy of the discharge is within 0.006cms because

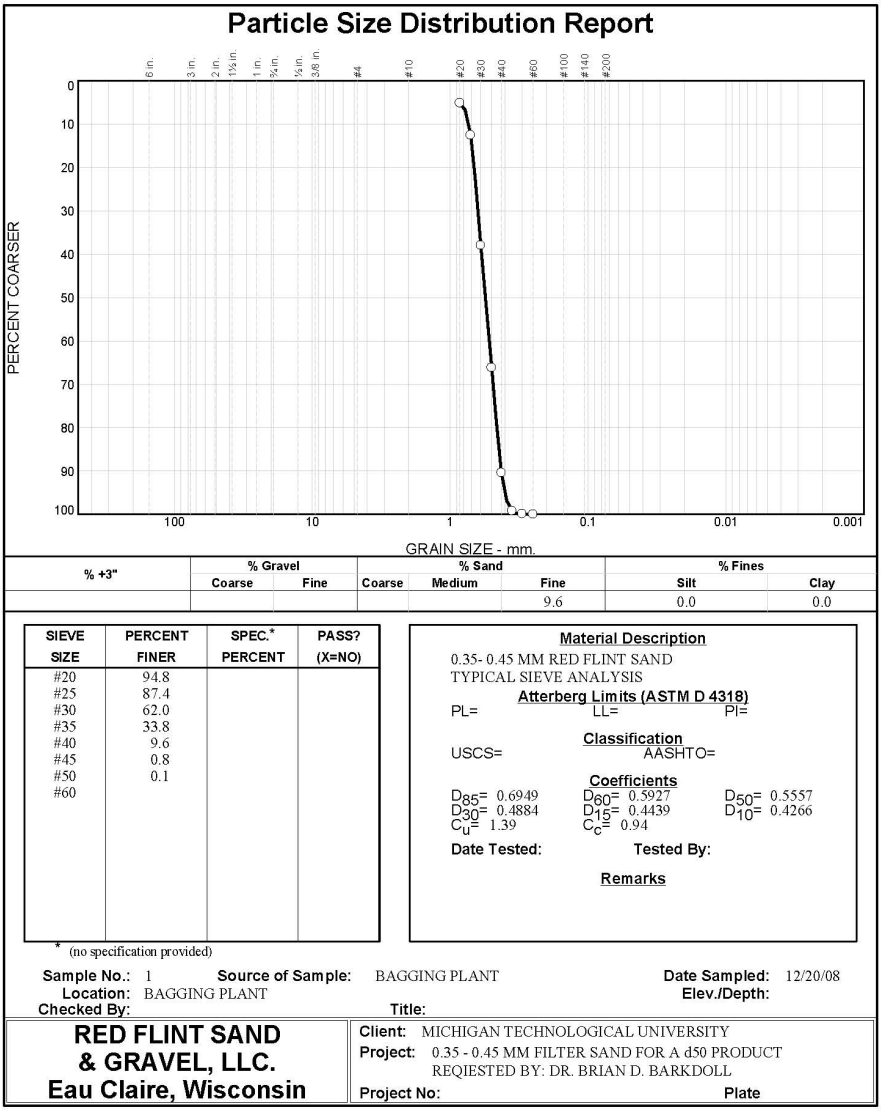

Figure 2.4.*Sediment size distribution for scour flume from manufacturer.*

the pump impellor rotation is constant ±0.005Hz, and the manometer has a 0.79mm accuracy (Champagne 2011).

A point gage was mounted on an instrument carriage that slid along support rails on the top of the side walls of the flume. This instrument, which has accuracy within 0.1mm, was used to measure the water surface and bed profiles (Champagne 2011).

To be sure equilibrium was reached, the scour depth was measured. For the initial scour stage, manual measurements were taken with a ruler because of the interference of suspended sediment. It took approximately 30 minutes for the initial scour stage to pass and the scour hole to become deep enough for measurements with the ADV. Measurements were taken using the ADV's depth function at ten-hertz intervals and were filtered to exclude visually-identified erroneous data. For any two-minute period, only the largest 25% of data collected was used due to the interruption of signal resulting from the occasional air bubble plume passing between the ADV and the scour hole. The data retained was then averaged into two-minute bins for ease of data analysis. The equilibrium scour conditions had been reached when a change in scour depth less than 0.5 percent was witnessed in a 2-hour period. Once equilibrium had been reached, the water surface profile was measured, followed by the bed profile. The equilibrium criterion was chosen after witnessing bed scour over the course of several days (Champagne 2011). Melville and Chiew (1999) discussed how using an equilibrium criteria that is less stringent, which would allow for a shorter experimental run time, would not adequately display full scour potential.

2.2.2 Stilling Basin Model

The spillway is a 1:30 scale model of one part of the SFWMD's S65E gate structure. The S65E gated structure is made up of six 9.15m long gates, giving the spillway a total length of 54.9m. The model is 0.457m wide, 0.1m high, and 0.23m long, as shown in Figure 2.5. The model spillway is immediately followed by a stilling basin with thrust blocks. The spillway is constructed out of aluminum, and the stilling basin and thrust blocks out of sealed wood. The 40mm, cubic thrust blocks are aligned in two rows offset from each other, and were attached with adhesive and screws. The stilling basin ends with a 40mm high triangular end sill constructed out of acrylic (Champagne 2011). Acrylic was used so the end sill could serve as an air diffuser for this study. The end sill was attached with adhesive.

In one set of experiments in this study, the end sill alone served as the air diffuser. In this case, nothing more was added to the aforementioned structure. In another set of experiments, an 8-cm rectangular piece extended out of the end sill. In this case, the rectangular piece served as the diffuser. Finally, in the third set of experiments, a 6-mm acrylic plate (8, 16, 24, 32, 40, 48, 56, 64, or 72cm) extended from the base of the acrylic end sill. Details of the configuration for air injection can be found in Chapter 3.

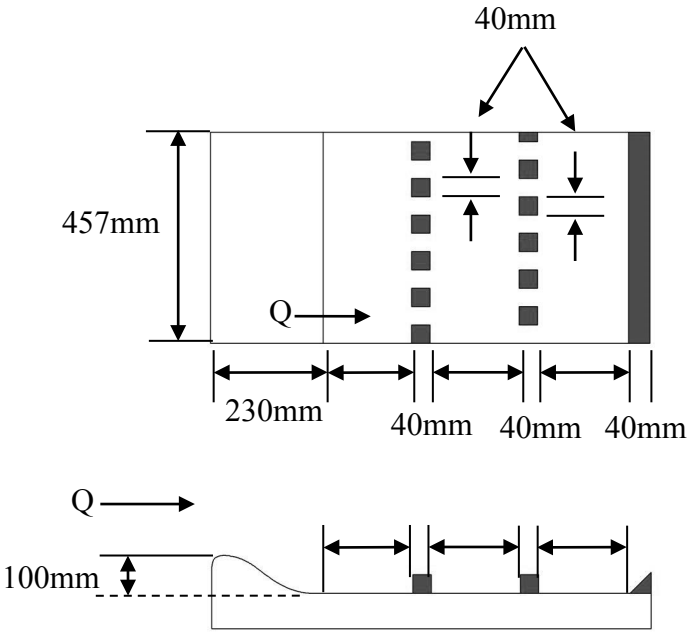

Figure 2.5. *Spillway and stilling basin model. Figure used with permission from Ted Champagne (Champagne 2011).*

Details of the upstream facing diffuser plate and the vertical facing diffuser plate are shown in Figures 2.6 and 2.7, respectively.

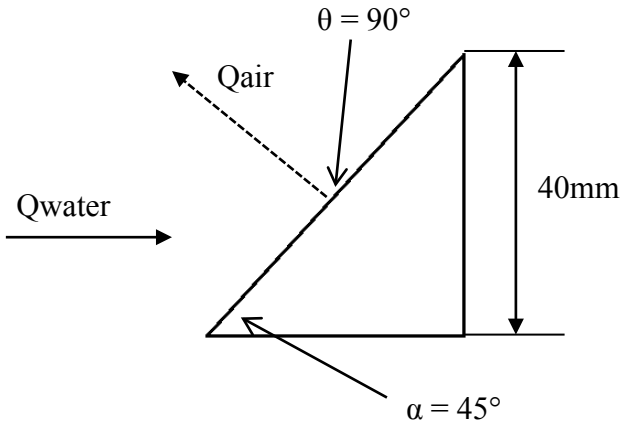

Figure 2.6. *End sill diffuser detail (UFDP).*

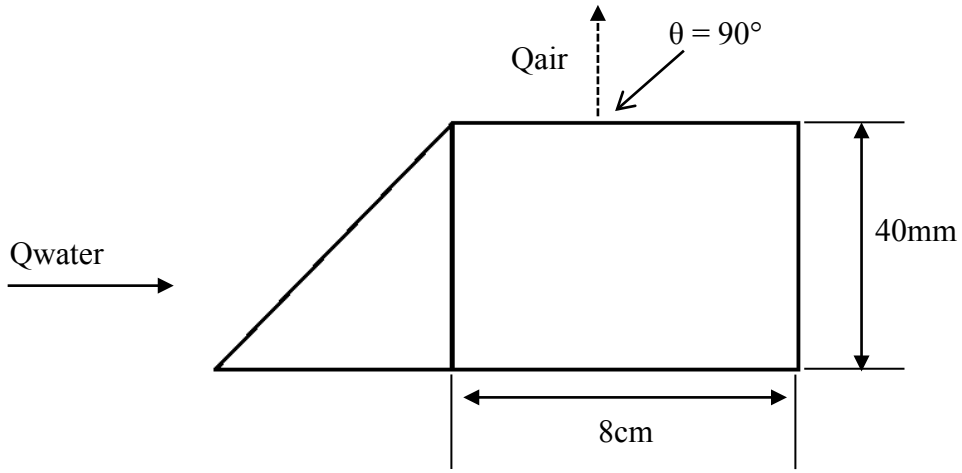

Figure 2.7. *Rectangular diffuser detail (VFDP).*

2.3 Data Collection

2.3.1 Acoustic Doppler Velocimeter

An acoustic Doppler velocimeter, also known as an ADV, was used to collect instantaneous three-dimensional velocity data and scour depth data throughout the experiments. The ADV is manufactured by Nortek AS, and is a Nortek Vectrino Velocimeter (Nortek 2013). In order to collect data, the ADV emits an acoustic signal in a cylindrical volume below the probe and measures the Doppler shift associated with the echo. Using this method of velocity measurement assumes that the particles which the sound is reflecting from are small enough that they have the same velocity of the water surrounding them (Champagne 2011).

An instrument carriage that ran the width of the flume supported the ADV and a point gage. This allowed the ADV and point gage to be positioned longitudinally, transversely, and vertically. Measurements were taken with the ADV using a downward-facing probe for both velocity and depth measurements; settings were configured differently for each type of measurement. The ADV measurements were controlled by Vectrino+ software, which was on the computer in the hydrodynamics laboratory. Before data was processed, it was run through the Nortek conversion software. Figure 2.8 shows the ADV and point gauge mounted to the carriage. Table 2.1 shows ADV software settings for each function (Champagne 2011).

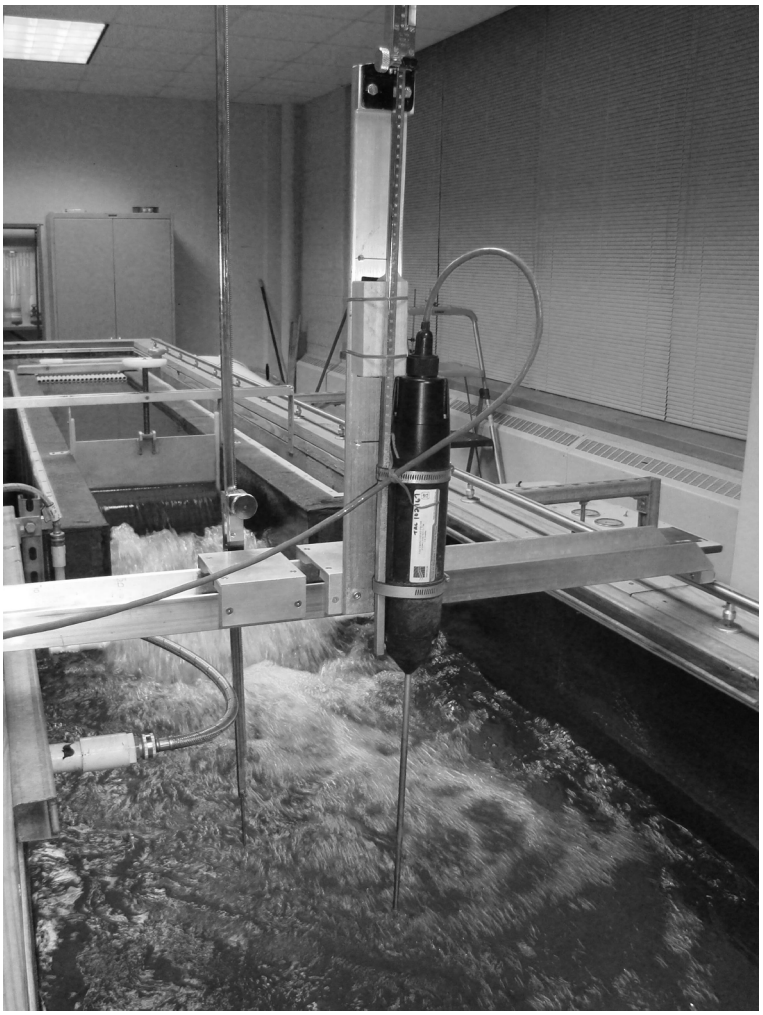

Figure 2.8. *Point gage and ADV mounted to instrument carriage. Figure used with permission from Ted Champagne (Champagne 2011).*

Table 2.1. *ADV configuration settings. Table used with permission from Ted Champagne (Champagne 2011).*

Setting	Velocity Function	Distance Check Function
Sampling rate (Hz)	200	10
Nominal velocity range (m/s)	±1.00	±0.30
Transmit length (mm)	1.8	2.4
Sampling vol (mm)	4	7.6
Power level	HIGH	HIGH

2.3.2 Photos and Videos

In addition to data collected by the ADV, photos and videos were taken of each experimental case, both while the case was running and of the empty bed. These were used to record visual observations after the experimental cases had reached equilibrium. The camera used for these experiments was a Sony CyberShot W120 camera, which can take photos up to 7.2 megapixels. Photos were used to better understand differences between cases.

CHAPTER 3: 2D AIR DIFFUSERS[1]

3.1 Experimental Design

A set of experiments was performed in order to determine how introducing a 2D diffuser plate with different air flow rates (Q_{air}) would affect scour downstream of the stilling basin structure.

The first configuration was a set of 0.04"-diameter holes drilled on the upstream face of an acrylic triangular end sill, which comprised the Upstream-Facing Diffuser Plate (UFDP). This configuration is shown in Figure 3.1. The end sill served, for the purpose of this experiment, as the diffuser plate. Five different arrangements were tested and the results were compared with a base experiment that included the end sill diffuser with no air injected. For the first case, one row of 70 holes was drilled into the diffuser. For each consecutive case, another row of 70 holes was drilled. For each new row of holes, an experiment was conducted (Barkdoll and Barlock 2011). Table 3.1 shows the diffuser configuration for each case.

The second configuration consisted of a set of 0.04"-diameter holes drilled into an acrylic, horizontal extension of the triangular end sill, thus comprising a Vertical-Facing Diffuser Plate (VFDP). This configuration is shown in Figure 3.2. The rectangular extension served, for the purpose of this experiment, as the diffuser plate. Six different arrangements were tested: the end sill with the rectangular piece without air injection and the end sill with the rectangular piece with air injection ranging from one to five rows of holes. The hole configuration was the same for one row of holes as for the previously described experiment, also shown in Table 3.1.

For each case the exit velocity of air was kept constant at a value determined by Champagne (2011) of 345.1 ft/s. The water discharge value was 0.0264m^3/s and was the largest discharge possible without overflowing the flume walls.

To test the worst scour conditions, all tests were done for clear water with no suspended sediment, since suspended sediment results in less scour due to its turbulence-dampening effects.

[1] Chapter 3 of this thesis was submitted as part of the Erosion Reduction by Air Entratinment Phase IV Task 3-Effect of 2D Diffuser Plate progress report to the client, the South Florida Water Management District in September 2011.

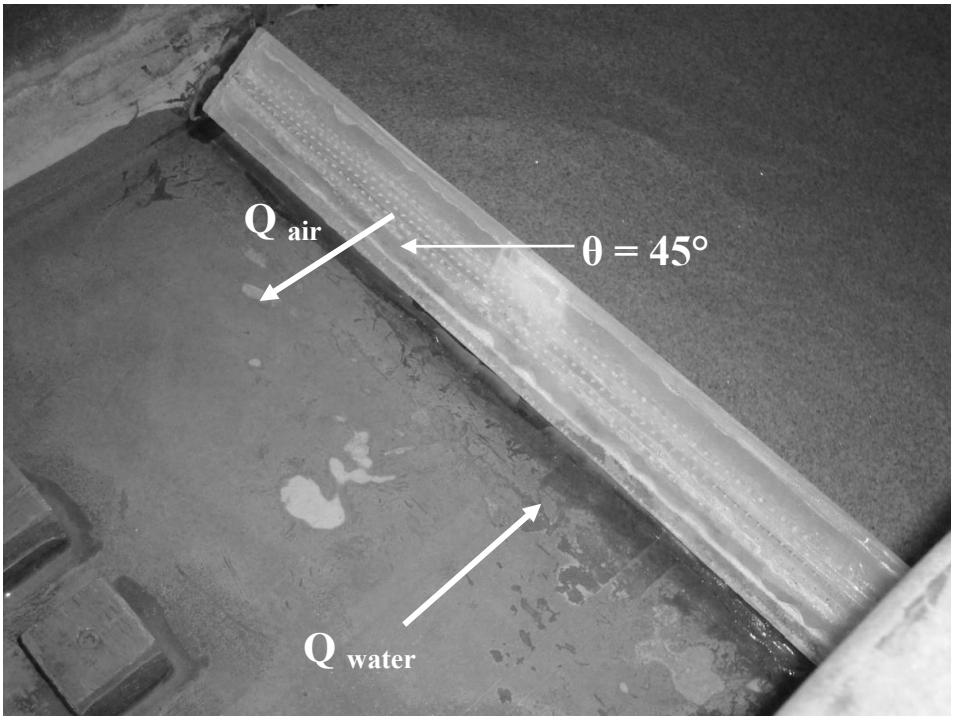

Figure 3.1.*Upstream-facing diffuser plate (UFDP). Refer to Figure 2.6 for side view.*

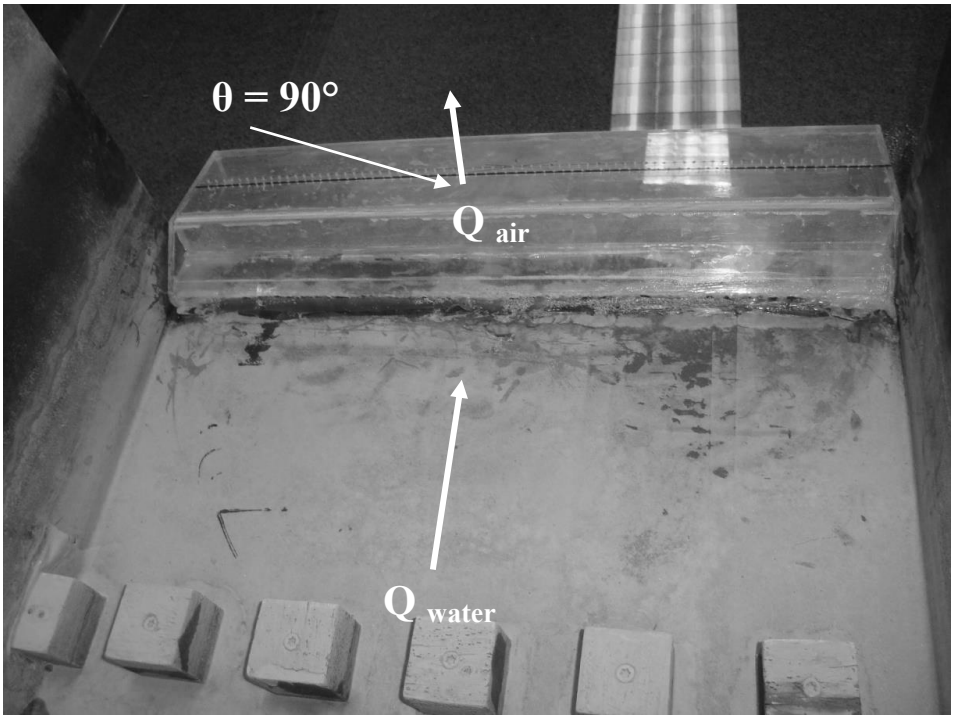

Figure 3.2.*Vertical-facing diffuser plate (VFDP). Refer to Figure 2.7 for side view.*

Table 3.1. *End sill diffuser experiment parameters.*

Diffuser Configuration	Number of Holes	Qair (scfm)
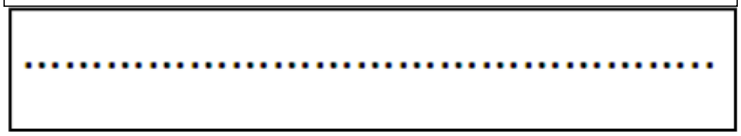	70	12.65
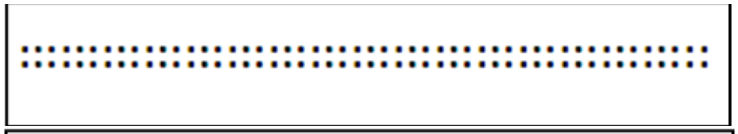	140	25.3
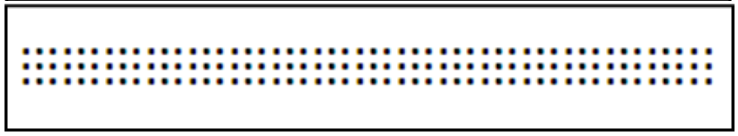	210	37.95
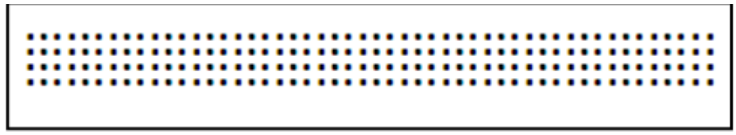	280	50.6
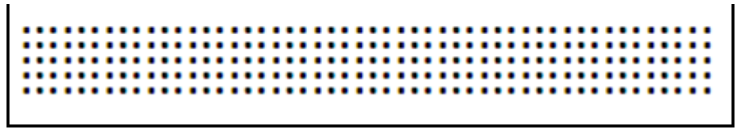	350	63.25

3.2 Experimental Procedure

For each experiment, the sediment was leveled in the scour section of the flume to the top of the stilling basin end sill. Next, the flume was filled with water to the desired flow depth, and the pump was turned on to the desired flow rate. Next, the air flow was turned on to the desired flow rate. Adjustments were made, if necessary, to the flow depth. The scour was measured in a location of expected deep scour with time until equilibrium was reached. Equilibrium was determined by scour measurements collected by the ADV when scour depth had changed less than 0.5 percent in a two-hour period. Once it was determined that equilibrium had been reached, the water surface profile was measured and photos and videos were taken. The flow was then stopped, and the water was drained from the scour chamber. Finally, the bed profile was measured manually using the point gauge. Each case took approximately two hours to set up, ten to twelve hours to reach equilibrium, and four hours to take measurements. One case could be completed in about two days (Barkdoll and Barlock 2011).

3.3 Results

3.3.1 Water Surface Profile

The water surface profiles for 0 to 5 rows of air holes in the UFDP are shown in Figure 3.3. Figure 3.4 shows the water surface profile for 0 to 5 rows of air holes in the VFDP. Water surface elevations were measured on the centerline of the flume. The water surface elevation at the end sill and in the stilling basin increased as air discharge is increased. However, in every case, the water surface elevation was unchanged upstream of the spillway crest (Barkdoll and Barlock 2011).

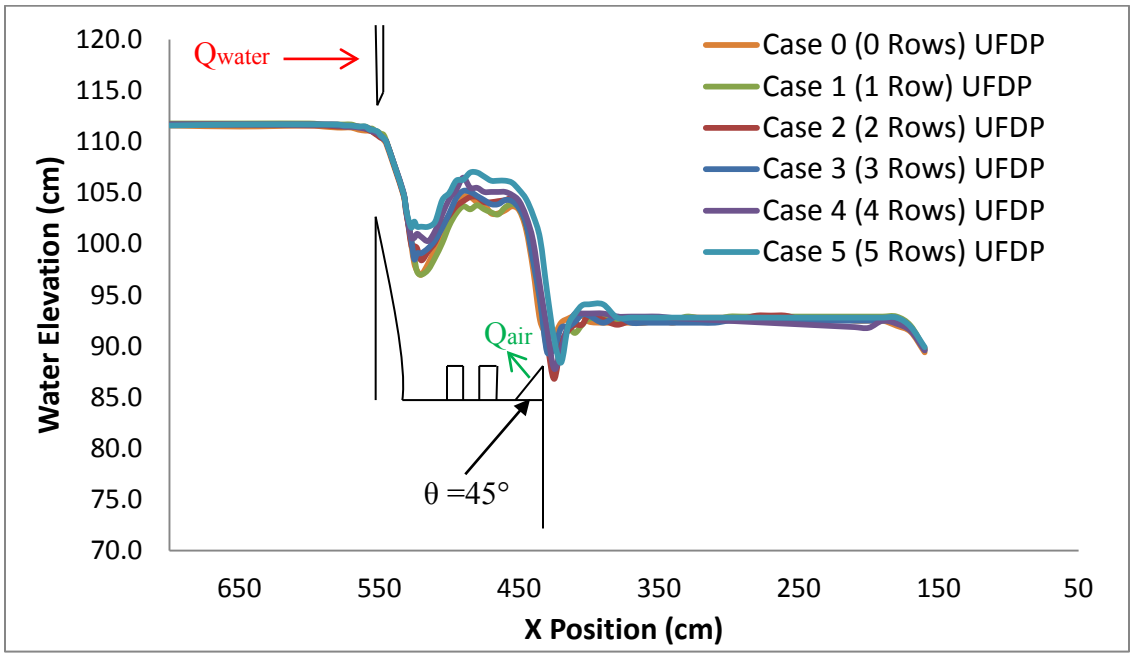

Figure 3.3. *Water surface profiles for varying cases with UFDP.*

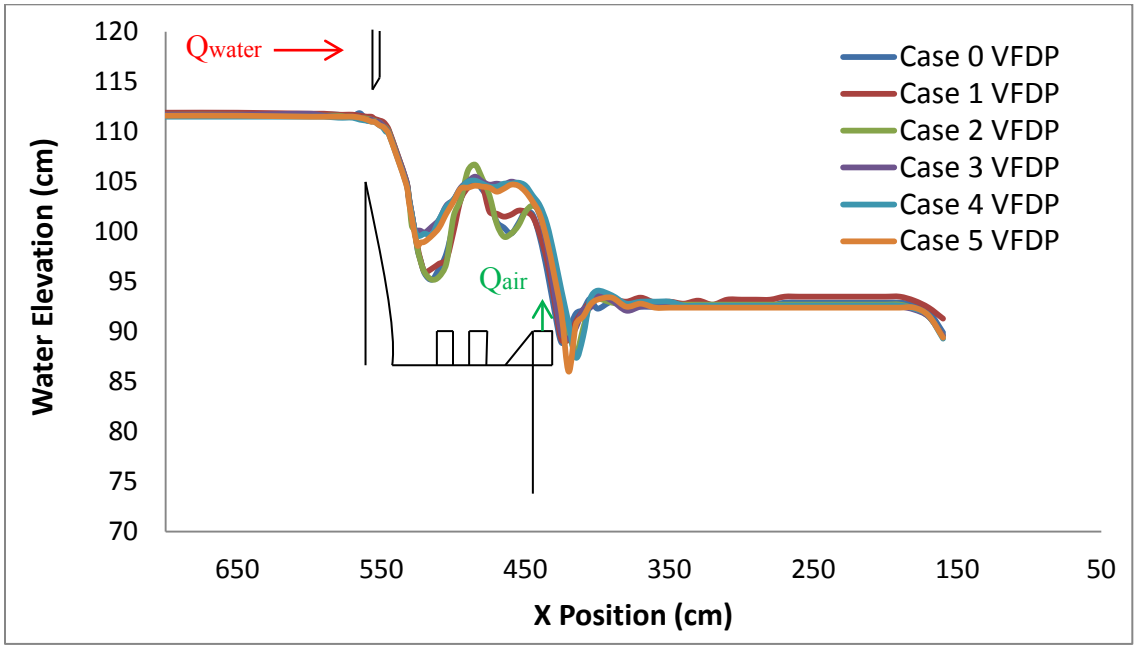

Figure 3.4. *Water surface profiles for varying cases with VFDP.*

Figures 3.5 through 3.10 show photographs for each of the six experimental cases (including the base case with no air injection) with the UFDP, while Figures 3.11 through 3.16 show the six cases for the VFDP. From these photographs, the increased whiteness and disturbance of the water by the injected air is shown clearly downstream of the end sill as the number of rows of air injection increase.

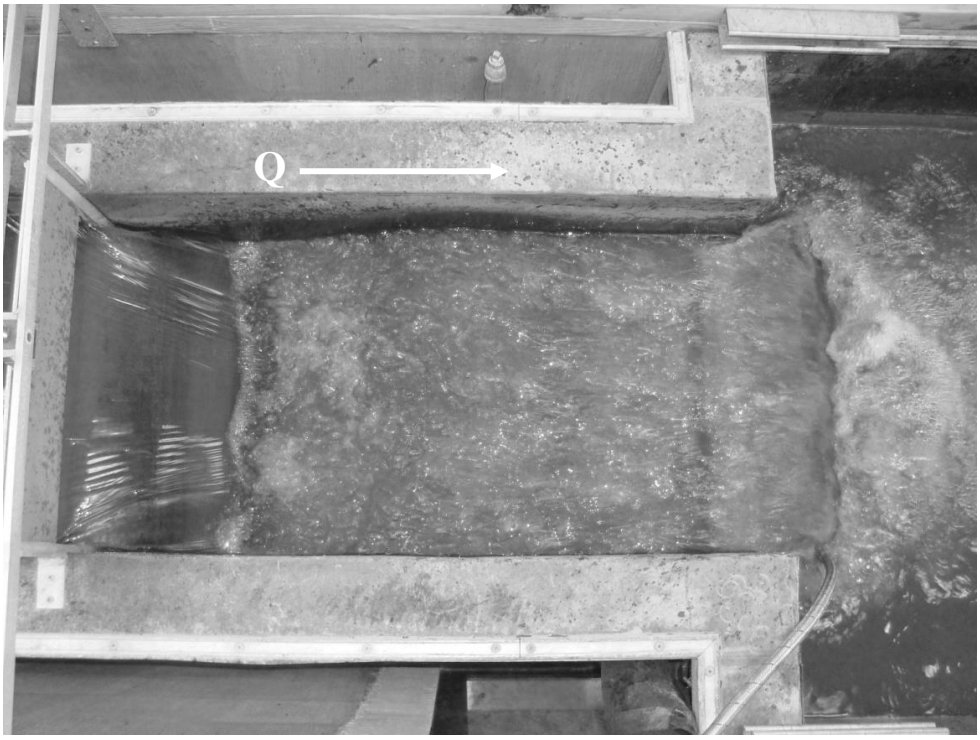

Figure 3.5. *Water surface photo without air with UFDP.*

Figure 3.6.*Water surface photo with 1 row of air holes with UFDP.*

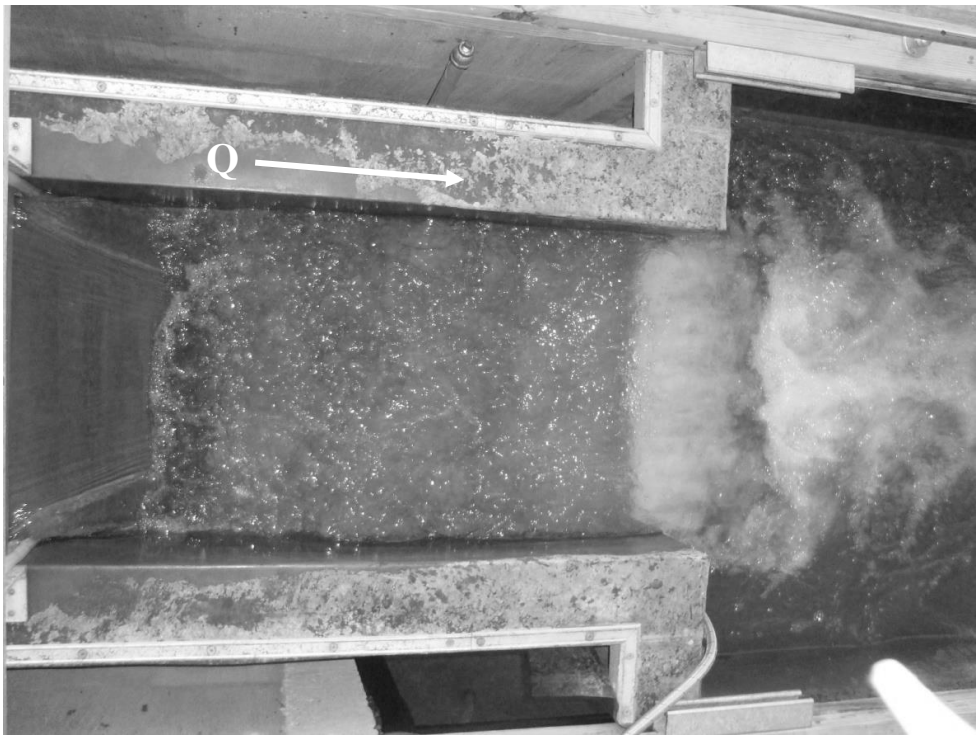

Figure 3.7. *Water surface photo with 2 rows of air holes with UFDP.*

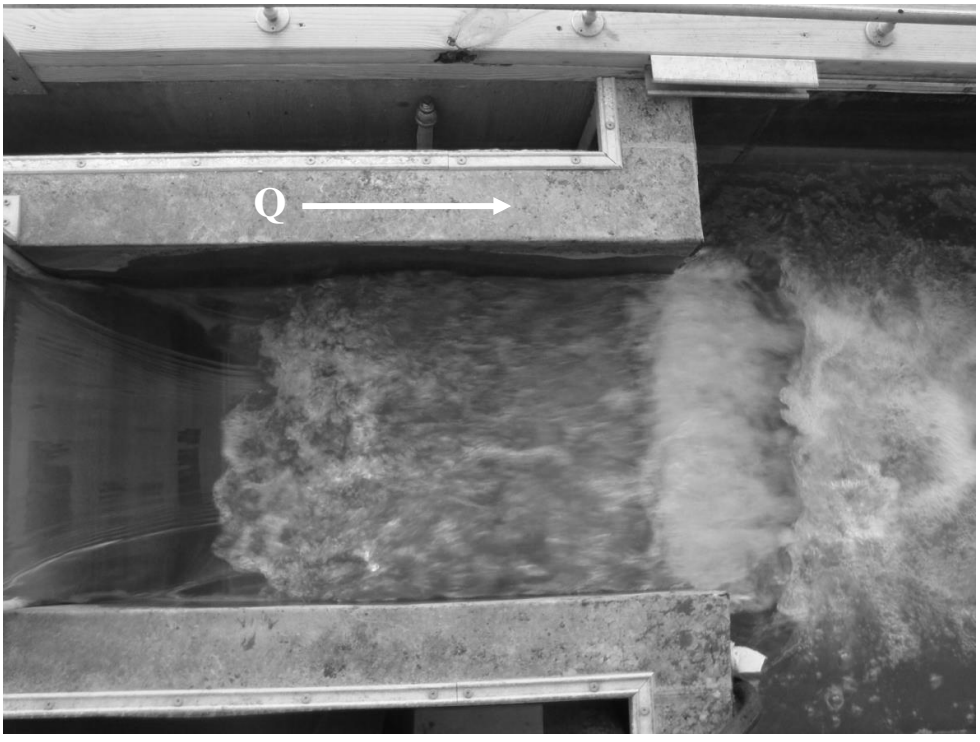

Figure 3.8.*Water surface photo with 3 rows of air holes with UFDP.*

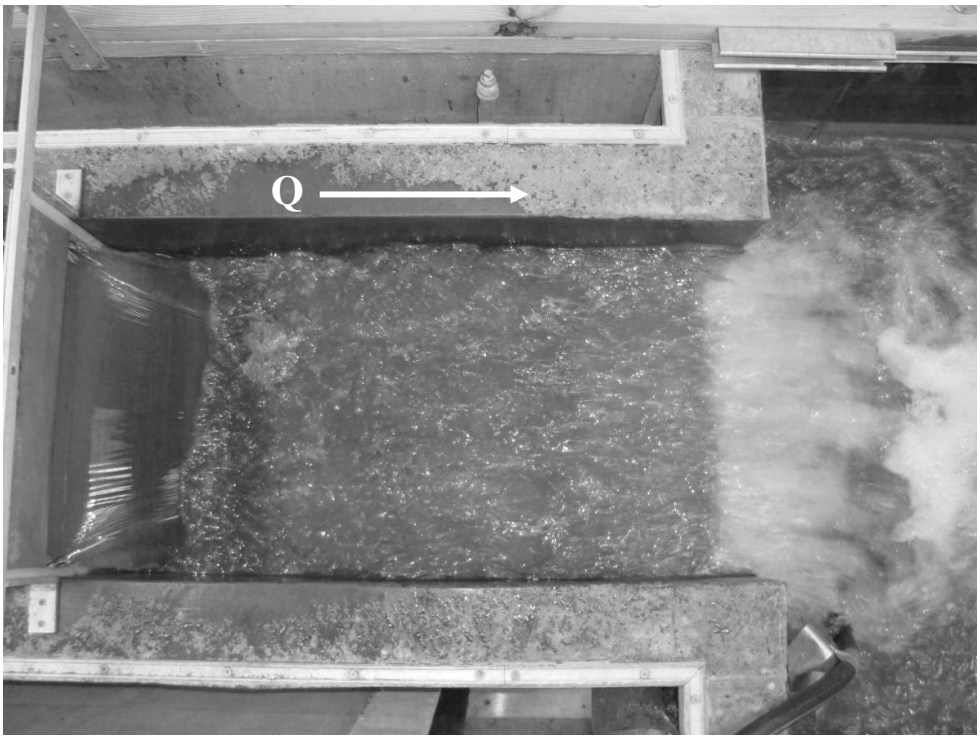

Figure 3.9.*Water surface photo with 4 rows of air holes with UFDP.*

Figure 3.10.*Water surface photo with 5 rows of air holes with UFDP.*

Figure 3.11. *Water surface photo with no air flow with VFDP.*

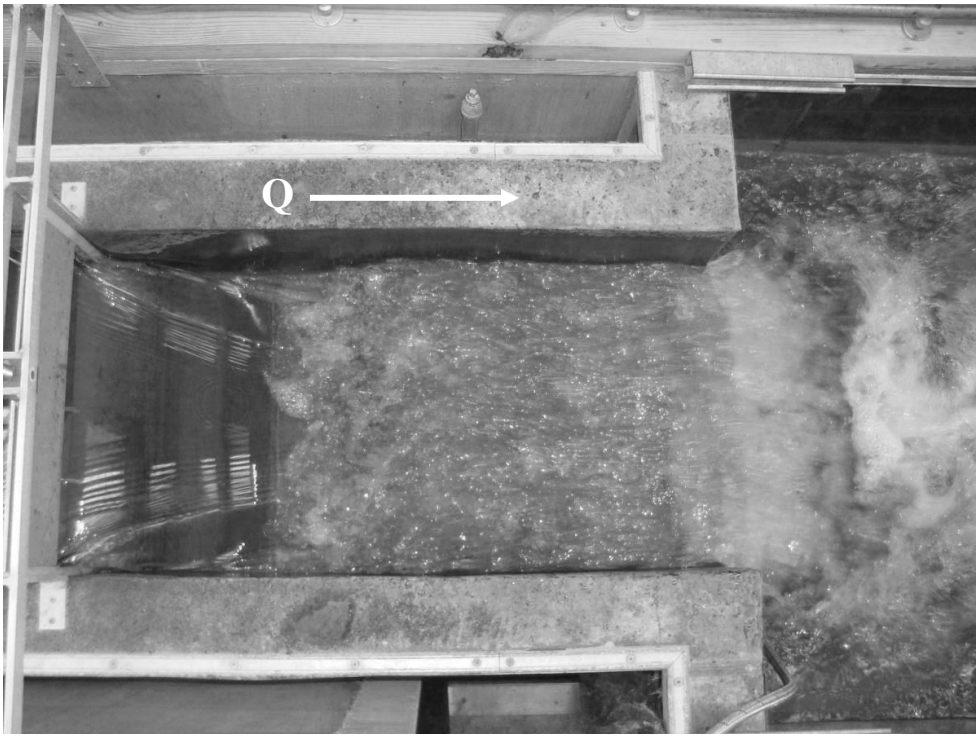

Figure 3.12. *Water surface photo with one row of air holes with VFDP.*

Figure 3.13.*Water surface photo with two rows of air holes with VFDP.*

Figure 3.14. *Water surface photo with three rows of air holes with VFDP.*

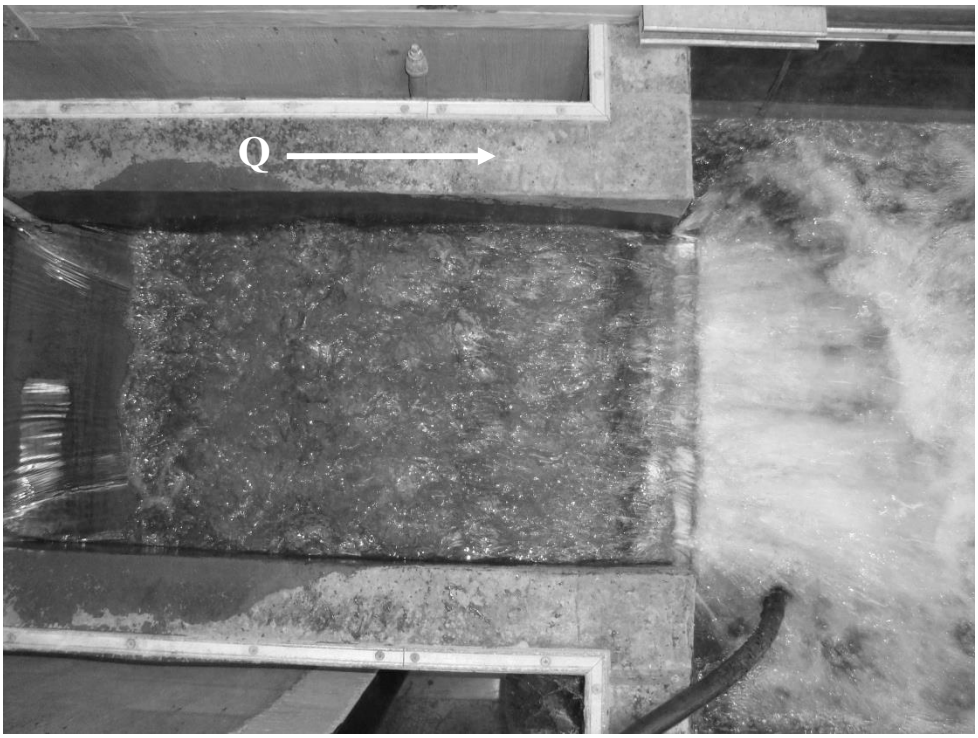

Figure 3.15. *Water surface photo with four rows of air holes with VFDP.*

Figure 3.16. *Water surface photo with five rows of air holes with VFDP.*

3.3.2 Scour Conditions

Contour plots for each air injection case with the UFDP are shown in Figures 3.17 through 3.22. The scour patterns for every air case are made up of lobes on either side of the major scour hole. The case with one row of air holes in the UFDP has an asymmetrical scour pattern. The base case with no air injection with the UFDP clearly has the largest scour hole, and it is evident that 5 rows of air injection cause the least volume of scour, calculated from the bed measurements using the point gage. Figures 3.23-3.28 show the contour plots for each case with the VFDP. It is also notable that the base case with no air injection with the VFDP caused approximately 20 cm less scour than the base case with no air for the UFDP. Table 3.2 shows the scour results from each case. It is important to note that with only one row of air injection in the VFDP, the volume of scour was less than with the UFDP with 2 or 3 rows of air injection, and 3 rows of air injection with the VFDP reduces scour volume to the same level as the UFDP with five rows. This shows that the VFDP is more effective at reducing scour than the UFDP (Barkdoll and Barlock 2011).

Photographs of the bed after reaching equilibrium with the UFDP are shown in Figures 3.29-3.34. Figures 3.35-3.40 show the bed equilibrium photos for the VFDP These photos show dunes forming upstream and on either side of the scour hole. These dunes are caused by the water flow separating into up- and downstream components as they make contact with the bed.

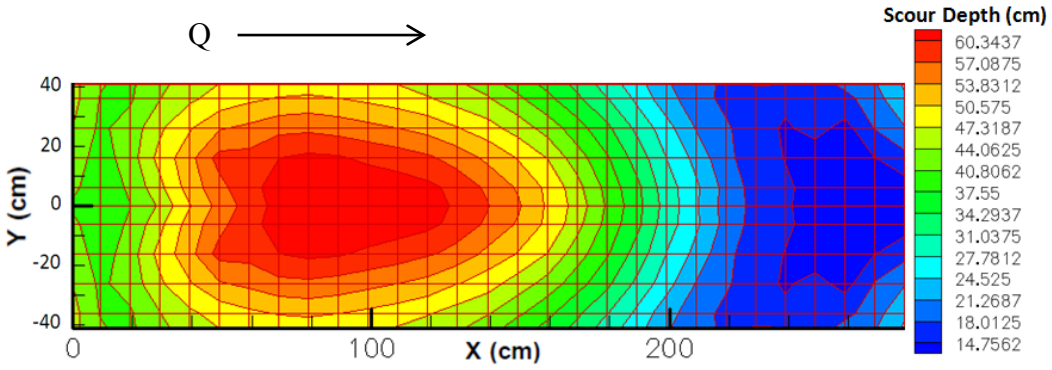

Figure 3.17. *Bed contour plot for zero rows of air holes with UFDP.*

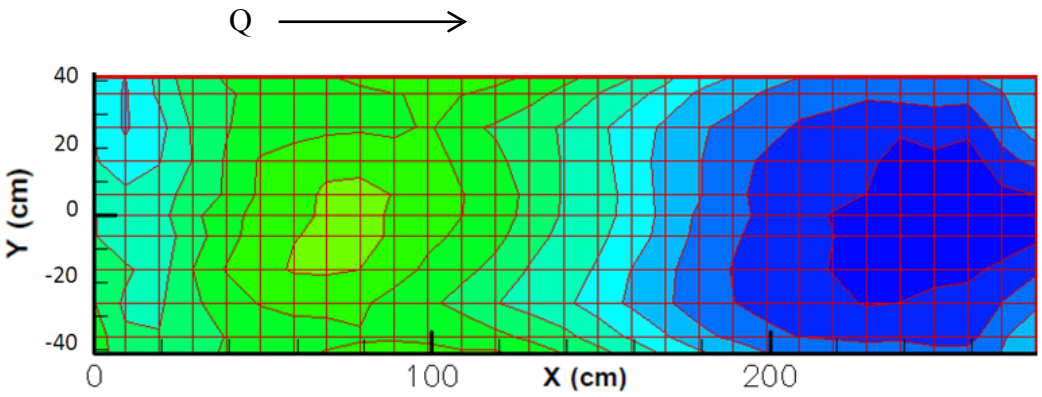

Figure 3.18. *Bed contour plot for one row of air holes with UFDP.*

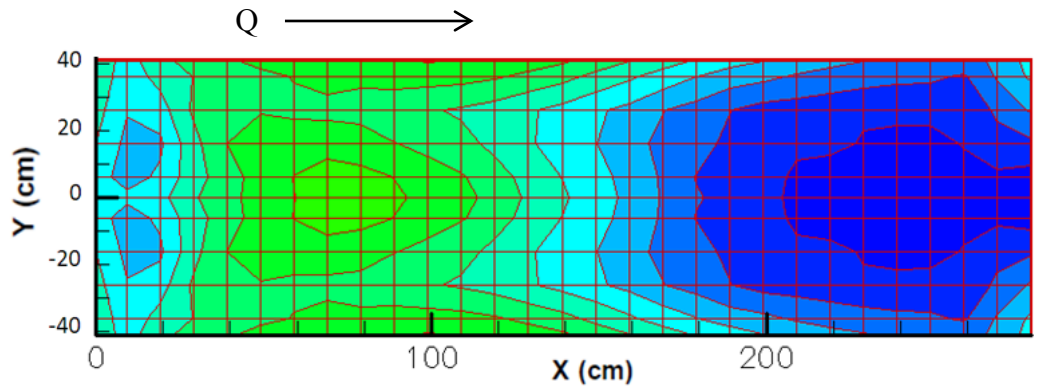

Figure 3.19. *Bed contour plot for two rows of air holes with UFDP.*

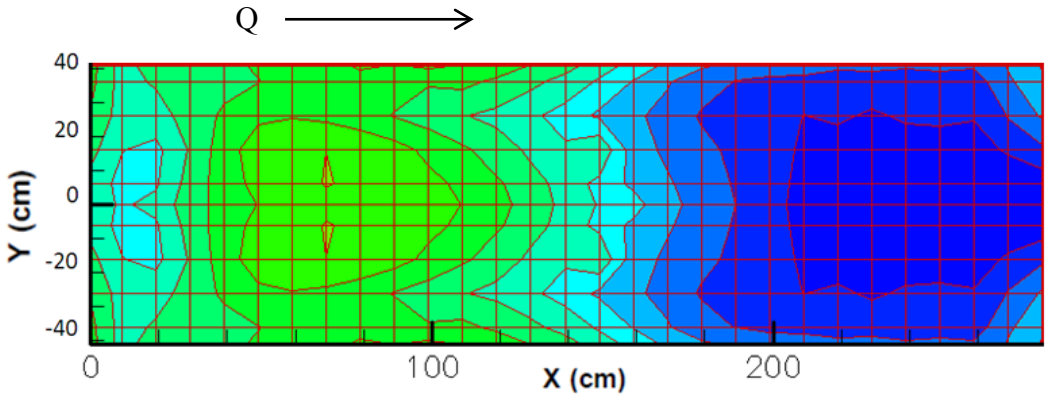

Figure 3.20. *Bed contour plot for three rows of air holes with UFDP.*

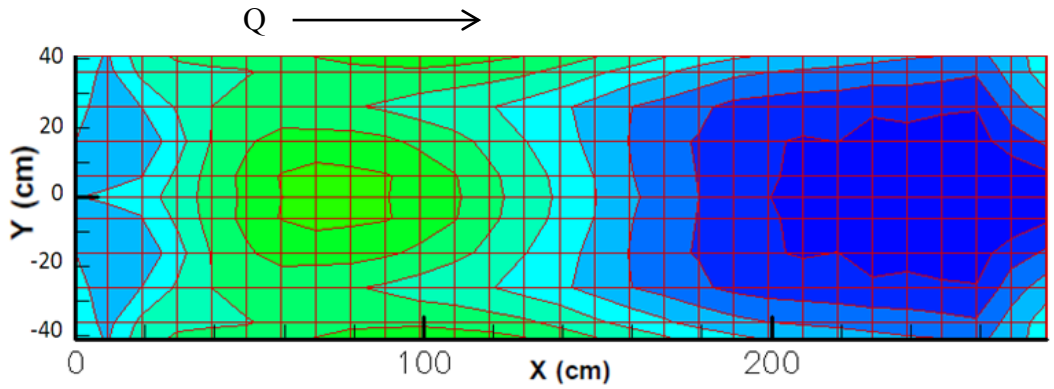

Figure 3.21. *Bed contour plot for four rows of air holes with UFDP.*

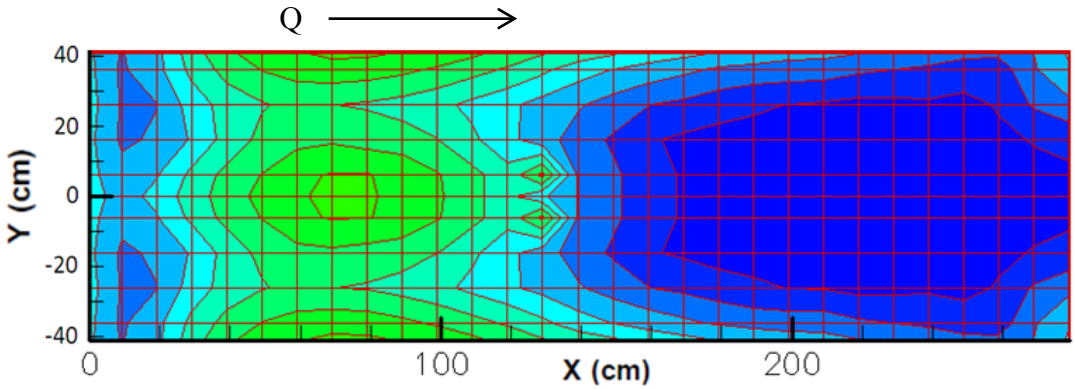

Figure 3.22. *Bed contour plot for five rows of air holes with UFDP.*

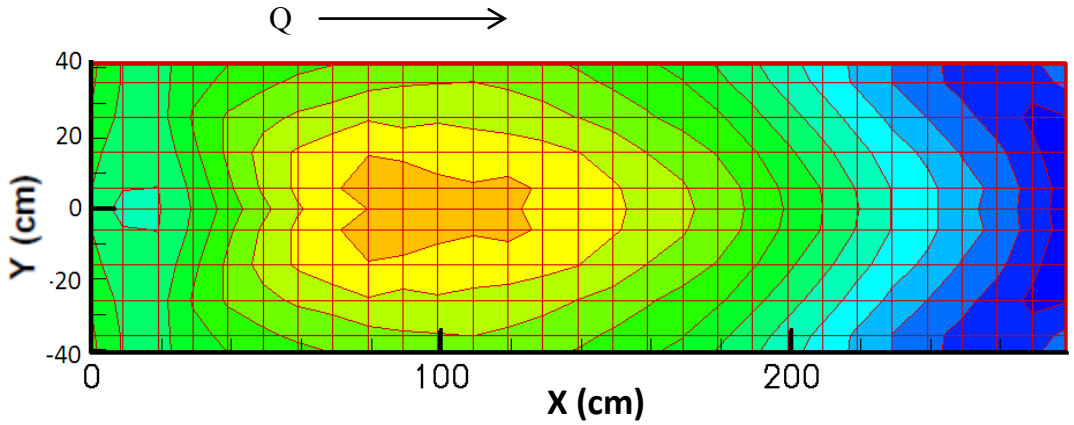

Figure 3.23. *Bed contour plot for zero air injection with VFDP.*

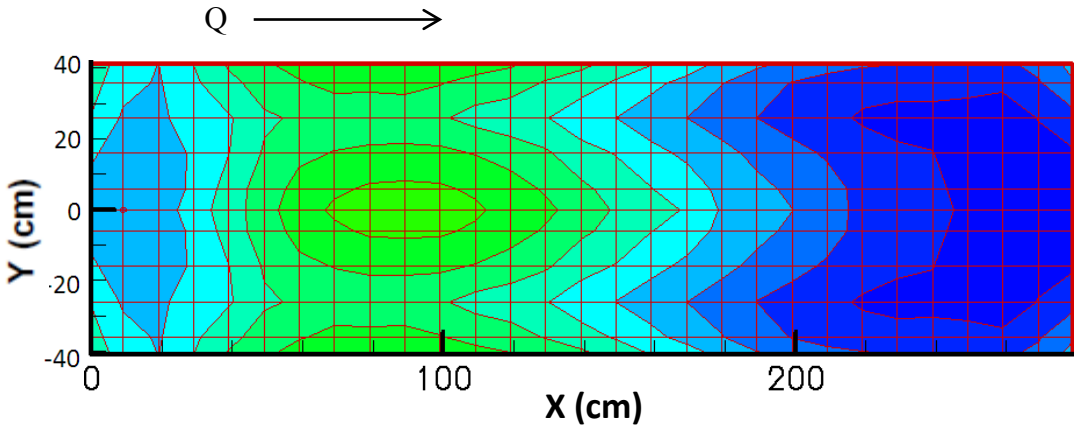

Figure 3.24. *Bed contour plot for one row of air injection with VFDP.*

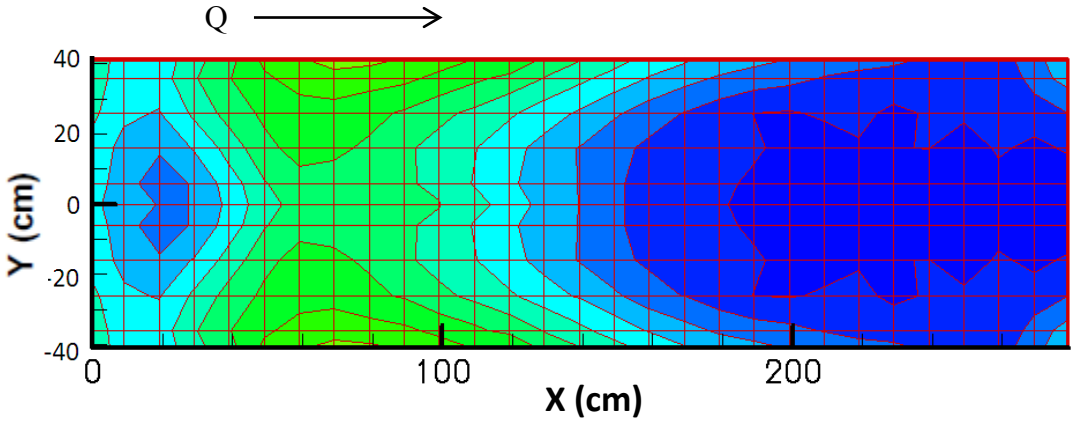

Figure 3.25. *Bed contour plot for two rows of air injection with VFDP.*

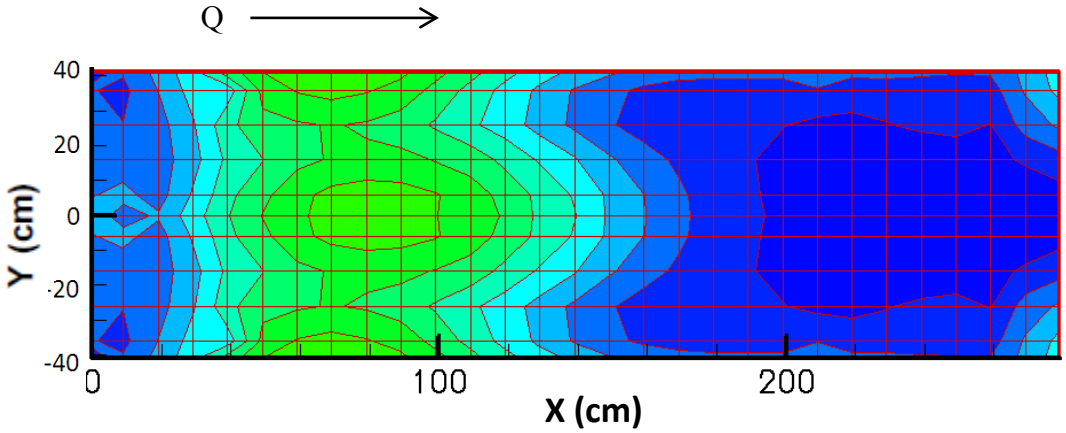

Figure 3.26. *Bed contour plot for three rows of air injection with VFDP.*

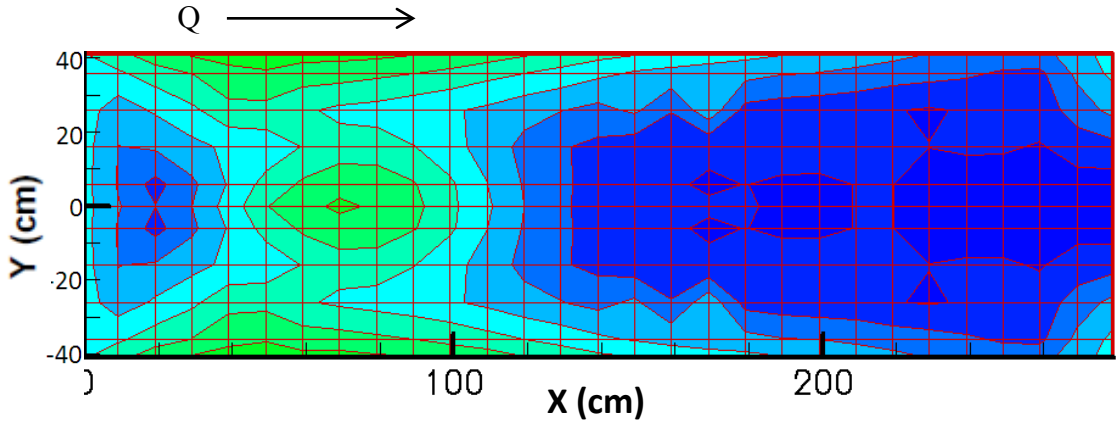

Figure 3.27. *Bed contour plot for four rows of air injection with VFDP.*

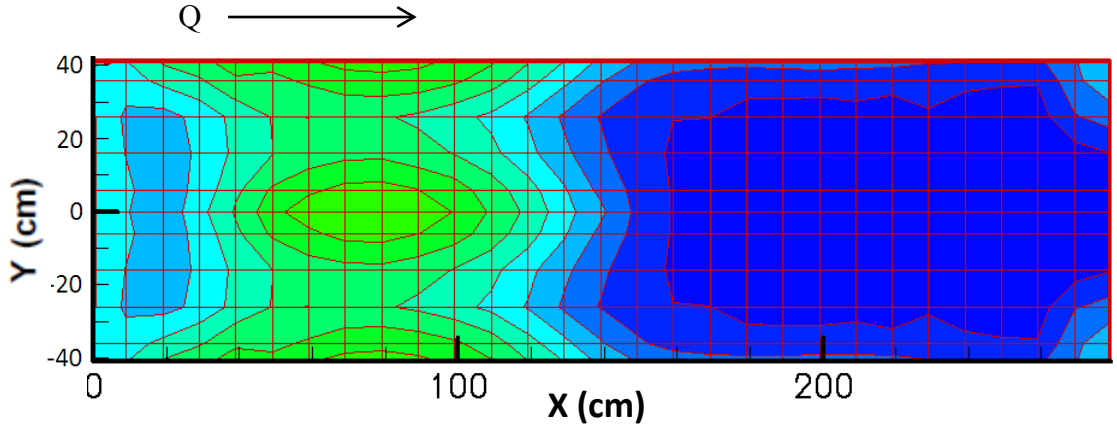

Figure 3.28. *Bed contour plot for five rows of air injection with VFDP.*

Table 3.2. *Scour volume for experimental cases.*

Number of Rows of Air Holes	Scour Volume (cubic meters)
UFDP	
0	0.79
1	0.51
2	0.47
3	0.48
4	0.44
5	0.41
VFDP	
0	0.73
1	0.46
2	0.42
3	0.41
4	0.39
5	0.39

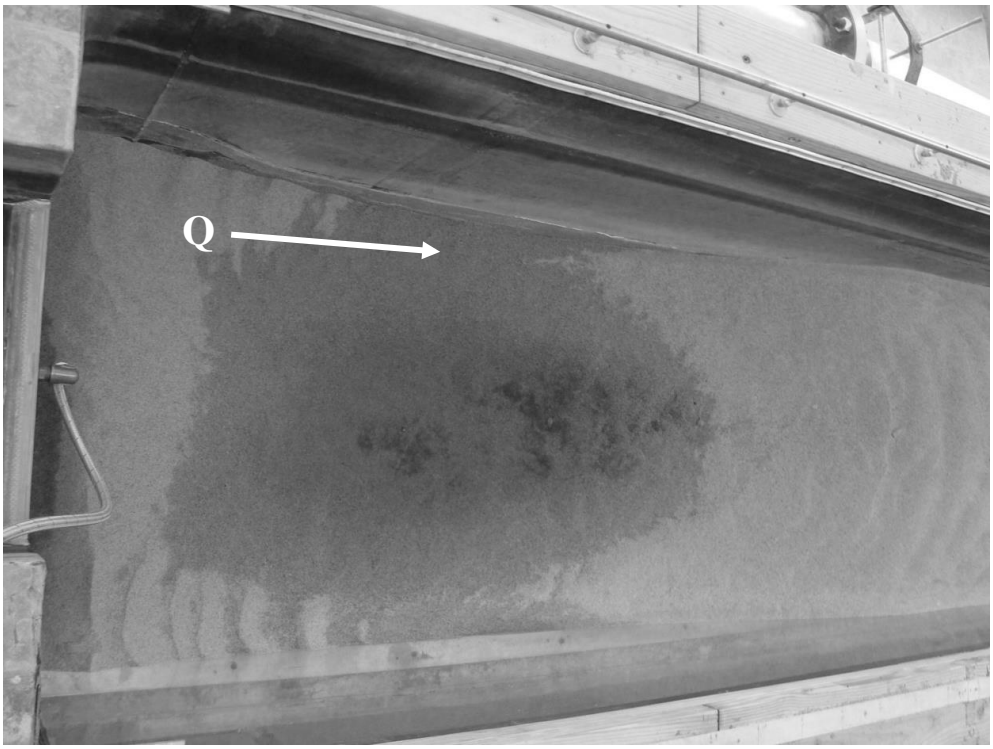

Figure 3.29. *Equilibrium bed photo for zero rows of air holes with UFDP.*

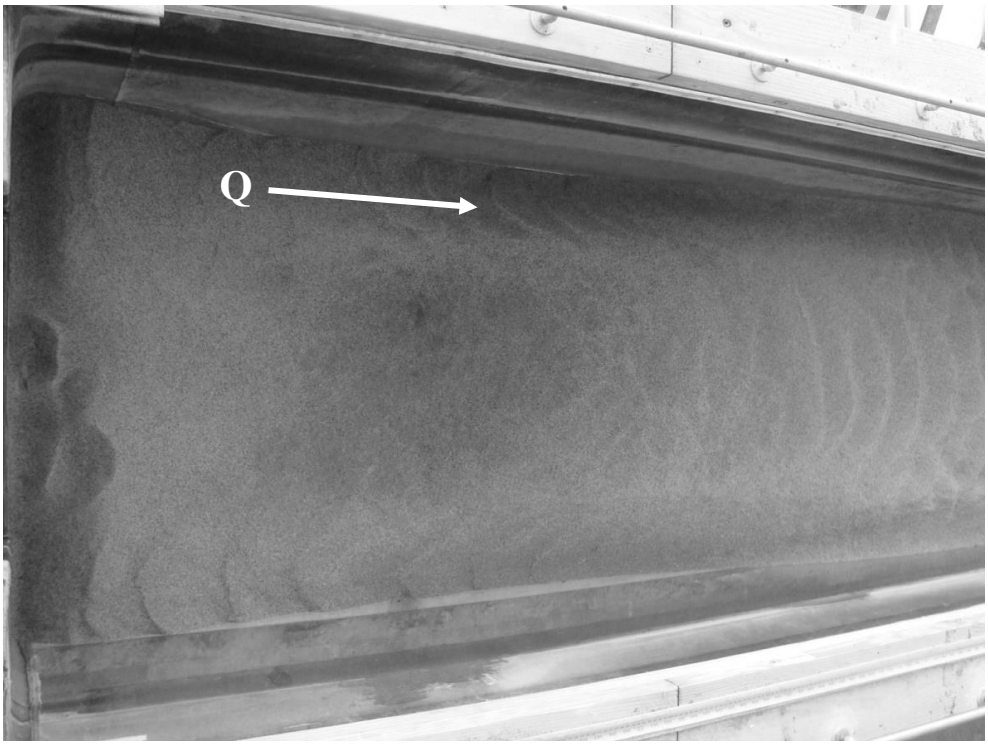

Figure 3.30. *Equilibrium bed photo for 1 row of air holes with UFDP.*

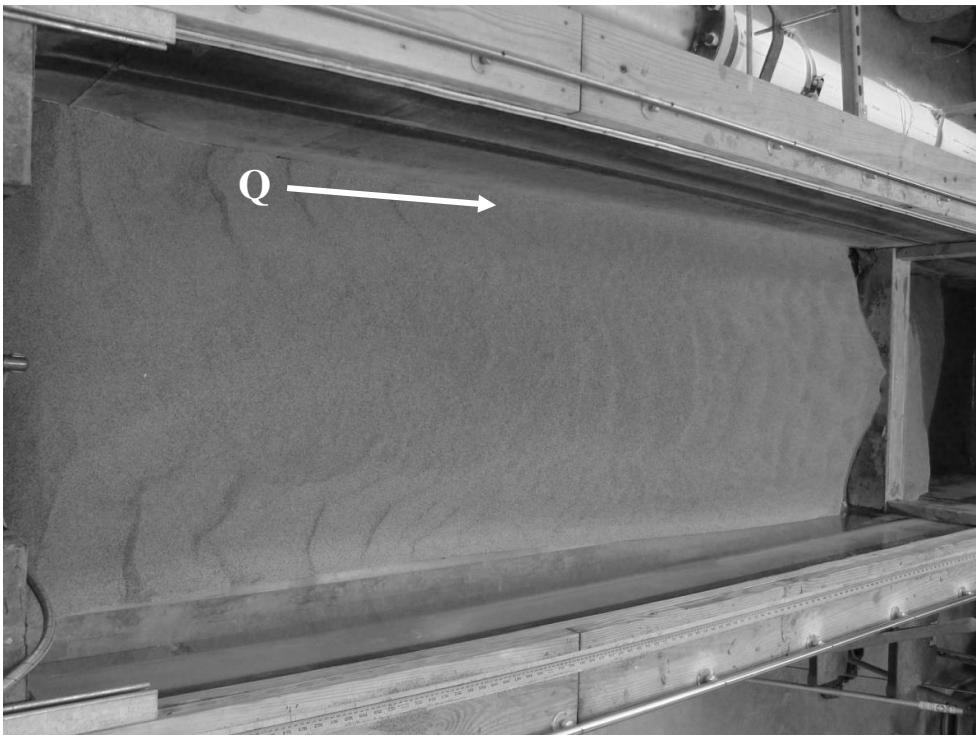

Figure 3.31. *Equilibrium bed photo for 2 rows of air holes with UFDP.*

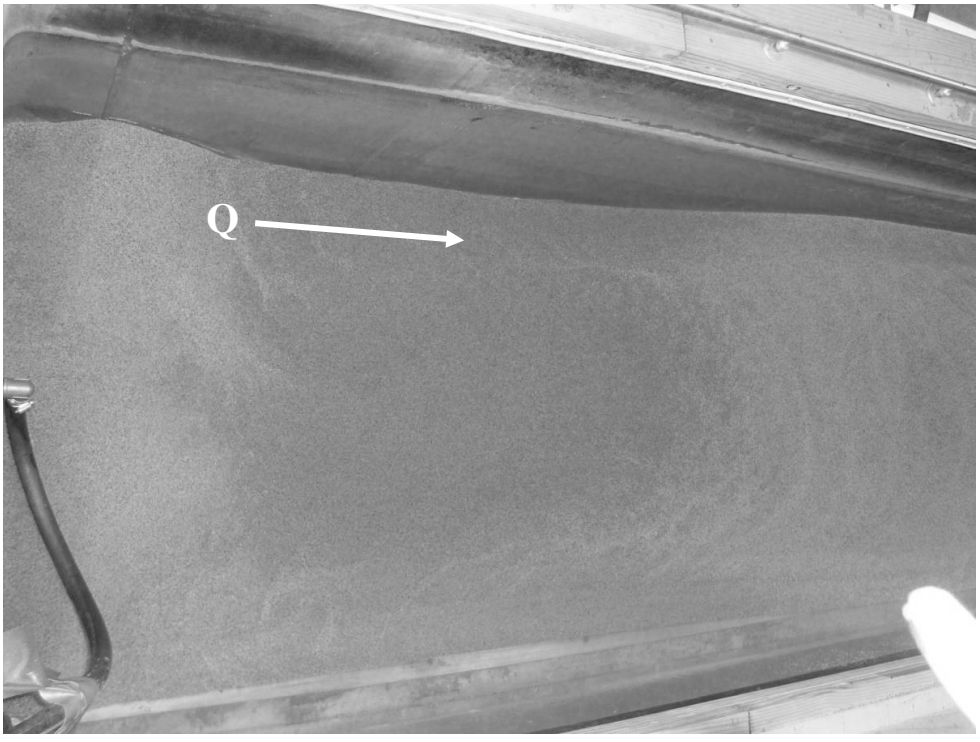

Figure 3.32. *Equilibrium bed photo for 3 rows of air holes with UFDP.*

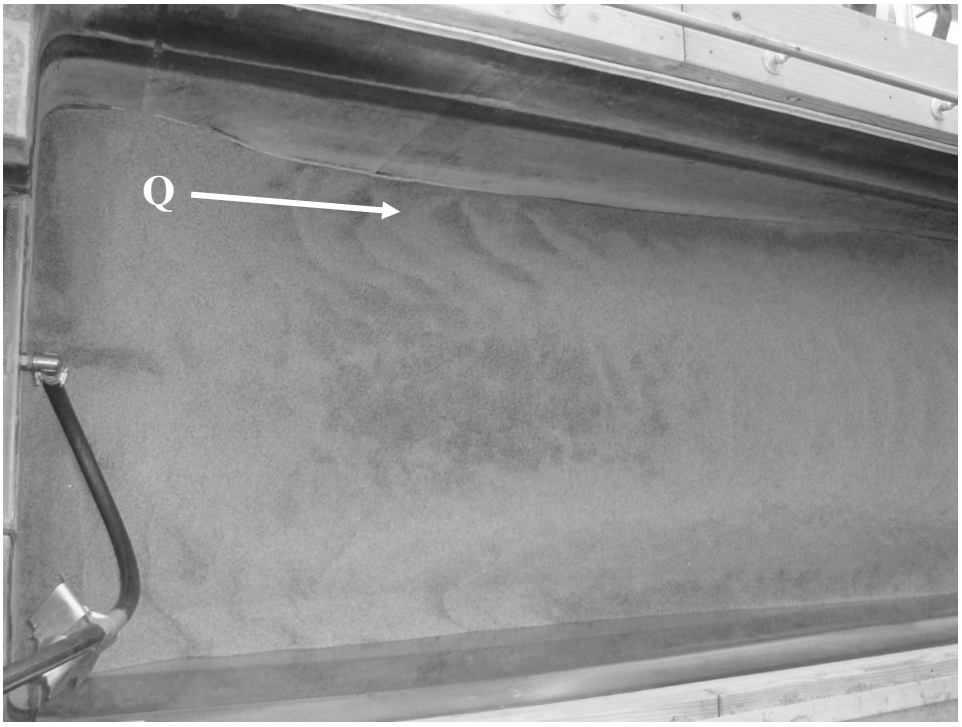

Figure 3.33. *Equilibrium bed photo for 4 rows of air holes with UFDP.*

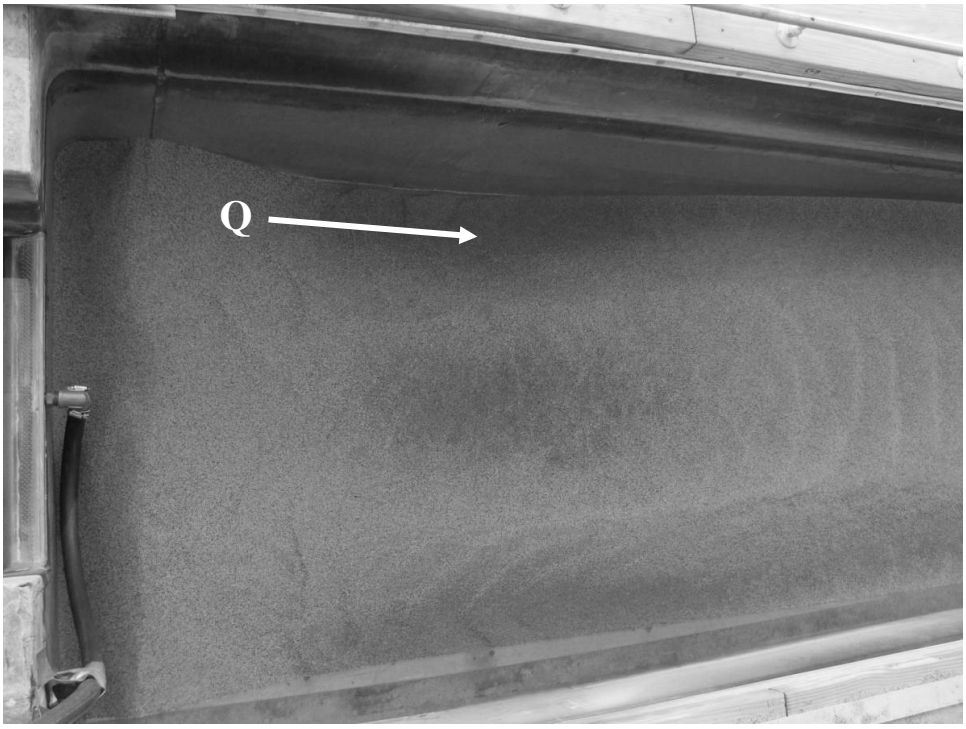

Figure 3.34. *Equilibrium bed photo for 5 rows of air holes with UFDP.*

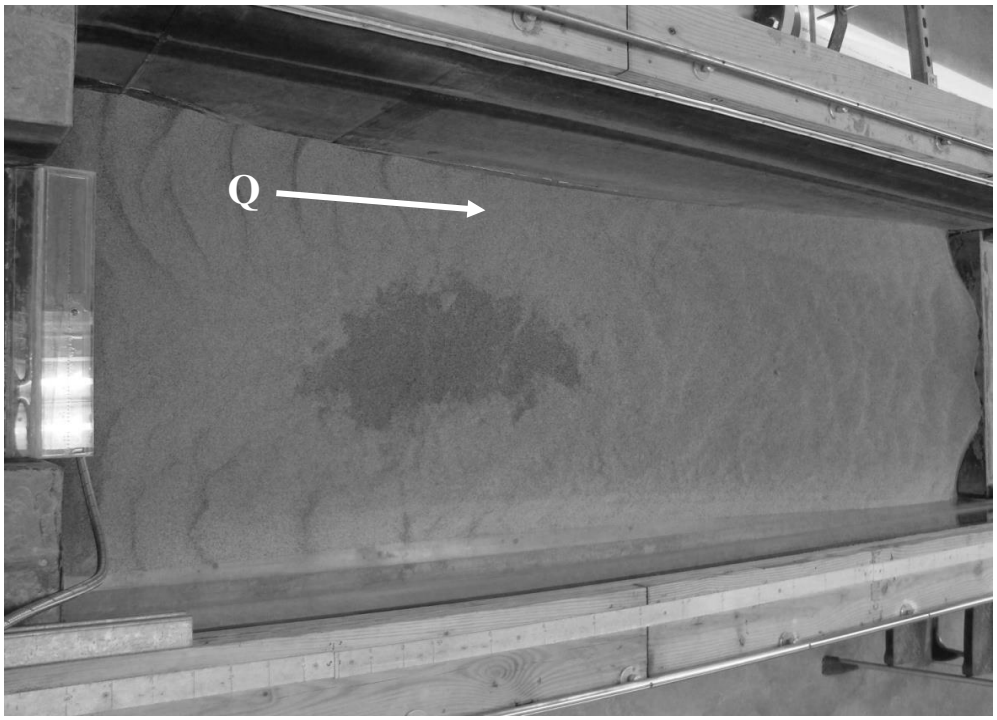

Figure 3.35. *Equilibrium bed photo for zero air injection with VFDP.*

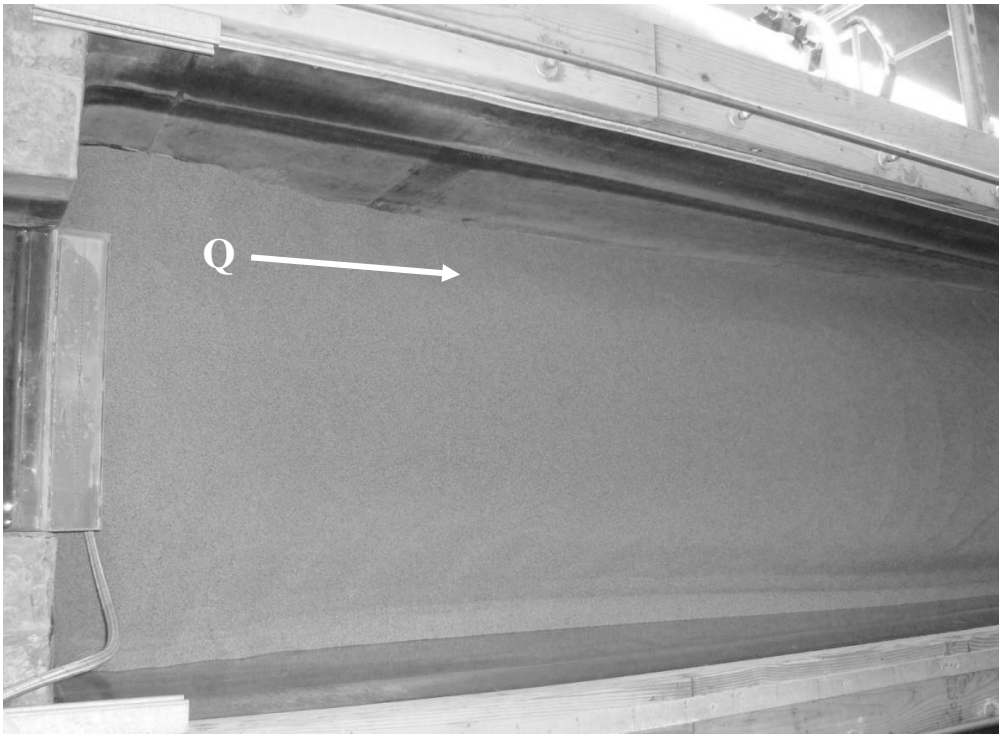

Figure 3.36. *Equilibrium bed photo for one row of air injection with VFDP.*

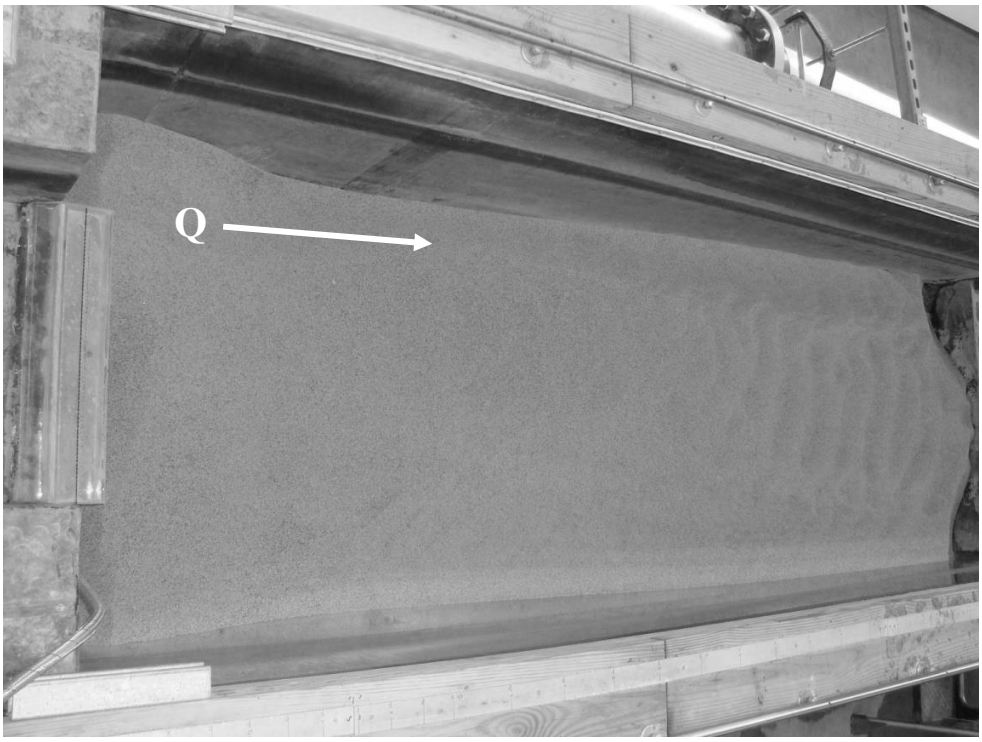

Figure 3.37. *Equilibrium bed photo for two rows of air injection with VFDP.*

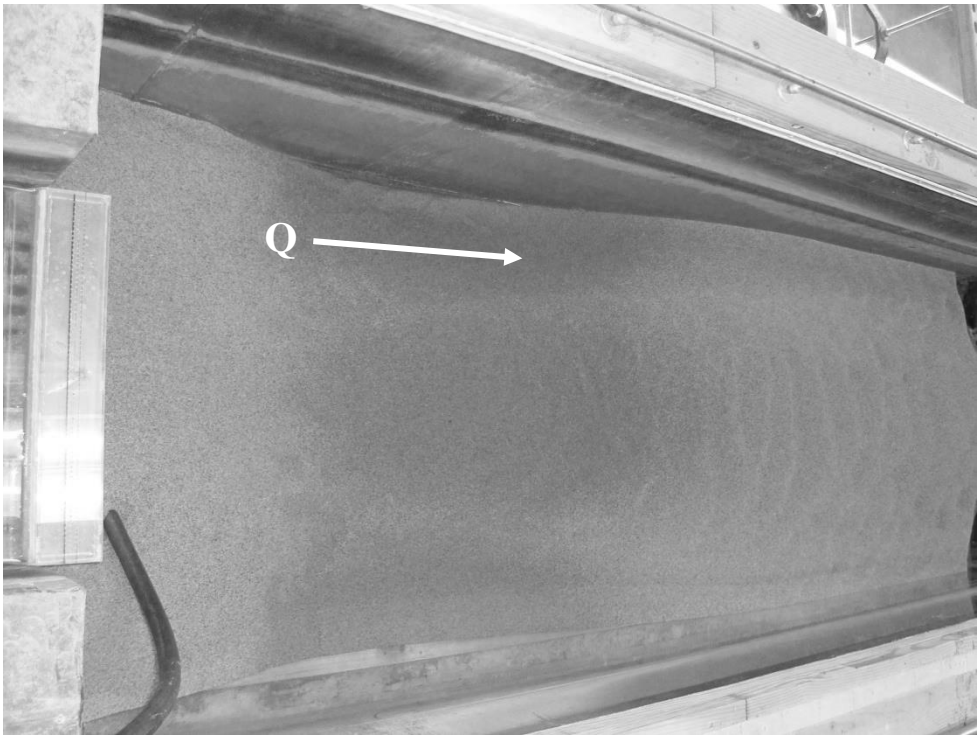

Figure 3.38. *Equilibrium bed photo for three rows of air injection with VFDP.*

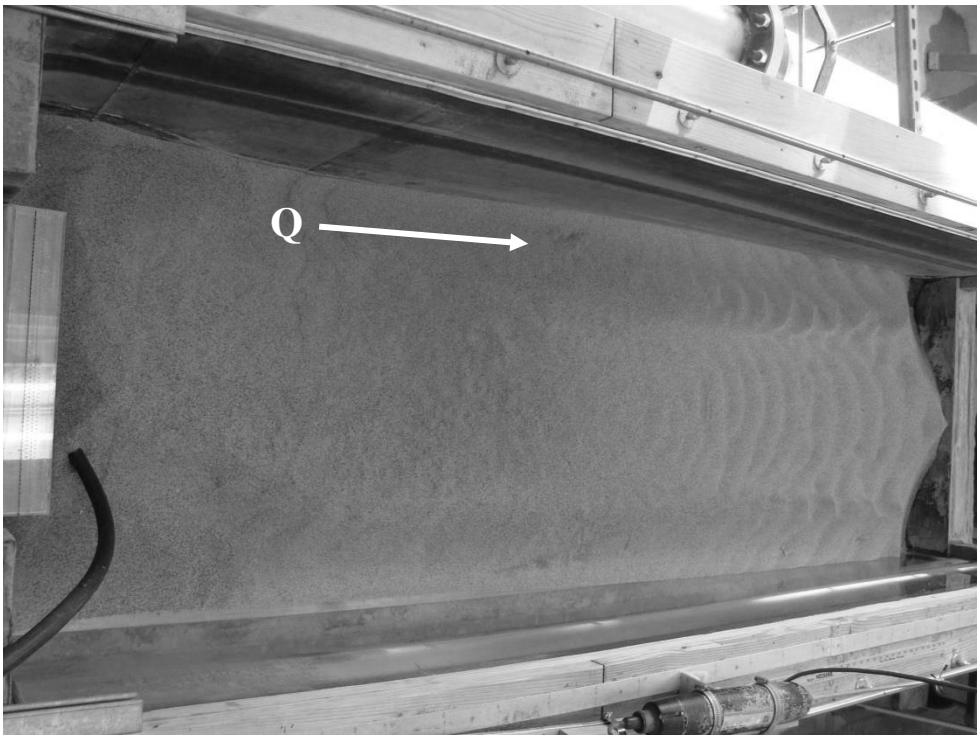

Figure 3.39. *Equilibrium bed photo for four rows of air injection with VFDP.*

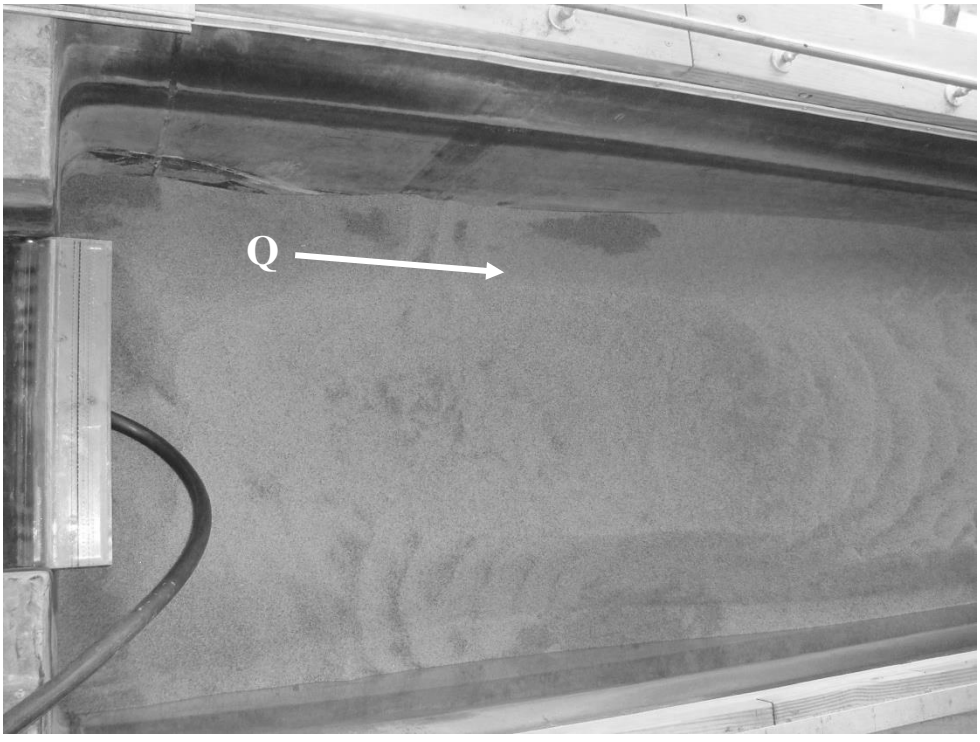

Figure 3.40. *Equilibrium bed photo for five rows of air injection with VFDP.*

Figures 3.41 and 3.42 are graphs of the centerline equilibrium bed profiles for the UFDP and VFDP, respectively. Again, it is evident that when there are five rows of air injection holes, the scour is reduced the most, and that the VFDP is more effective at reducing scour than the UFDP.

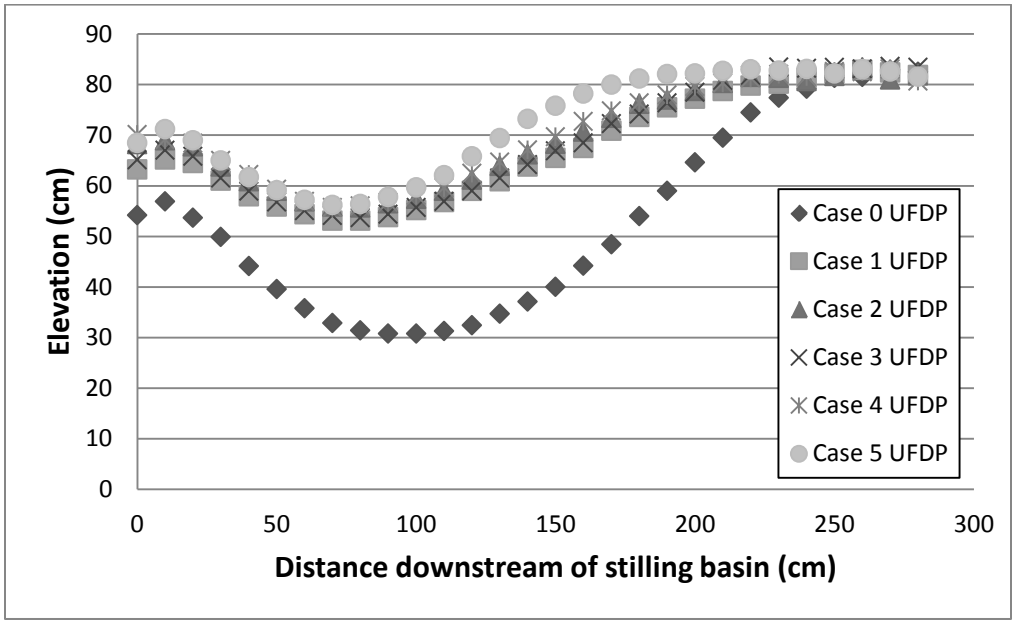

Figure 3.41. ***Centerline bed elevation for UFDP.***

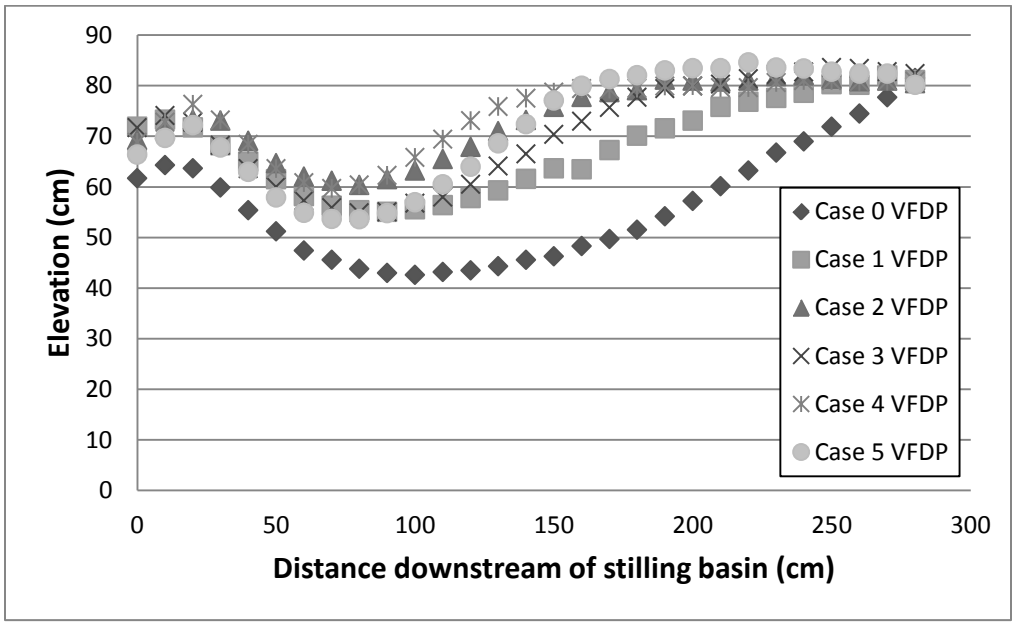

Figure 3.42. ***Centerline bed elevation for VFDP.***

Figure 3.43 shows the bed elevation at the worst scour point near and away from the structure for every case. It can be seen that in all air injection cases, scour is reduced, but five rows of air injection holes reduces scour the most, both near and away from the structure. Scour away from the structure is a similar depth in each case, but scour near the structure varies more from case to case. Again, scour is less with the VFDP than with the UFDP. Figure 3.44 plots the volume of scour away from the structure in each case. Again, it can be seen that five rows of air injection cause the least amount of scour (Barkdoll and Barlock 2011).

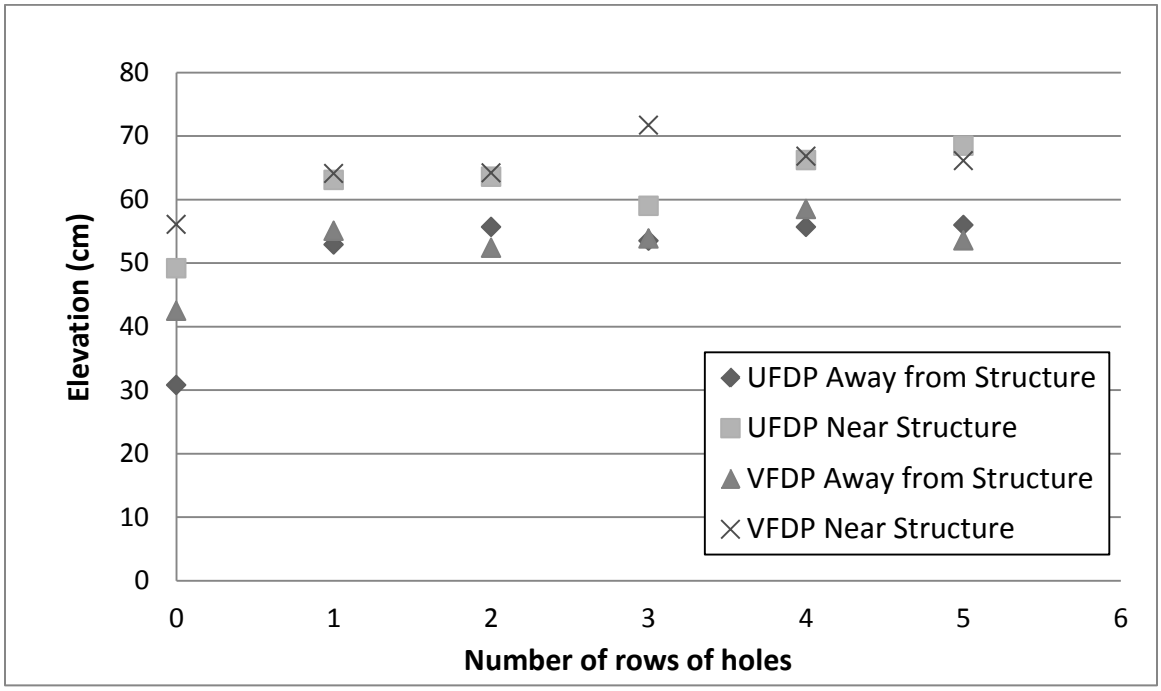

Figure 3.43. *Maximum scour depth near and away from the structure.*

Thinking about these results in terms of the large-scale, existing structure, the important thing to consider is the scour depth near the structure. The scour depth near the structure is the location of scour that causes the most concern. Scour below the foundation bottom will result in structural failure, but it would be a conservative estimate to say that scour at the structure that is below half the height of the structure is dangerous. In the case of these studies, the trials that were considered effective were those that left remaining sediment height well above the lower half of the structure.

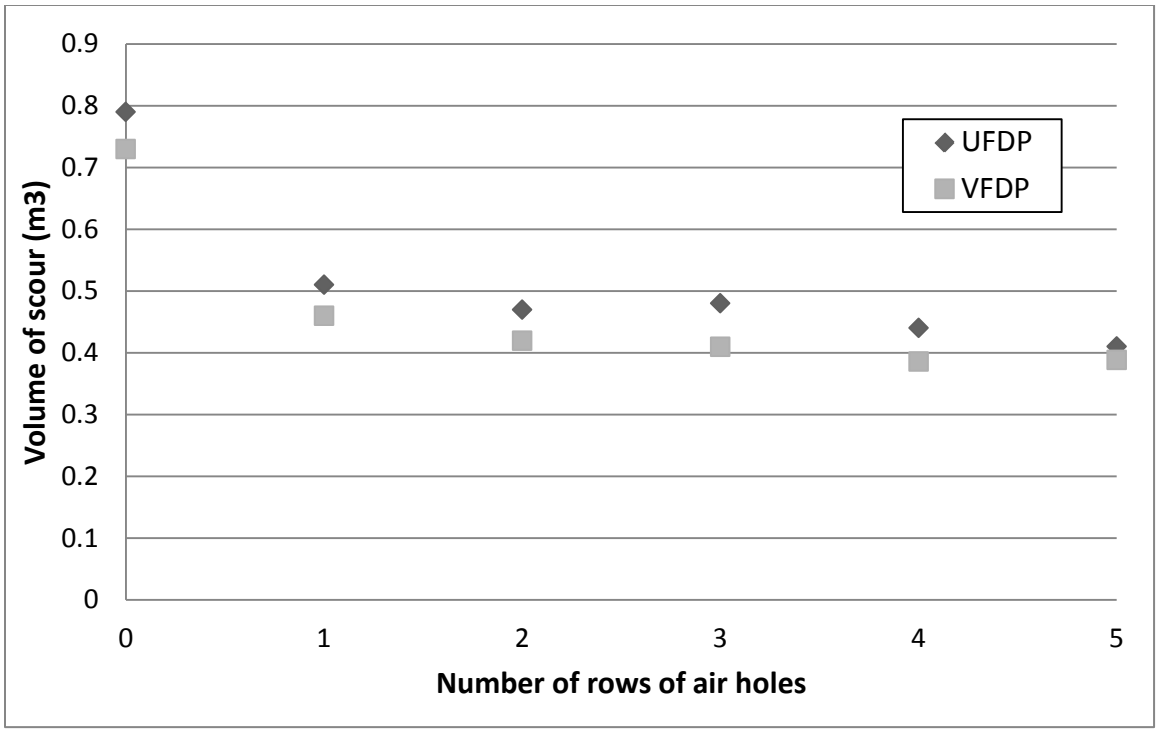

Figure 3.44. *Volume of scoured sediment for different cases.*

3.3.3 Velocity and Turbulence Measurements

Figures 3.45 through 3.50 show the water velocity profiles near the stilling basin exit (6 cm upstream of the stilling basin face). As expected, the velocity increases further from the bed. Figures 3.45 and 3.46 agree with the hypothesis that air injection decreases longitudinal velocity, which in turn, reduces scour. Figures 3.51 through 3.62 show the turbulence intensities in the *x*-, *y*- and *z*-directions and the anisotropic ratios and anisotropy of turbulence, respectively. It can be seen that one or two rows reduce turbulence but more rows than that increase the turbulence again.

The turbulence intensities in the longitudinal, transverse and vertical directions, respectively, were calculated with the following equations:

$$TI_u = \frac{\sqrt{\overline{(u')^2}}}{U};\ TI_v = \frac{\sqrt{\overline{(v')^2}}}{U};\ TI_w = \frac{\sqrt{\overline{(w')^2}}}{U}$$

Where TI_u, TI_v and TI_w are the turbulence intensities, and *u'*, *v'* and *w'* are the turbulent velocity fluctuations in their respective directions, with the prime superscript denoting the

amount away from the mean value as obtained by the filtered velocity signal from the ADV. The velocity data was filtered by removing the largest value of any acceleration greater than that of the acceleration due to gravity. The anisotropy of turbulence in the cross section was calculated with the following equation:

$$ANI = \frac{\overline{v'^2} - \overline{w'^2}}{\overline{v'^2}}$$

The anisotropy ratios were calculated using the following equations:

$$v_r{}' = \frac{\overline{v'^2}}{\overline{u'^2}};\ \ w_r{}' = \frac{\overline{w'^2}}{\overline{u'^2}}$$

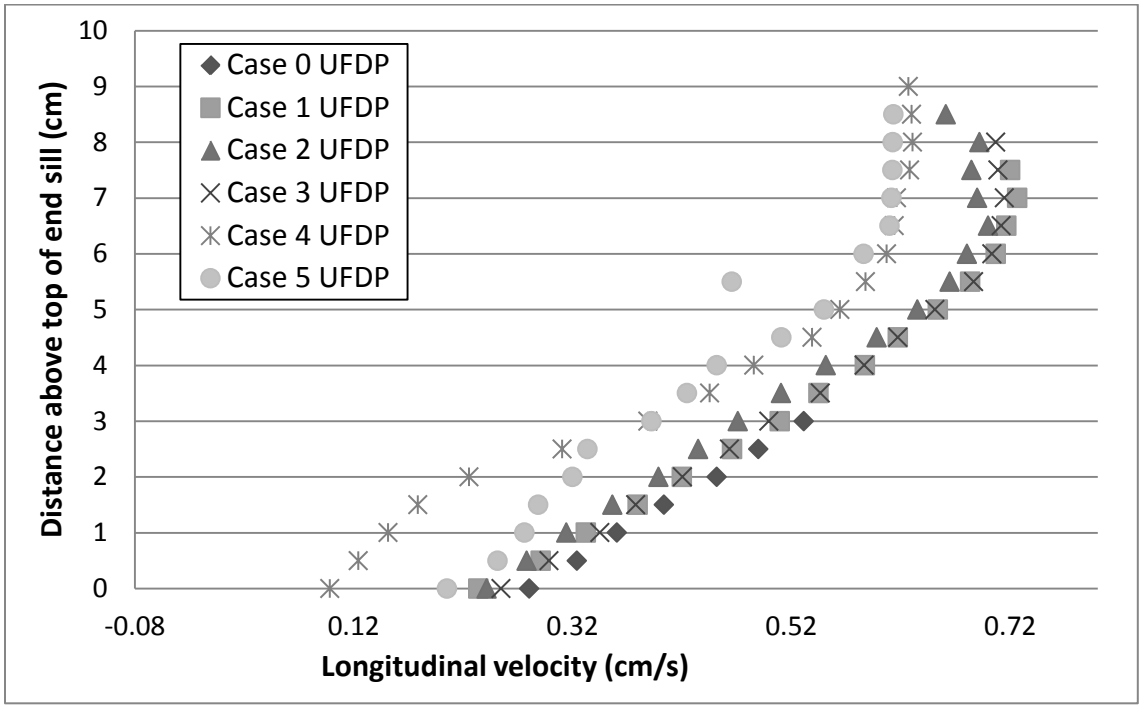

Figure 3.45. *Longitudinal velocity measurements for each case with the UFDP.*

In Figure 3.45, there is a single data point that looks like it could potentially be an outlier. This could be due to filtering uncertainties.

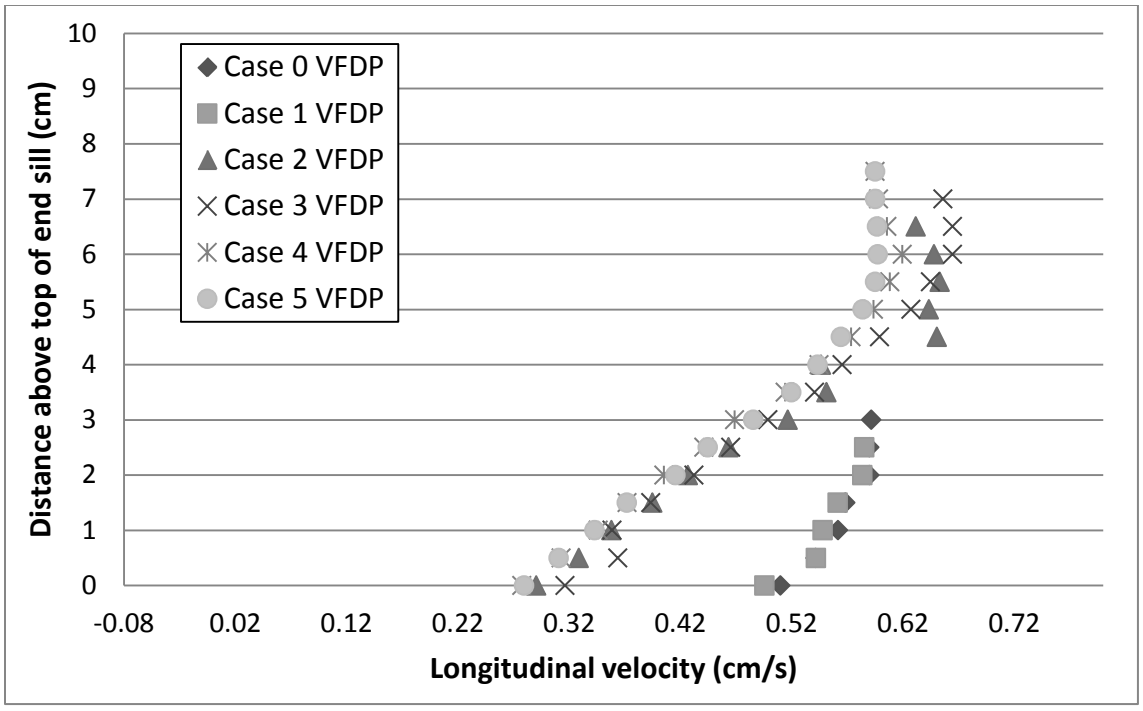

Figure 3.46. *Longitudinal velocity measurements for each case with the VFDP.*

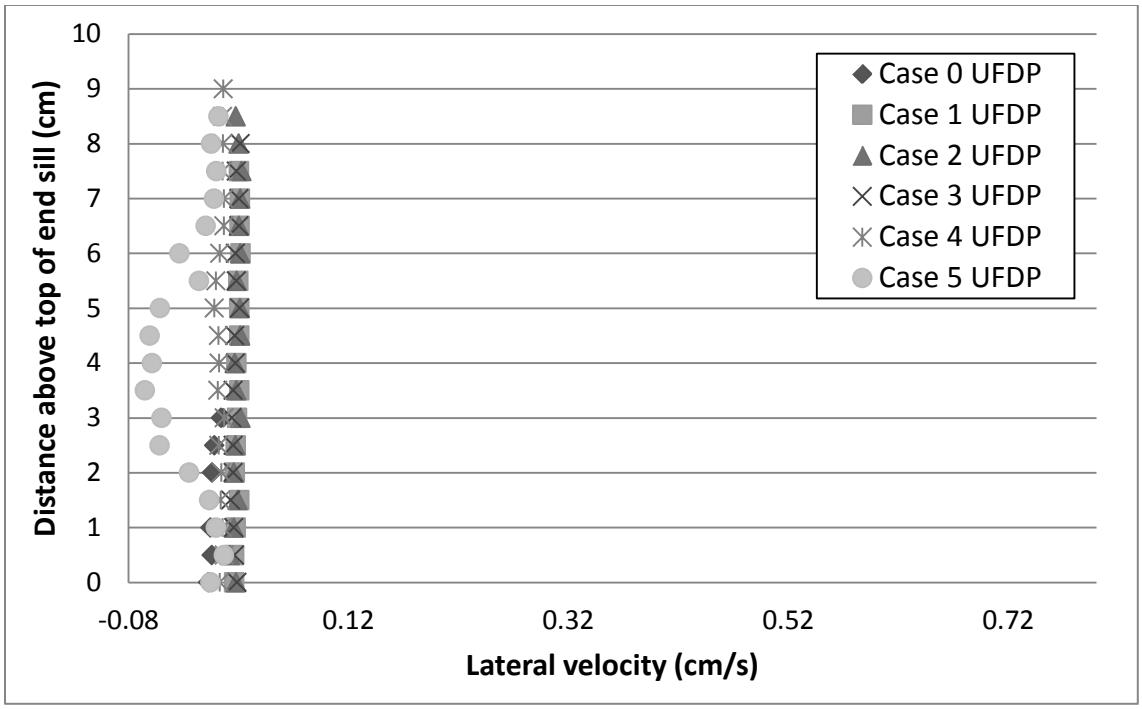

Figure 3.47. *Lateral velocity measurements for each case with the UFDP.*

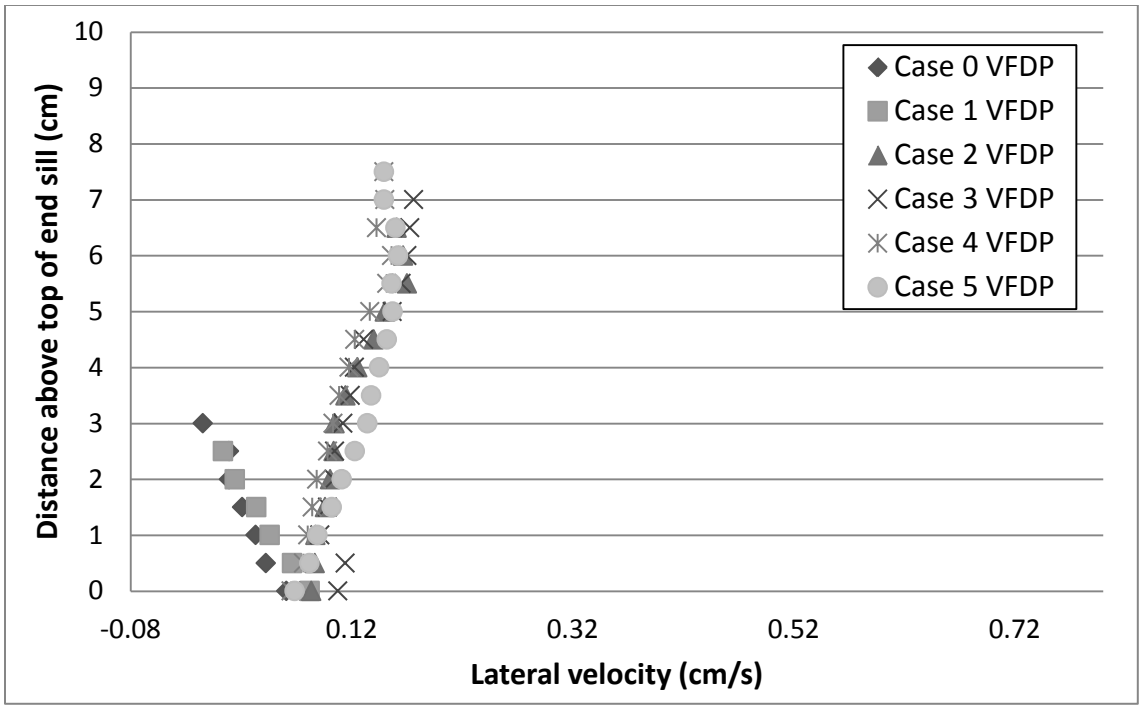

Figure 3.48. *Lateral velocity measurements for each case with the VFDP.*

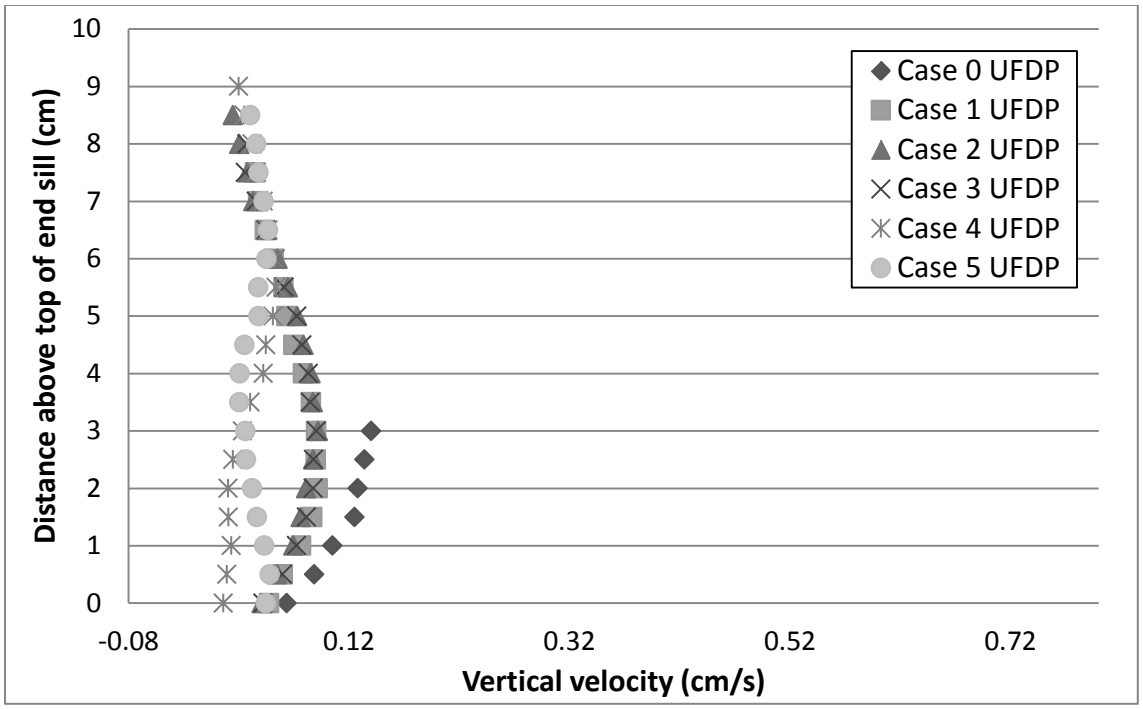

Figure 3.49. *Vertical velocity measurements for the UFDP.*

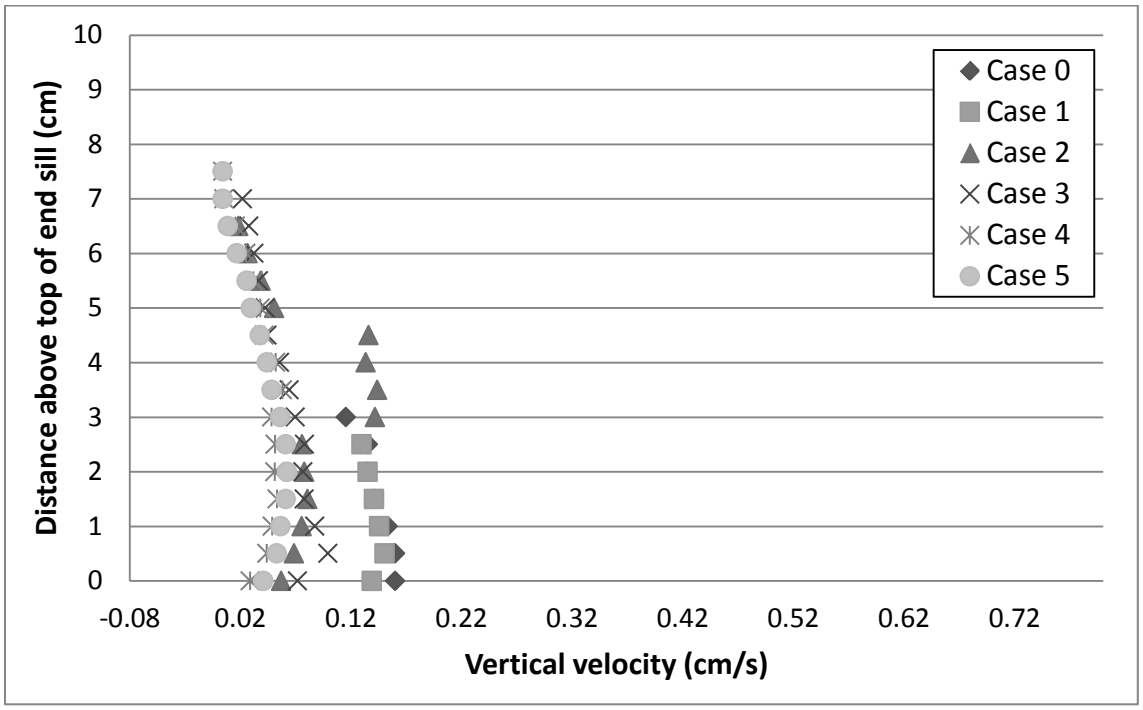

Figure 3.50. *Vertical velocity measurements for the VFDP.*

Figures 3.51 and 3.52 reflect the turbulence intensities in the x-direction for the UFDP and VFDP, respectively. The two diffusers appear to have an opposite effects on the turbulence. In the cases tested with the UFDP, higher turbulence values are witnessed in the cases of more air injection. However, with the VFDP, higher turbulence values are observed in the cases with less or no air injection. It is theorized that in the cases involving the UFDP, the air causes a backwater effect on the flow but increases turbulence and, hence, scour. However, with the VFDP the air is injected as the flow is exiting the structure which reduces turbulence.

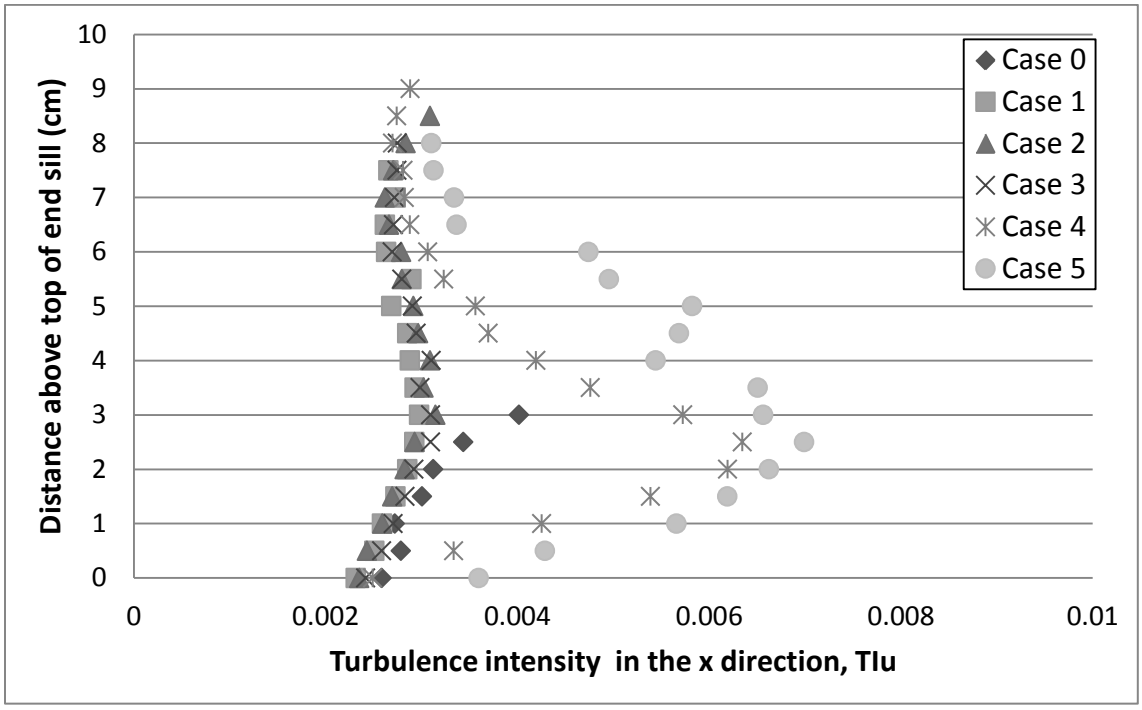

Figure 3.51.*Turbulence intensity in x direction for the UFDP.*

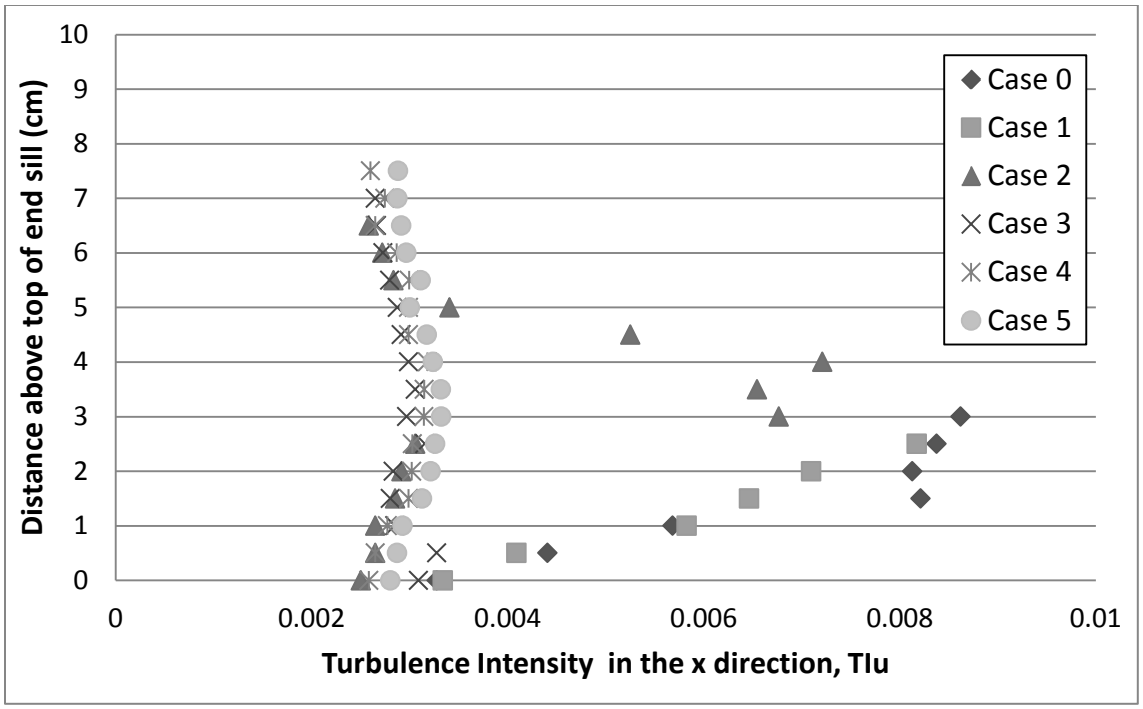

Figure 3.52. *Turbulence intensity in x direction for the VFDP.*

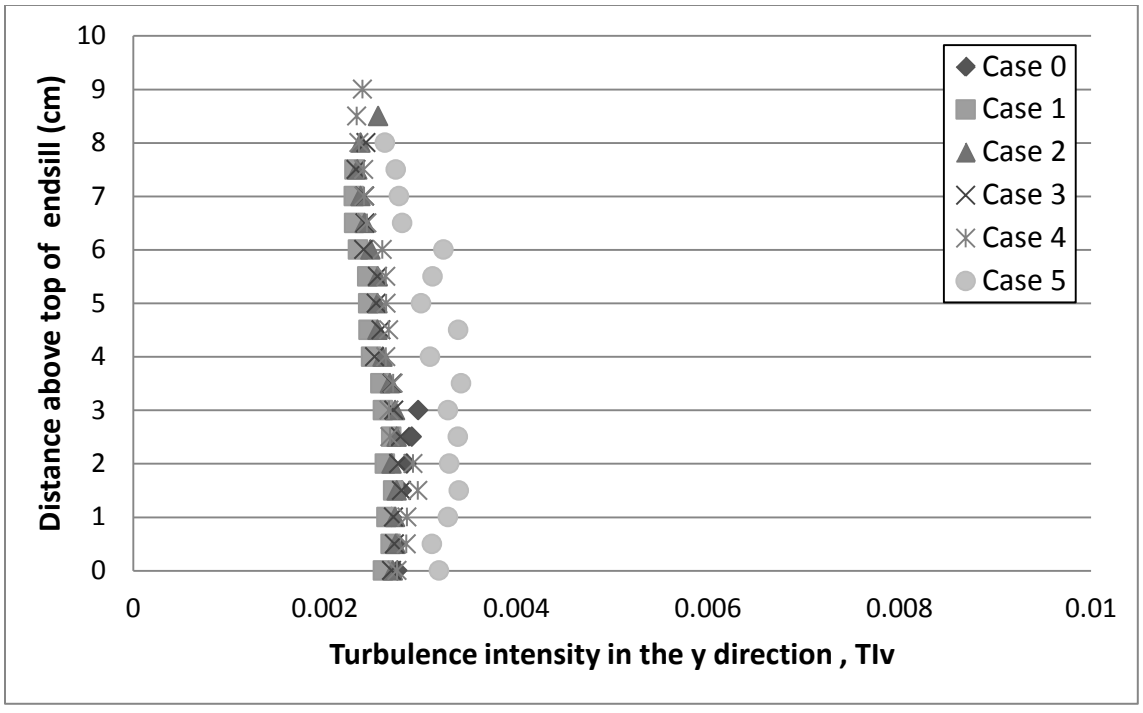

Figure 3.53. *Turbulence intensity in the y direction (transverse) for the UFDP.*

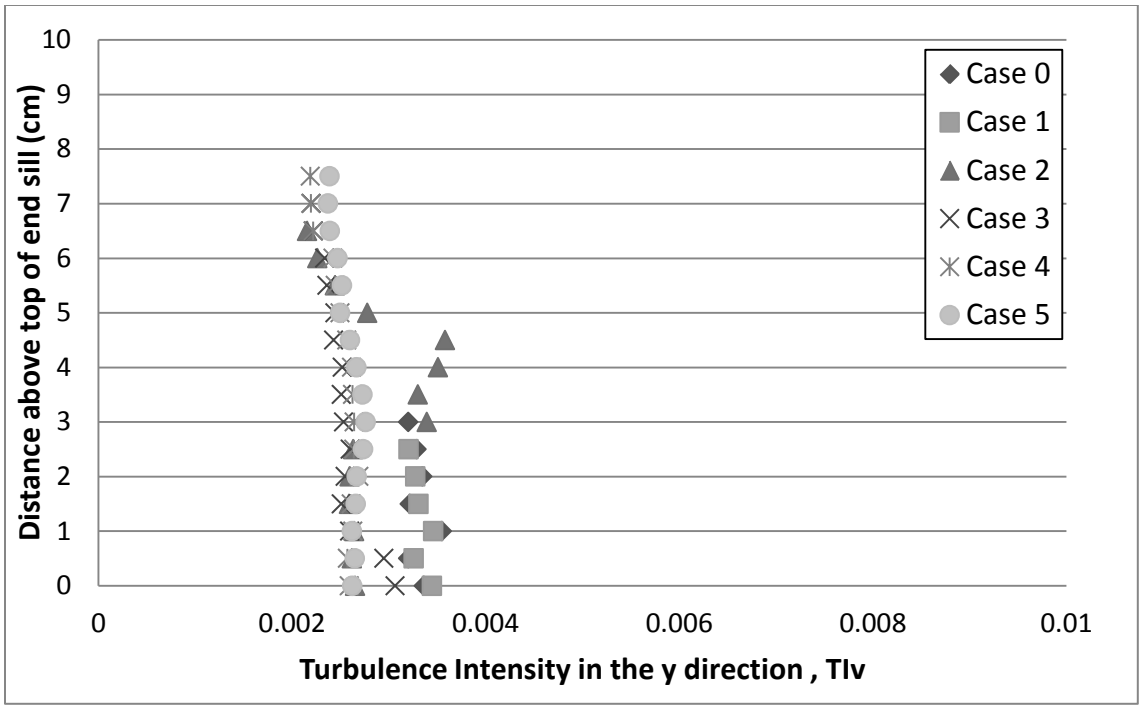

Figure 3.54. *Turbulence intensity in the y direction (transverse) for the VFDP.*

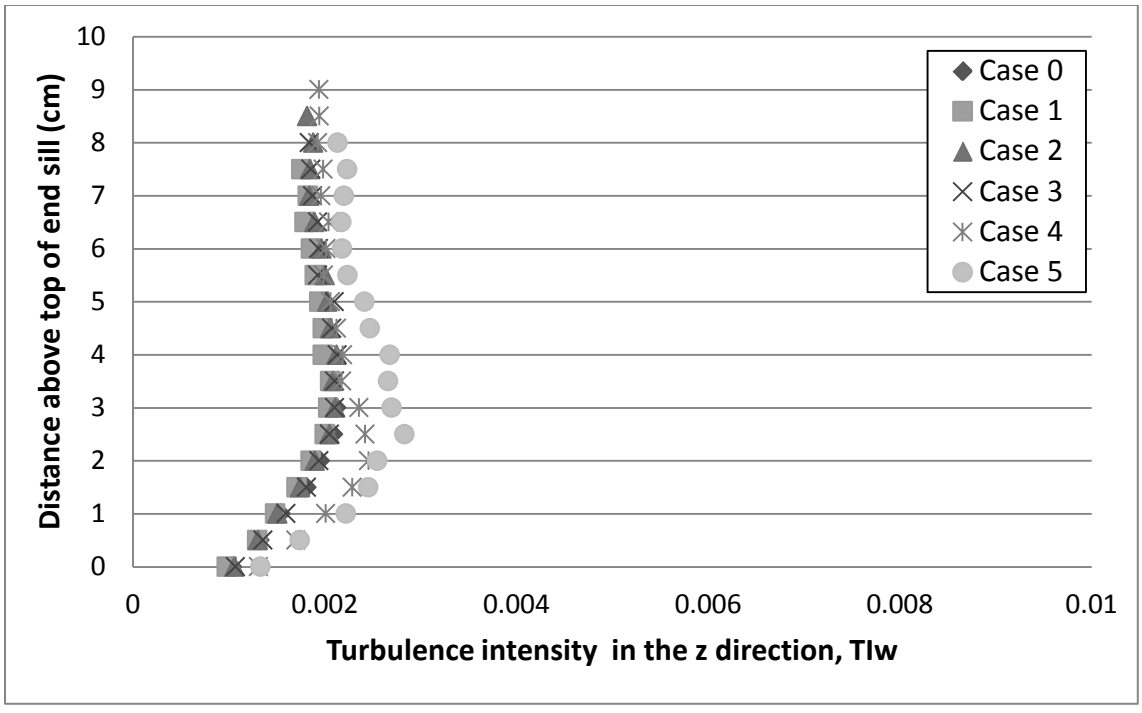

Figure 3.55. *Turbulence intensity in the z direction (vertical) for the UFDP.*

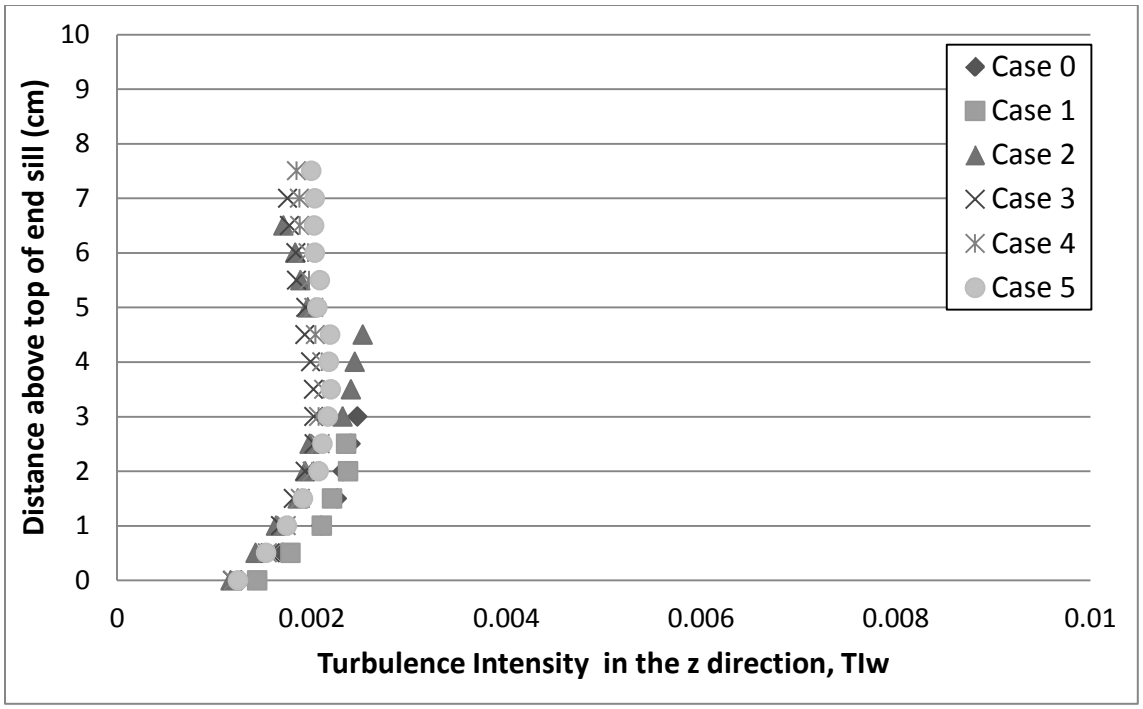

Figure 3.56. *Turbulence intensity in the z direction (vertical) for the VFDP.*

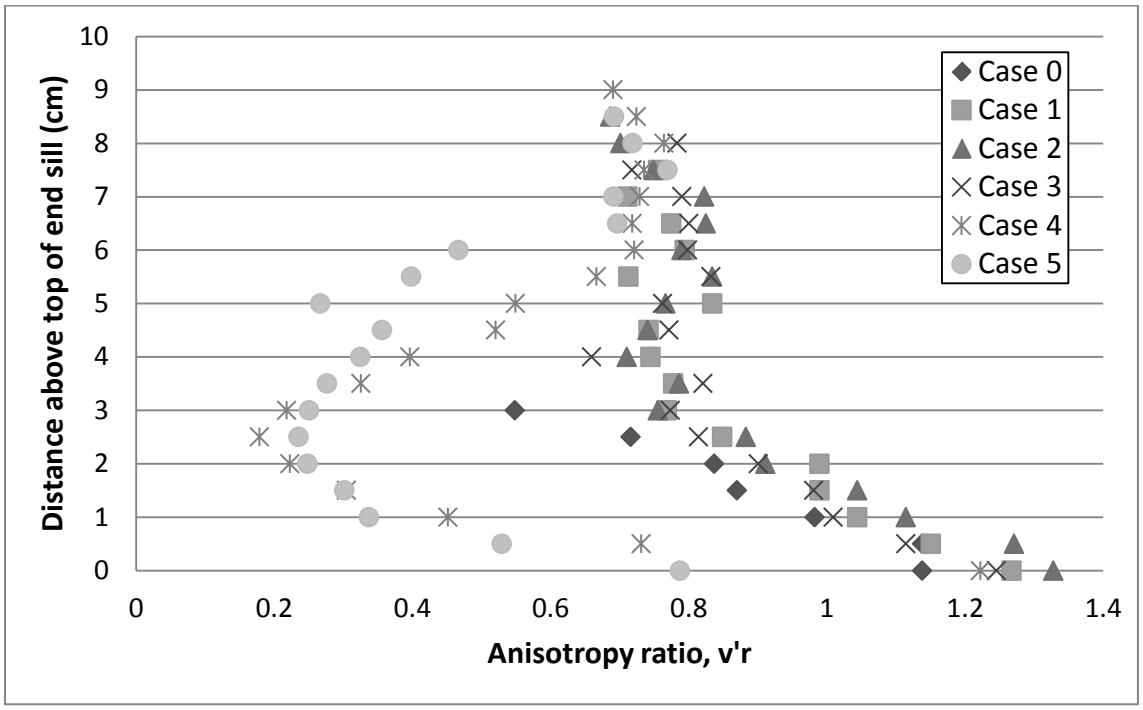

Figure 3.57. *Anisotropy ratio with respect to the v-component (transverse) for the UFDP*

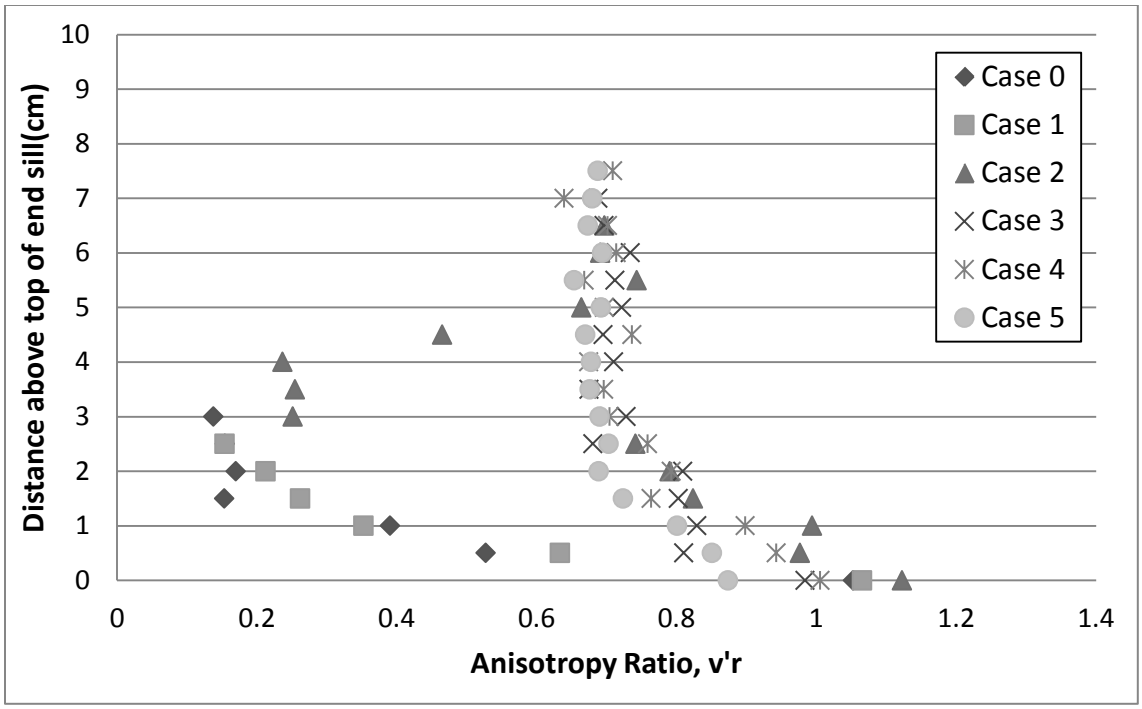

Figure 3.58. *Anisotropy ratio with respect to the v-component (transverse) for the VFDP*

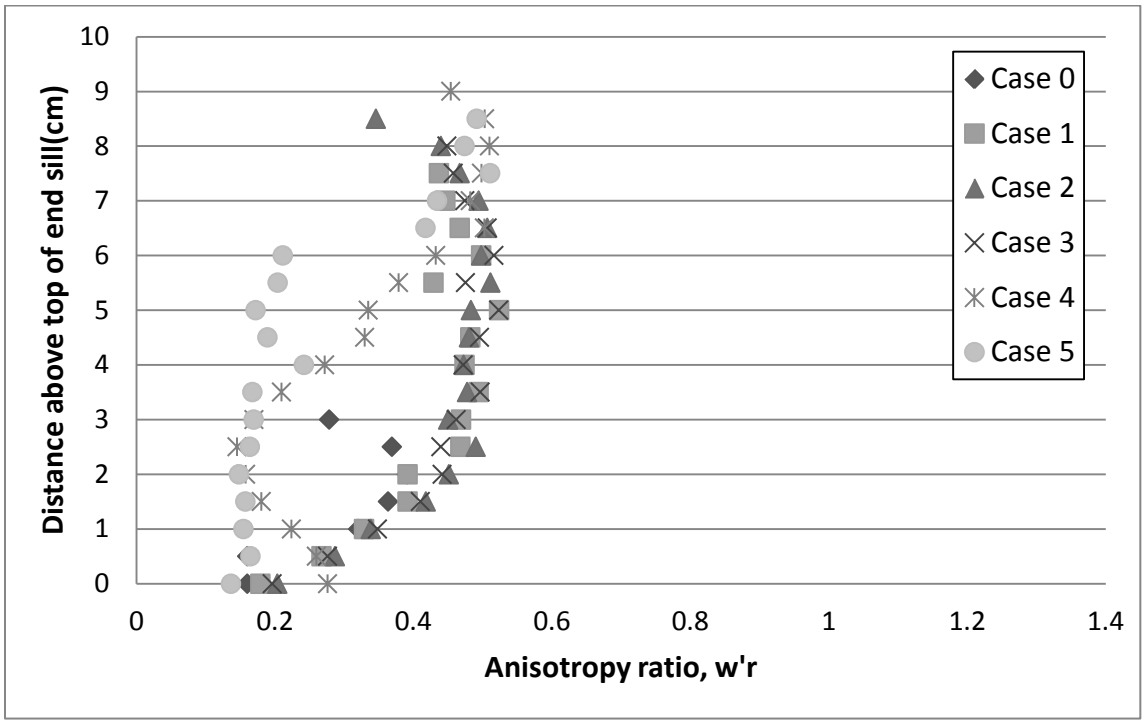

Figure 3.59. *Anisotropy ratio with respect to the w-component (vertical) for the UFDP.*

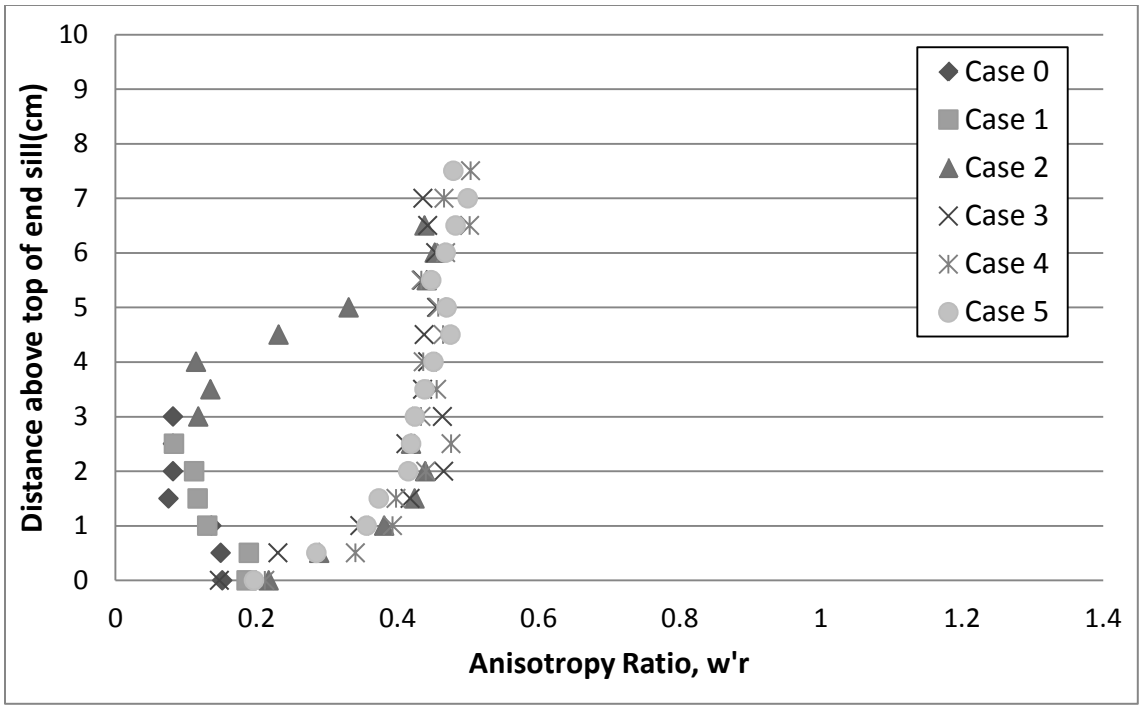

Figure 3.60. ***Anisotropy ratio with respect to the w-component (vertical) for the VFDP.***

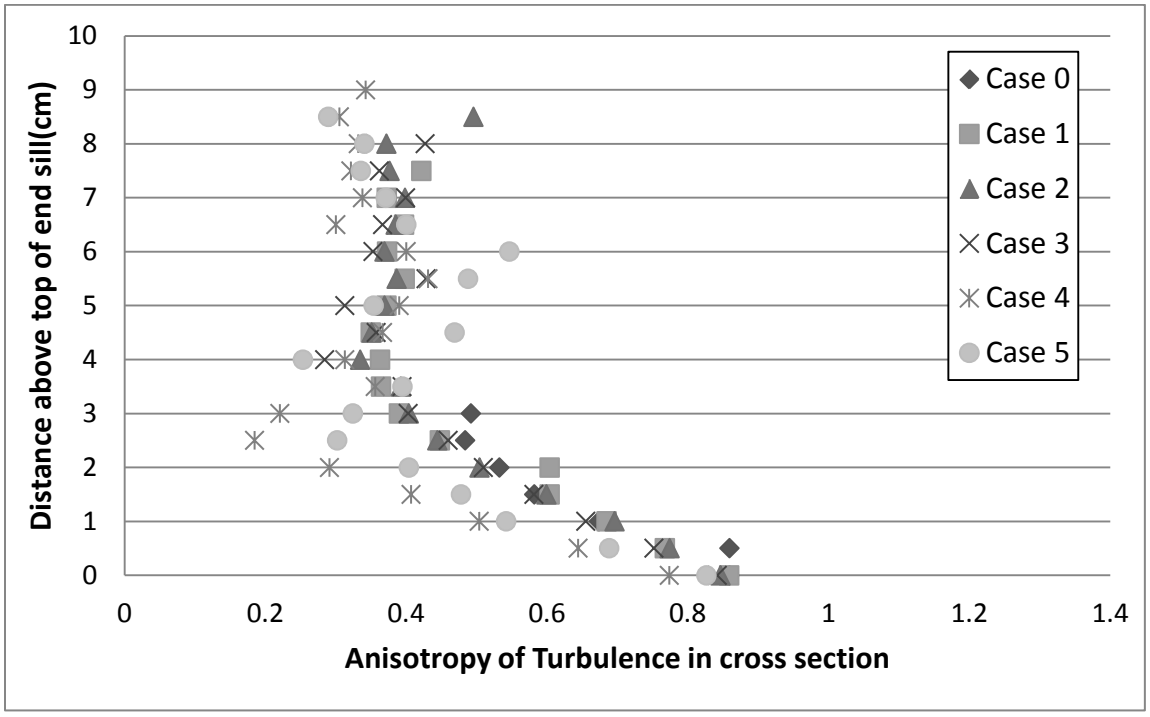

Figure 3.61. *Anisotropy of turbulence in cross section for the UFDP.*

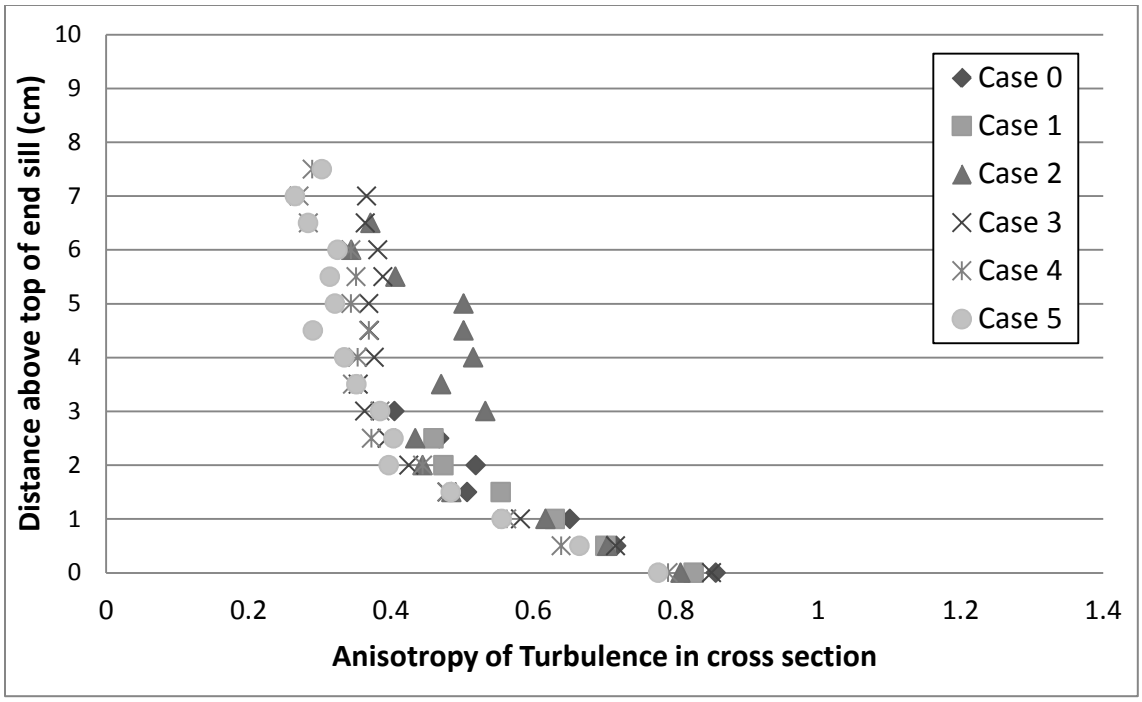

Figure 3.62. *Anisotropy of turbulence in cross section for the VFDP.*

3.4 Conclusions

From the experiments described here it can be seen that increasing the spatial extent (number of rows of holes in the 2D diffuser):

1. Increases the stilling basin flow depth but not enough to affect the flow depth upstream of the stilling basin.
2. Increases the amount of bubbles
3. Decreases the scour depth both near and away from the stilling basin
4. Decreases the streamwise exit velocity
5. Decreases streamwise exit turbulence
6. Decreases streamwise exit turbulence anisotropy.

Increasing the spatial extent of diffuser holes decreases scour but requires an accompanying air flow rate. There is only a marginal gain in scour reduction, however, past one row of holes. The Vertical-Facing Diffuser Plate reduced scour volume more than the Upstream-Facing Diffuser Plate for all conditions tested.

These conclusions lead to the following understanding of the role of air injection on scour: air injection causes a backwater effect on the exiting flow thereby raising the flow depth and consequently retarding the exit velocity, turbulence, and turbulence anisotropy. These combine to reduce the amount of exiting flow energy and therefore, scour depth.

This effect is exacerbated by the Vertical-Facing Diffuser Plate due to the closer proximity of the air injection location to the stilling basin exit which organizes the bubbles nearer to the water surface as seen more so than the Upstream-Facing Diffuser Plate (Barkdoll and Barlock 2011).

To relate back to the large-scale problem at the S65E gate, it was estimated that a safe depth of scour is that which leaves remaining sediment at a height greater than half of the total structure height. It is assumed that the air injection would not be running at normal conditions, but only when heavy rainfall causes high flow rates, threatening the structure. This study simply proves that air injection does reduce scour; it does not focus on implementation. The optimal value of air injection ratio for maximum scour reduction was found by Champagne (2011) to be $Q_{air}/Q_{water}=0.28$.

CHAPTER 4: FLAT EXTENSION PLATE

After the air diffuser experiments were completed, it was observed that with the rectangular diffuser that extended from the end sill, the volume of scoured sediment was reduced even without air injection. This lead to the hypothesis that a flat plate extending from the end sill would reduce scour. This solution would be much less energy intensive by not requiring compressed air.

4.1 Experimental Design

A set of experiments was performed in order to determine how introducing a flat plate extending from the existing end sill top would affect scour downstream of the control structure. Ten different plate lengths were tested, shown below in Table 4.1.

Table 4.1. *Plate lengths tested in extension plate study.*

Plate Length (cm)	Case Number
0	1
8	2
16	3
24	4
32	5
40	6
48	7
56	8
64	9
72	10

Each of the plates was created using pieces of acrylic that extended from the base of the end sill. Each plate had supporting side walls that prevented water from escaping over the sides of the plate, ensuring that the total flow was exiting at the end of the plate (Figure 4.1).

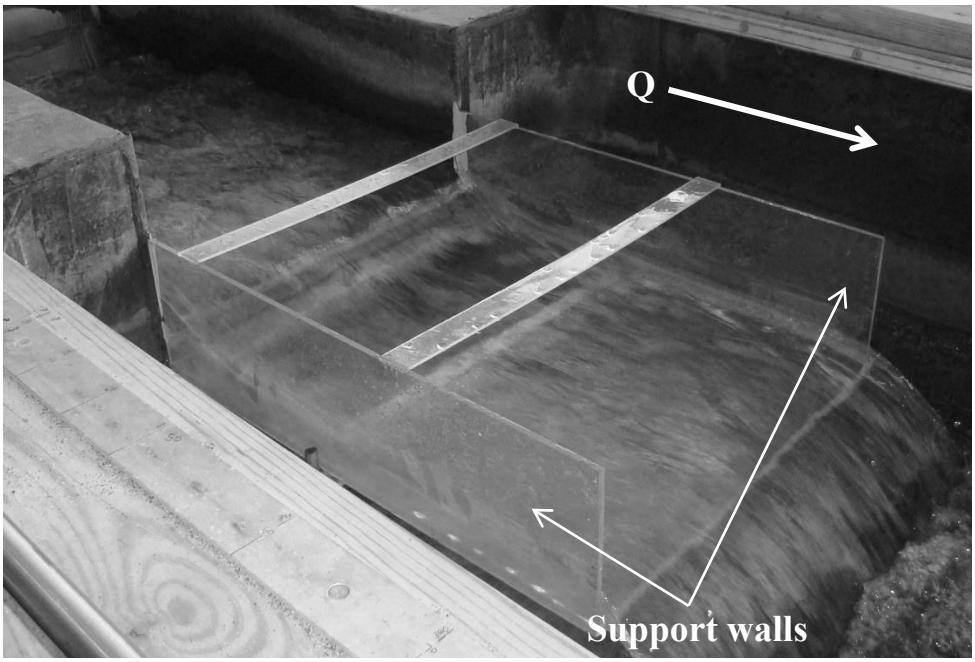

Figure 4.1. *Extension plate (Lp=56cm) showing support walls.*

The discharge wwas chosen to ensure that the scour hole did not encroach on the downstream end of the scour chamber. This reduced water discharge corresponded to the design discharge for Gate S65E as shown by the following. The discharge in the model was 0.023 cms, and the scale was 1:30. The design discharge that the S65E structure was designed to pass safely was 680 cms. Only one of the six gates on the gated spillway was modeled, however, so the design flow in the laboratory is 680 cms divided by the six gates, which is 113 cms.

Assuming that the Froude Number of the model equals that of the prototype, $F_m = F_p$ it can be shown that $Q_m = \left(\frac{1}{30}\right)^{5.2} * Q_p = 0.023\ cms$, which happens to match the design flow exactly.

Therefore the discharge used in the experiments corresponded exactly to the prototype design discharge.

4.2 Experimental Procedure

For each experiment, the sediment was leveled in the scour section of the flume to the top of the stilling basin end sill. Next, the flume was filled with water to the desired flow depth, and the pump was turned on to the desired flow rate. The air flow was then turned on to the desired flow rate. Adjustments were made, if necessary, to the flow depth. The scour was measured in a location of expected deep scour with time until equilibrium was

reached. Equilibrium was determined by scour measurements collected by the ADV when the scour depth changed less than 0.5 percent in a two-hour period. Once it was determined that equilibrium had been reached, the water surface profile was measured and photos and videos were taken. Next, the flow was stopped, and the scour chamber was drained. Finally, the bed profile was measured manually using the point gauge. It took approximately two hours to set up the experiment, 12-14 hours for the experiment to reach equilibrium, and four hours to take the measurements. One case could be completed in about two days.

4.3 Results

4.3.1 Water Surface Profile

The water surface profiles for all ten plate lengths are shown in Figure 4.2. Water surface elevations were measured on the centerline of the flume. The water surface elevation at the end sill increases with plate length, as is shown Figure 4.3. However, in every case, the water surface elevation was unchanged upstream of the spillway crest.

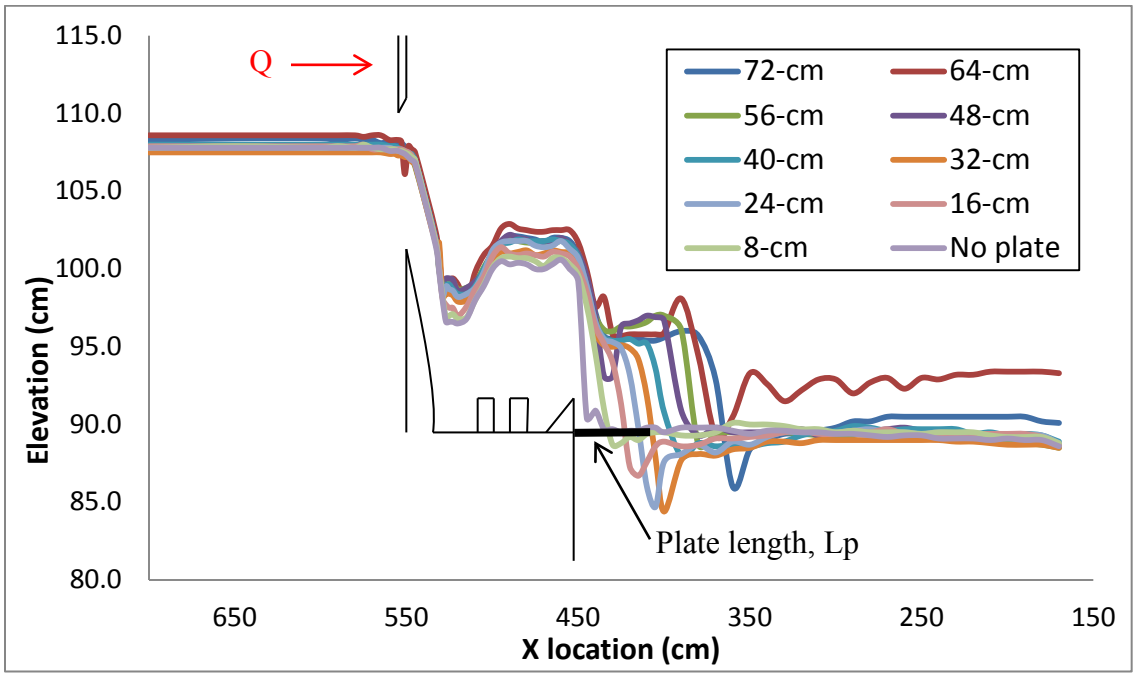

Figure 4.2. *Water surface profile for all ten plate lengths.*

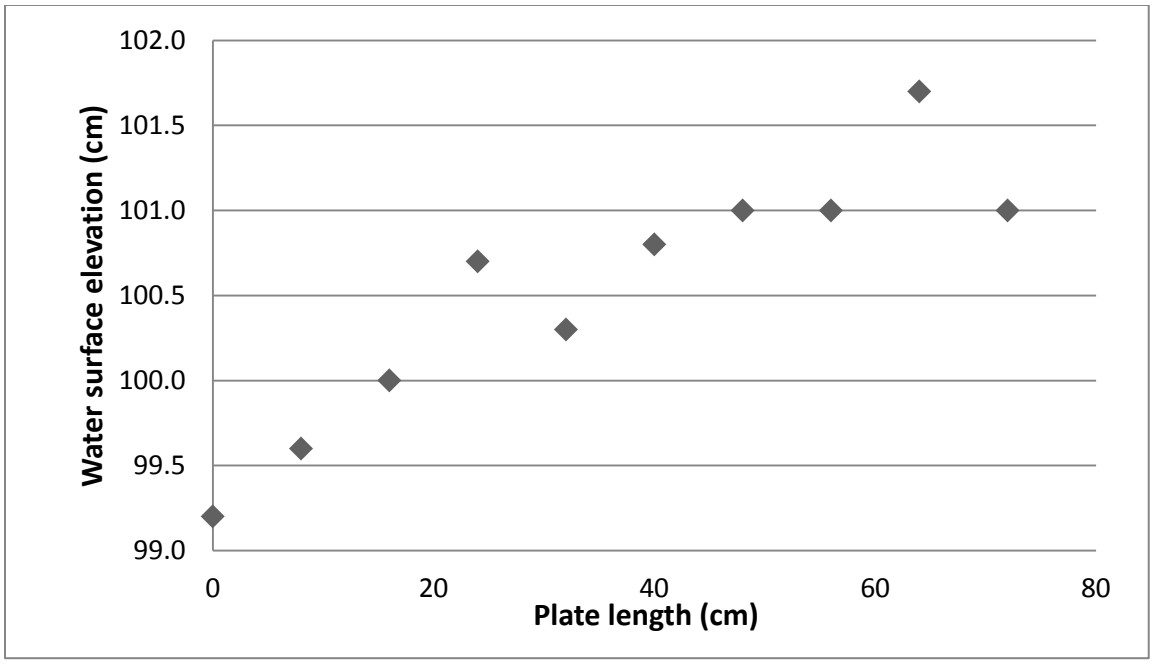

Figure 4.3. *Water surface elevation (WSE) at end sill for each plate length. Refer to Figure 4.4 for sampling location.*

In Figure 4.3, it appears that the data points for the 32-cm and 64-cm plates do not follow the trend of the rest of the plate lengths. The most likely cause for this inconsistency is human error. The water surface profiles were measured with the point gauge manually. Because the water is flowing while this measurement is taken, the water level is constantly fluctuating, making it difficult to get an exact reading.

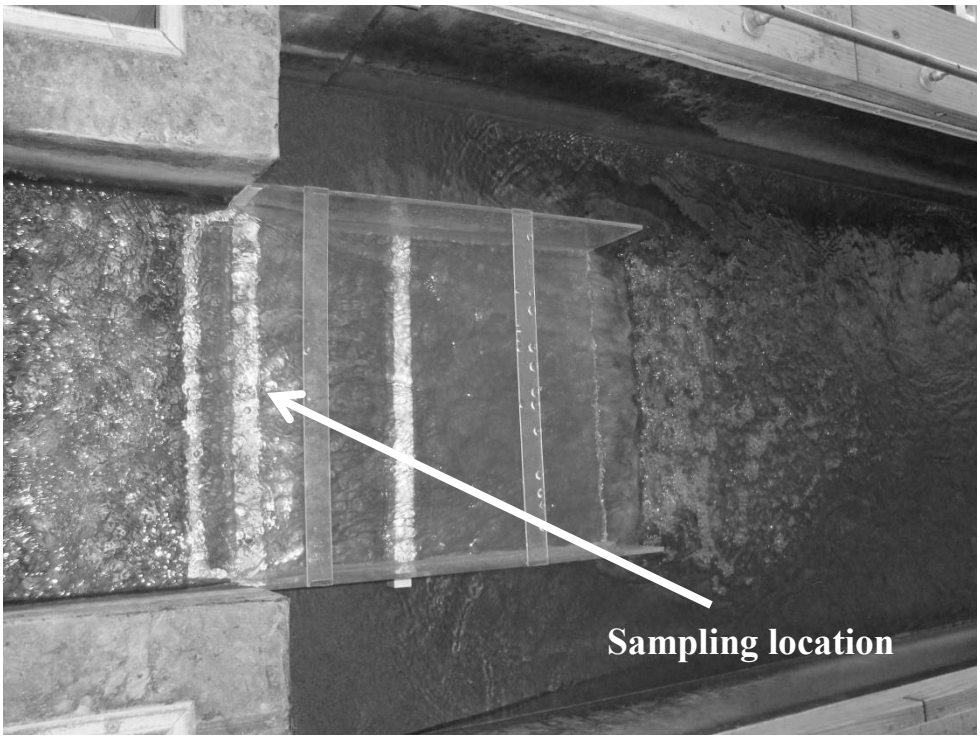

Figure 4.4. *Sampling location for WSE data points shown in Figure 4.3. Location was the same for each plate length, (Lp=56cm in this figure).*

Figure 4.4 shows a support that hangs from the sides of the flume, while the previous plates had a support buried in the sand below the flume. It was assumed that neither of these supports affected the flow or scour.

Figures 4.5-4.14 show photographs of water exiting the stilling basin and flowing over the plate for each of the ten experimental cases.

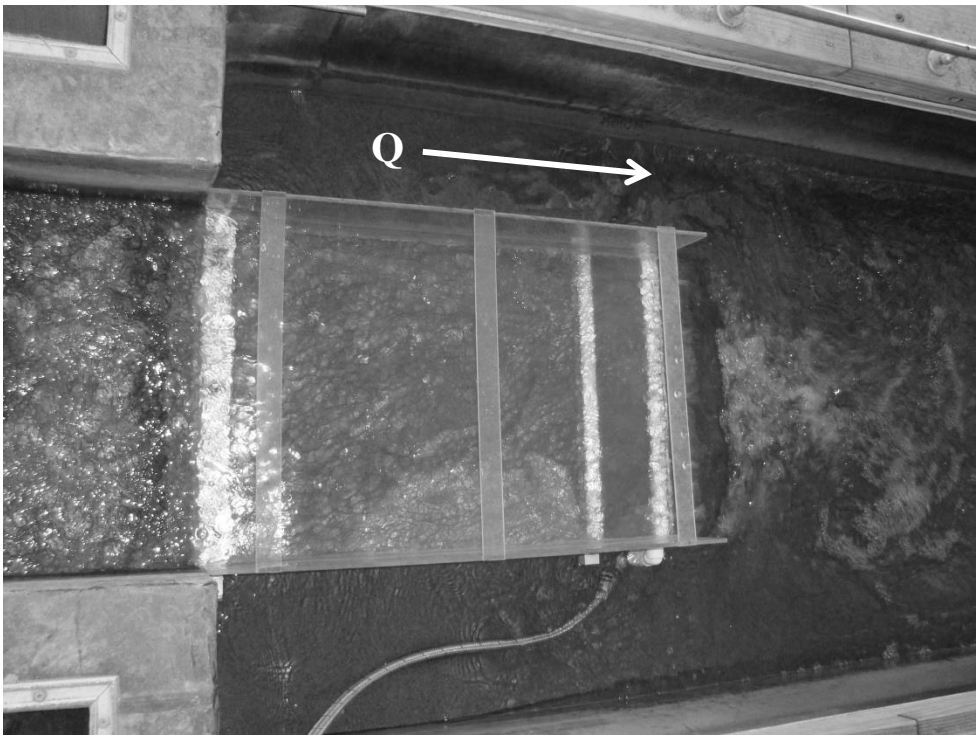

Figure 4.5. *Water surface photo with 72-cm plate.*

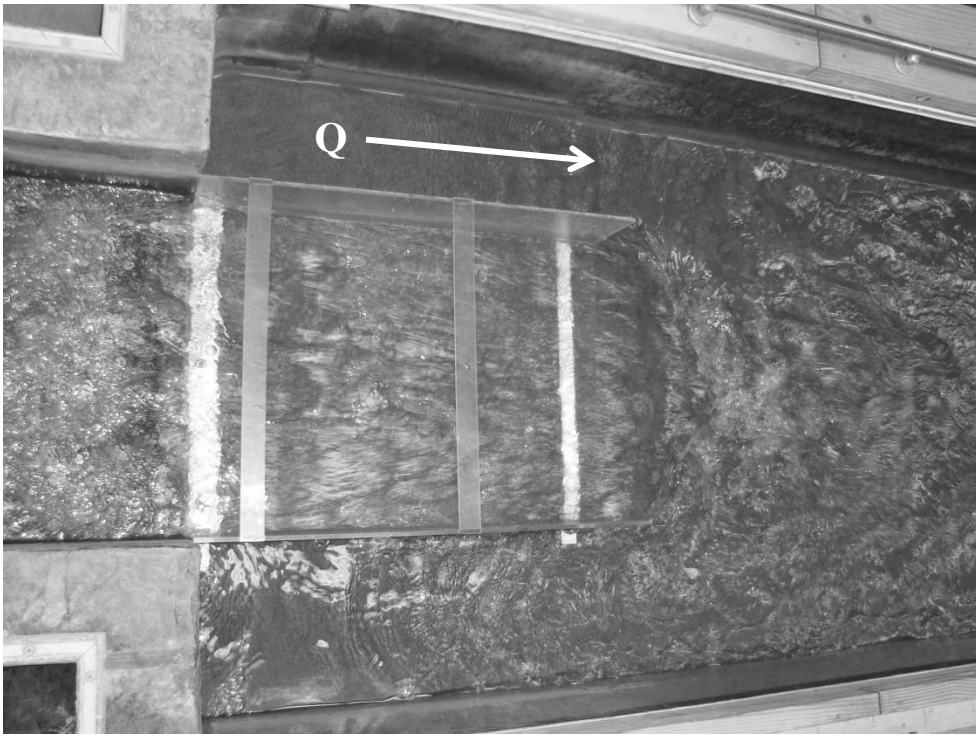

Figure 4.6. *Water surface photo with 64-cm plate.*

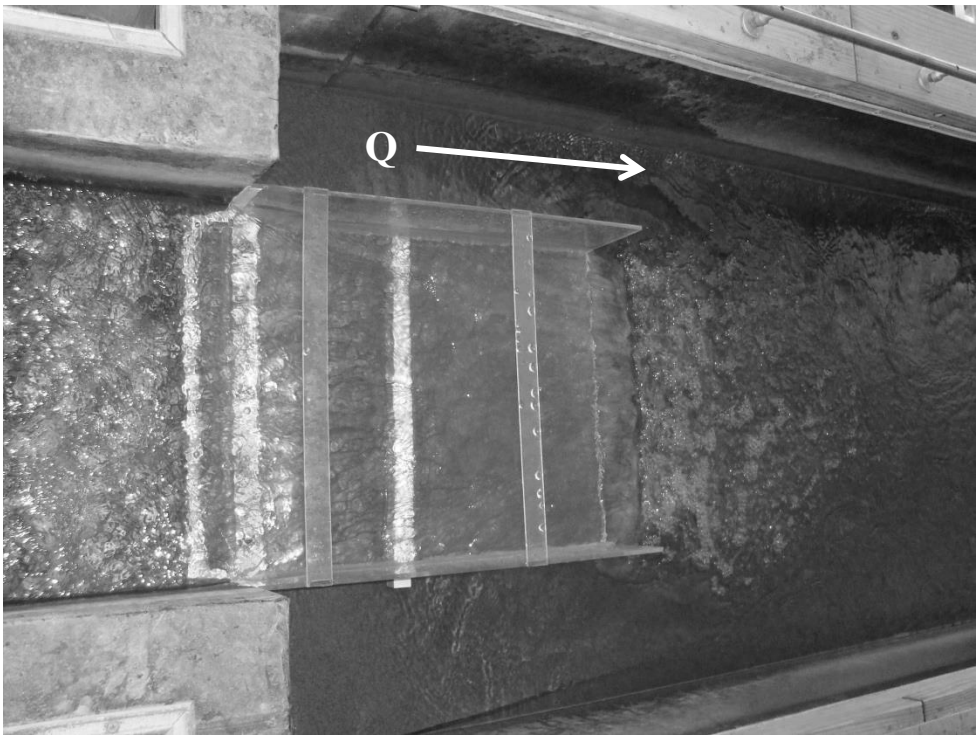

Figure 4.7. *Water surface photo with 56-cm plate.*

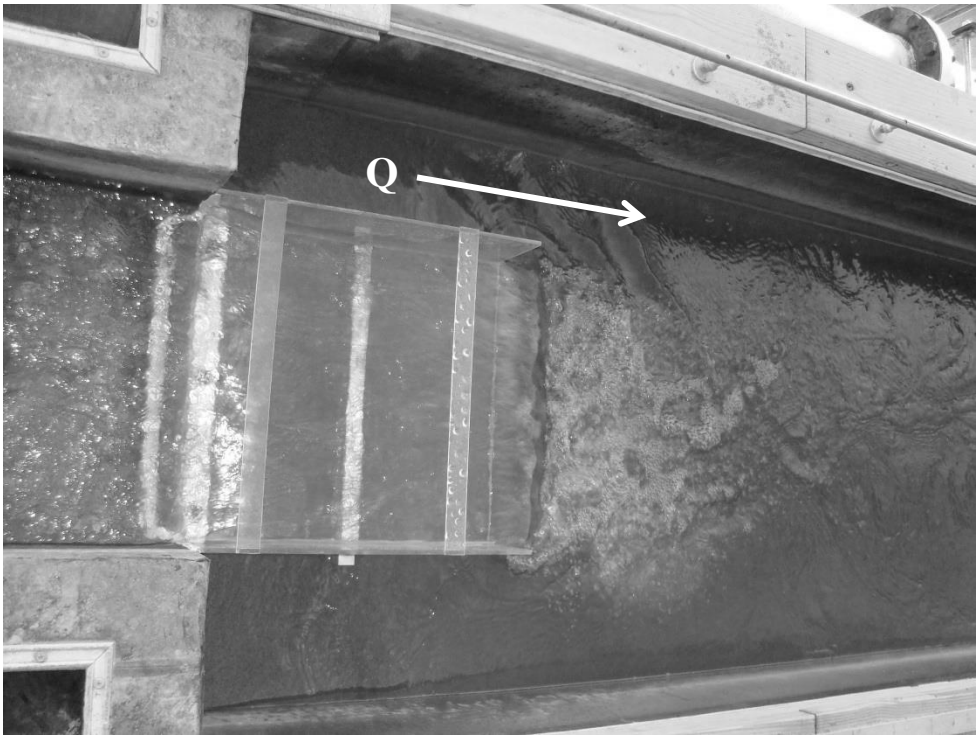

Figure 4.8. *Water surface photo with 48-cm plate.*

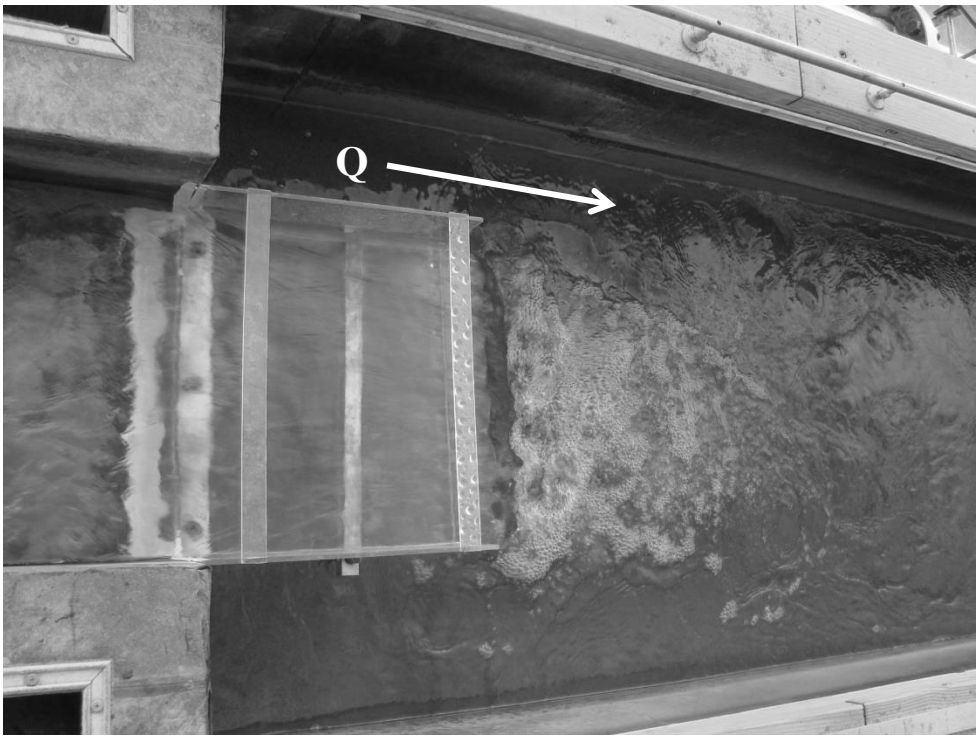

Figure 4.9. *Water surface photo with 40-cm plate.*

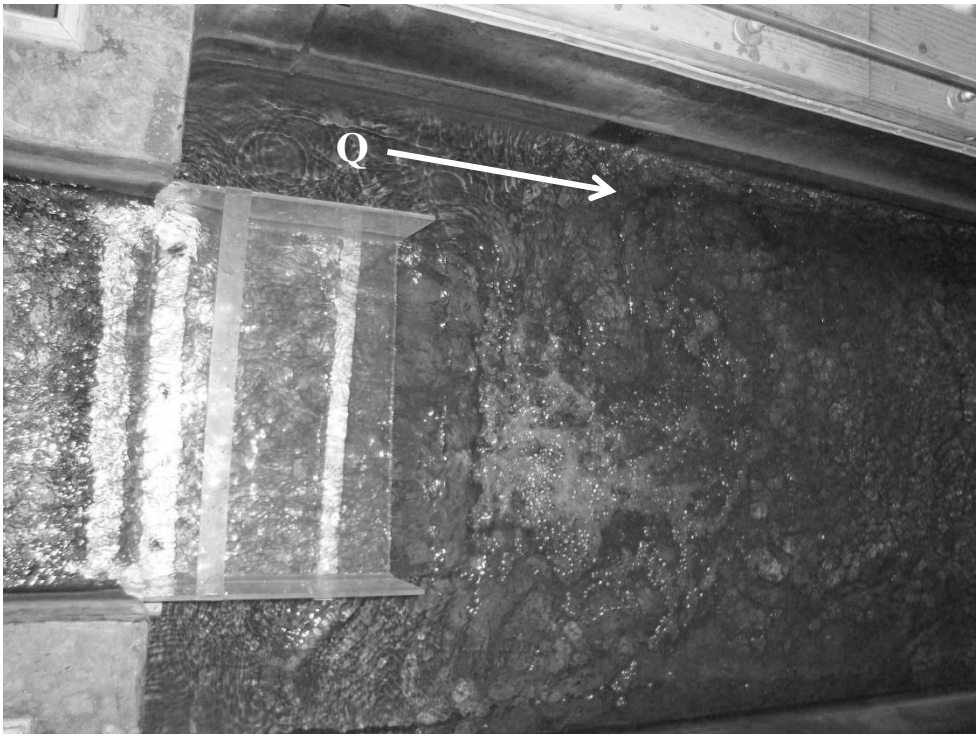

Figure 4.10. *Water surface photo with 32-cm plate.*

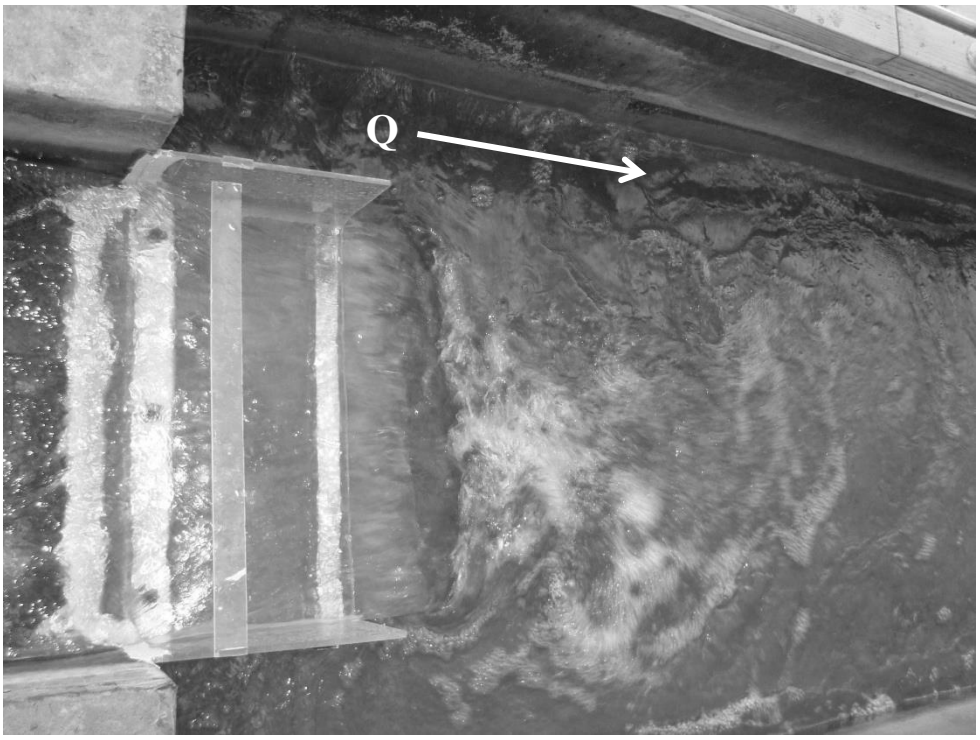

Figure 4.11. *Water surface photo with 24-cm plate.*

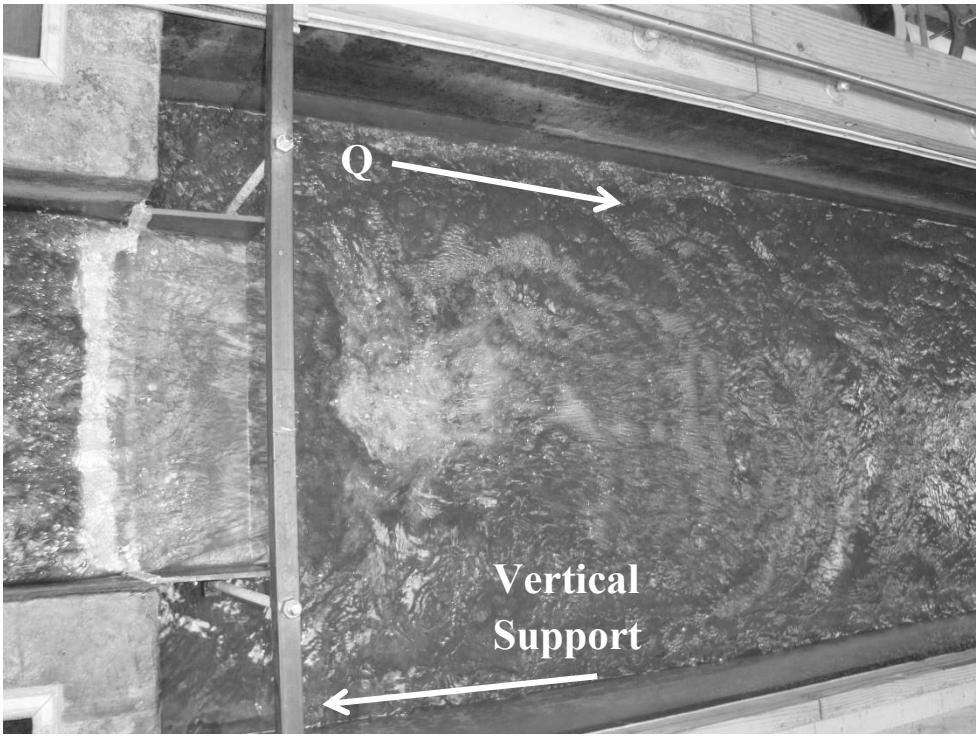

Figure 4.12. ***Water surface photo with 16-cm plate.***

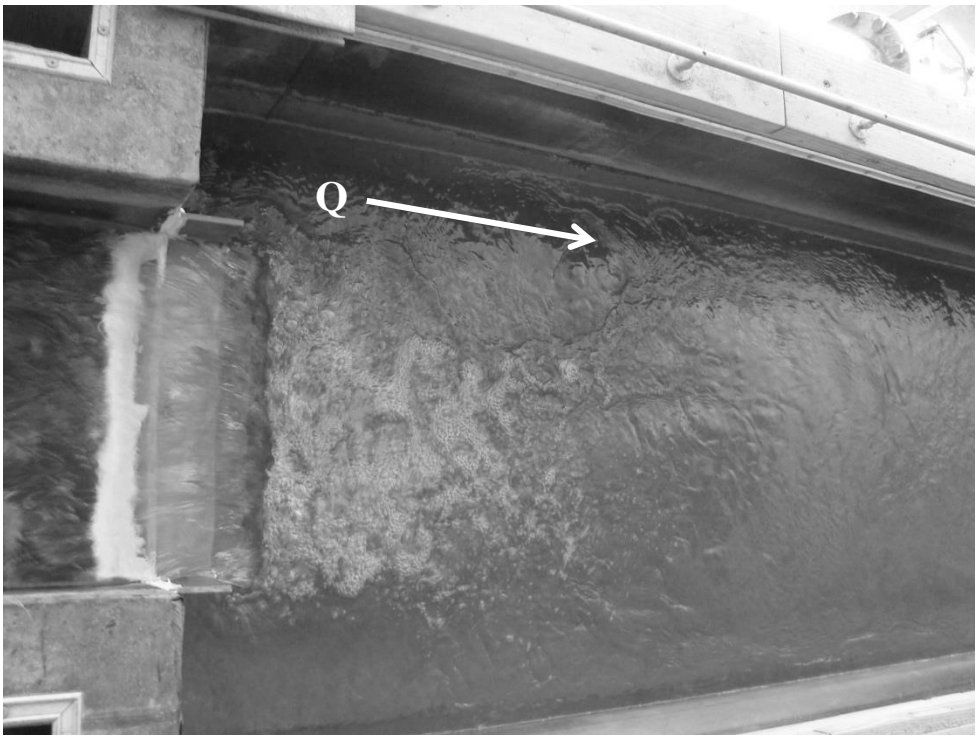

Figure 4.13. *Water surface photo with 8-cm plate.*

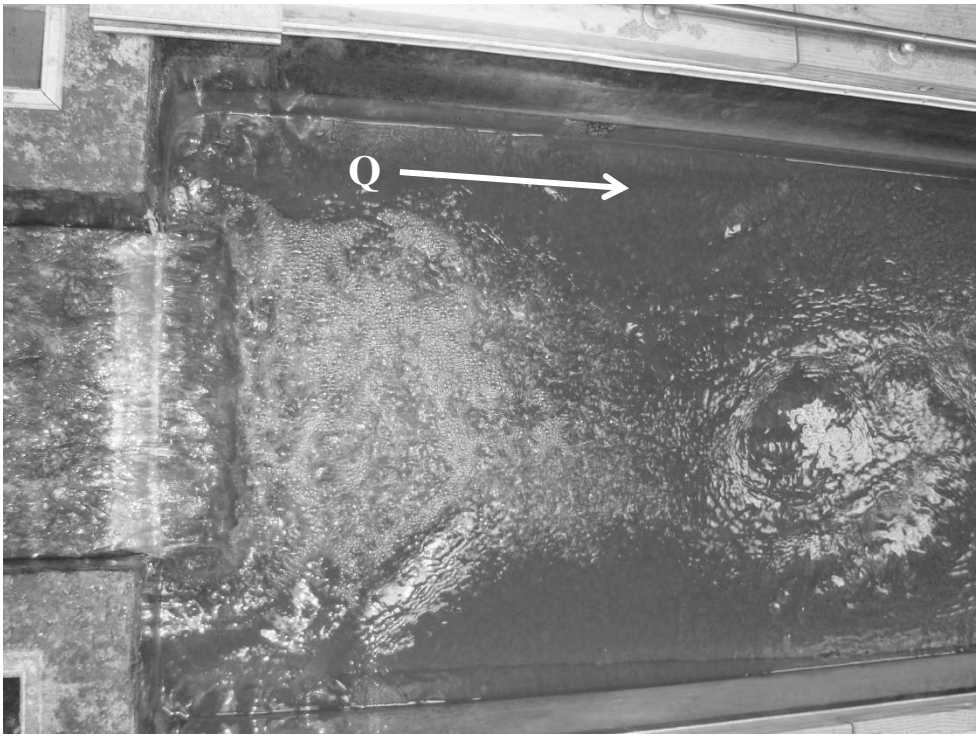

Figure 4.14. *Water surface photo with no plate.*

4.3.2 Scour Conditions

Contour plots for each plate length are shown in Figures 4.15 through 4.24. The scour patterns for some air cases are made up of lobes on either side of the major scour hole, while in others, there is only the main scour hole. The case with no plate has the largest scour hole closest to the structure. Increasing plate lengths push the deepest point of scour further downstream, which is illustrated in Figure 4.25. Plate lengths of 72, 64, 32, 24, and 16 cm decreased the volume of scour, while the remaining plate lengths scoured into a steeply-sloped scour hole. For those steeply-sloped holes, the location of deepest scour was further downstream with increasing plate lengths. Figure 4.26 illustrates the aforementioned pattern with the centerline bed profiles for each plate length.

Photographs of the bed after reaching equilibrium are shown in Figures 4.27 through 4.36. These photos show dunes forming upstream and on either side of the scour hole. These dunes are caused by the water flow separating into up- and downstream components as they make contact with the bed.

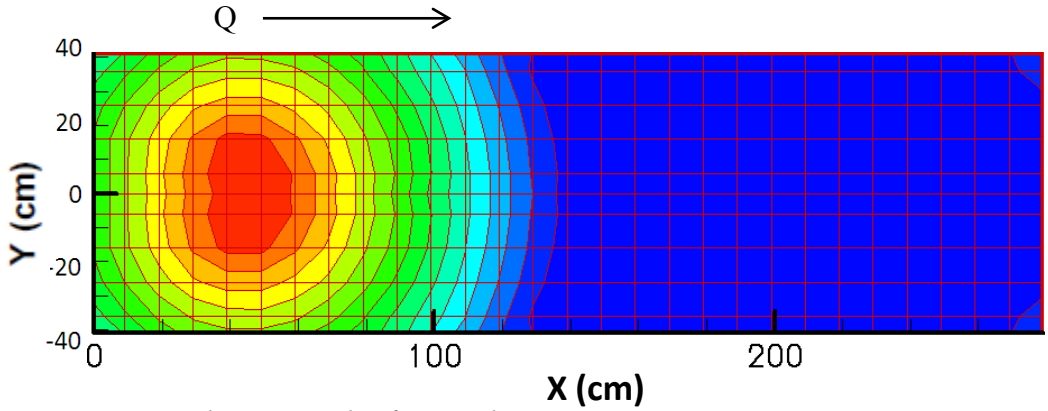

Figure 4.15. *Bed contour plot for no plate extension.*

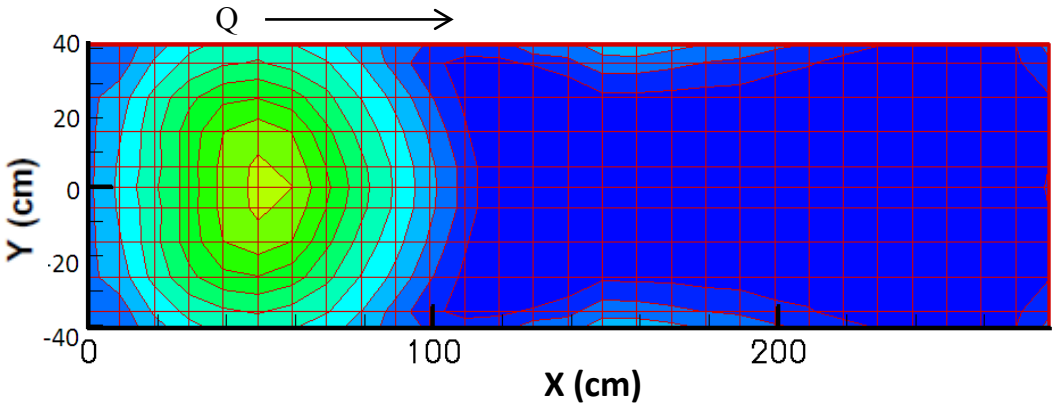

Figure 4.16. *Bed contour plot for 8-cm plate extension.*

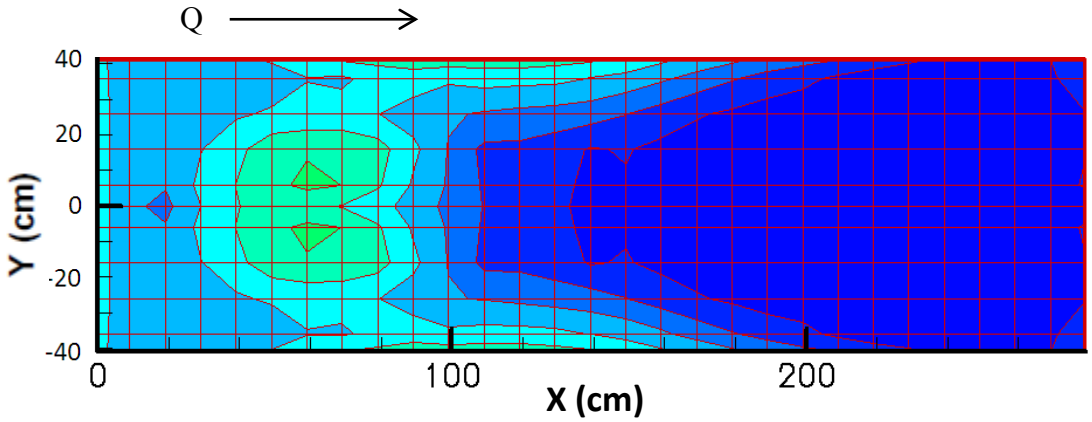

Figure 4.17. *Bed contour plot for 16-cm plate extension.*

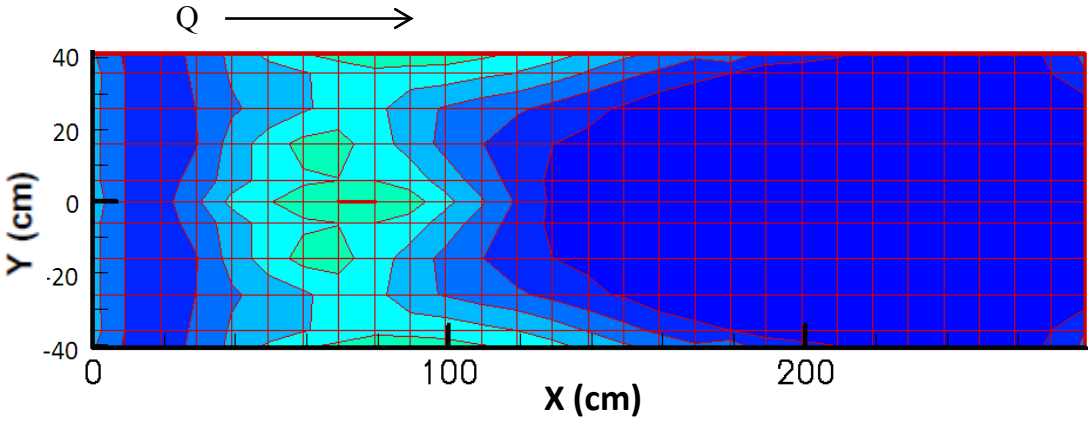

Figure 4.18. *Bed contour plot for 24-cm plate extension.*

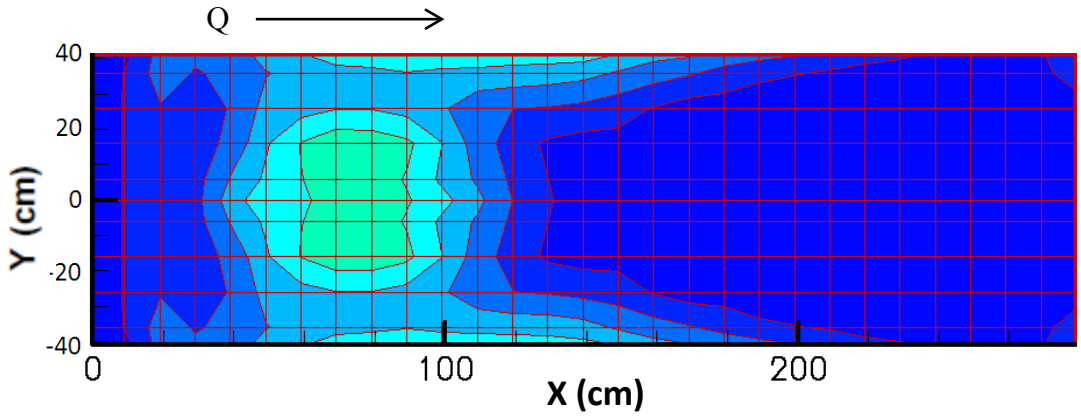

Figure 4.19. *Bed contour plot for 32-cm plate extension.*

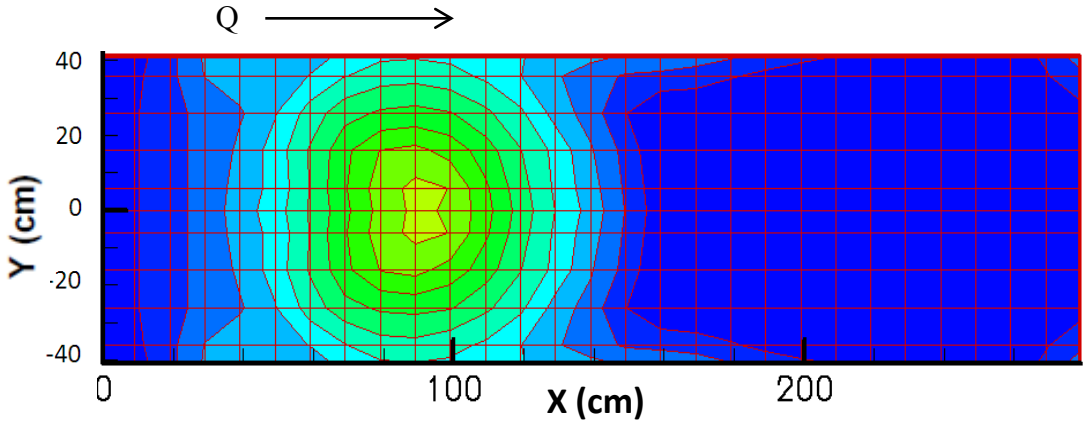

Figure 4.20. *Bed contour plot for 40-cm plate extension.*

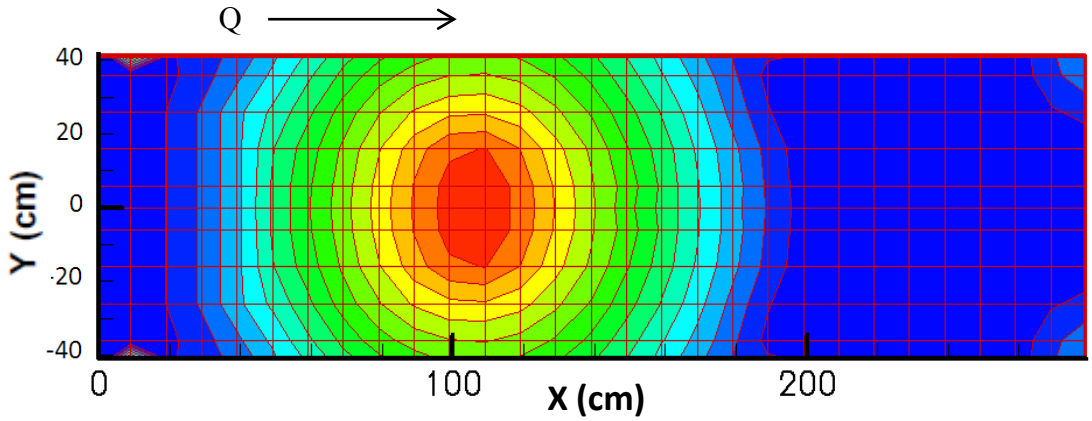

Figure 4.21. *Bed contour plot for 48-cm plate extension.*

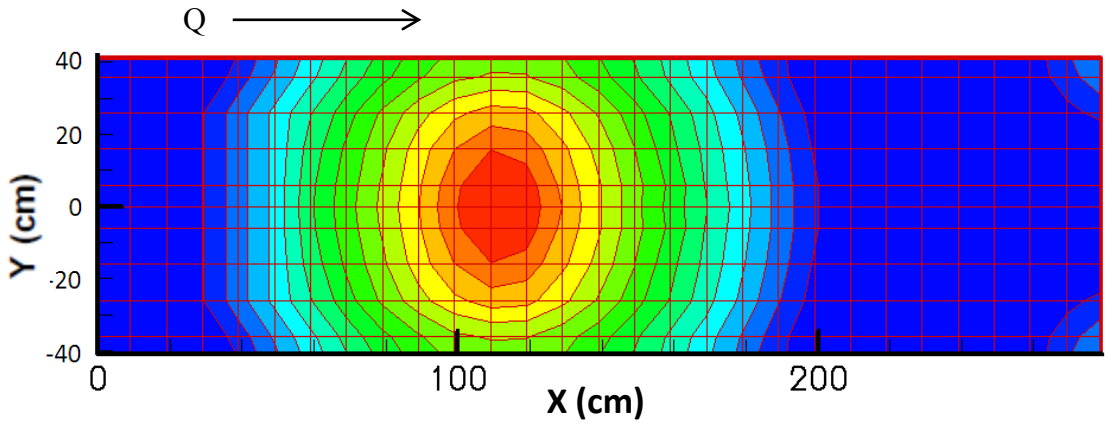

Figure 4.22. *Bed contour plot for 56-cm plate extension.*

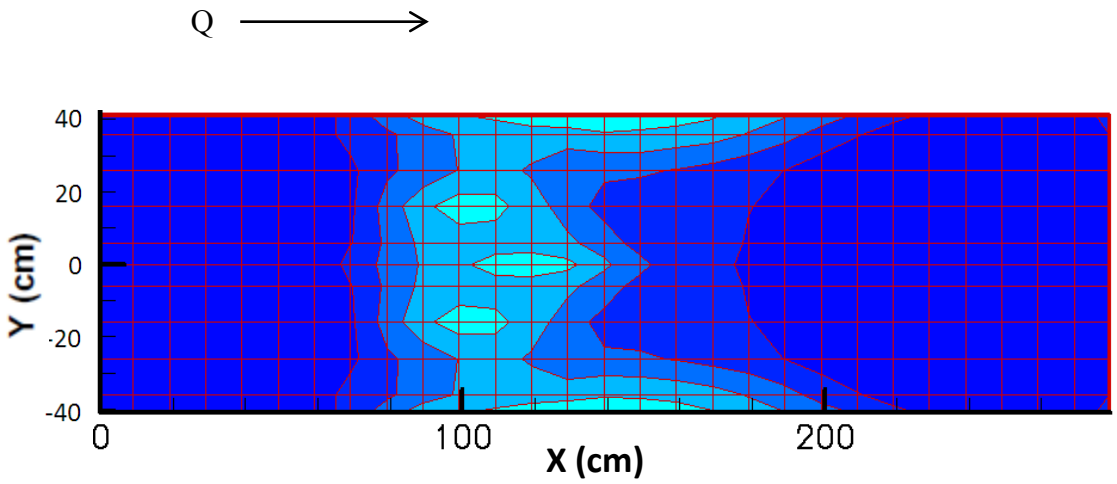

Figure 4.23. *Bed contour plot for 64-cm plate extension.*

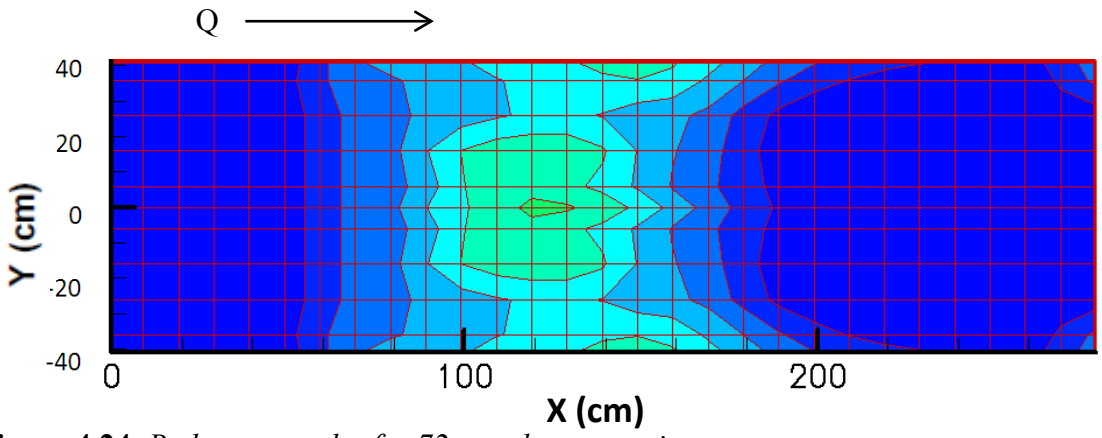

Figure 4.24. *Bed contour plot for 72-cm plate extension.*

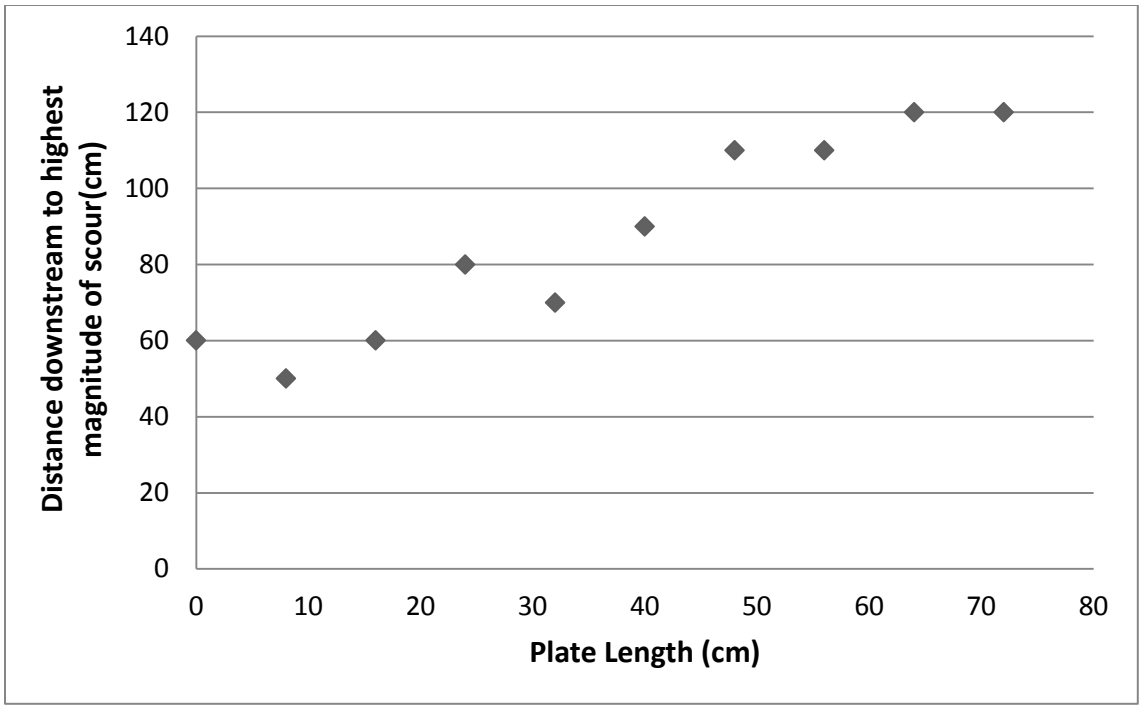

Figure 4.25. *Distance downstream along centerline to point of worst scour for each plate length.*

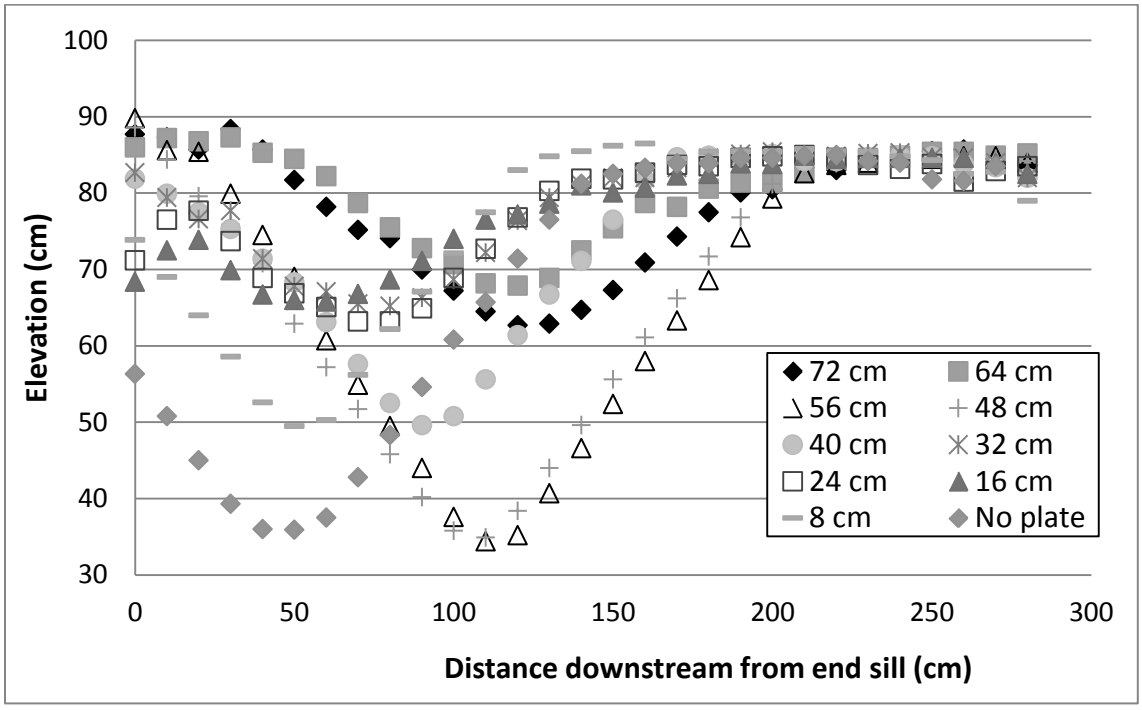

Figure 4.26. *Centerline bed profiles for each plate length.*

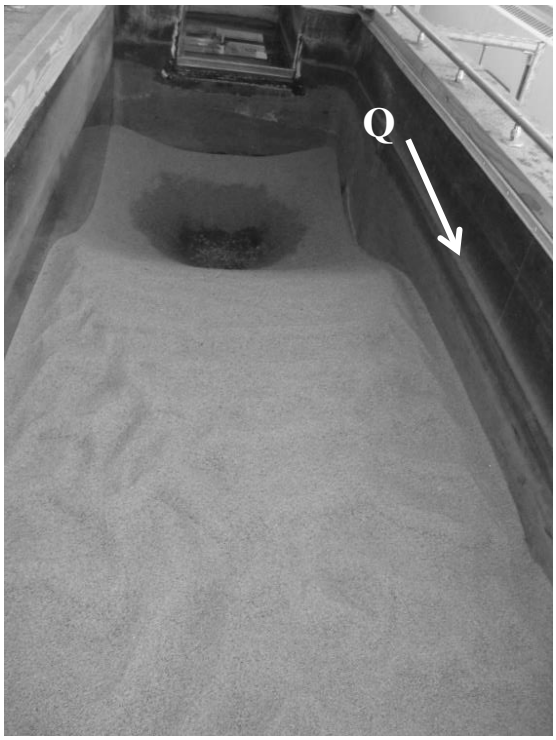

Figure 4.27. *Equilibrium bed photo for no plate.*

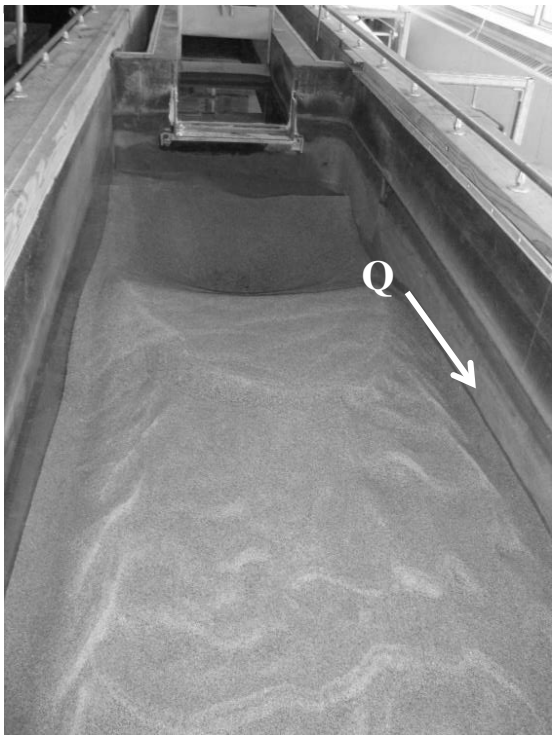

Figure 4.28. *Equilibrium bed photo for 8-cm plate.*

Figure 4.29. *Equilibrium bed photo for16-cm plate.*

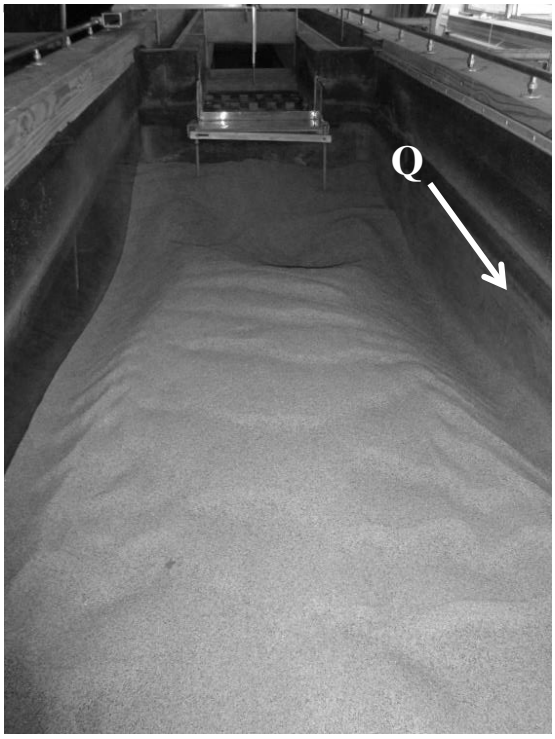

Figure 4.30. *Equilibrium bed photo for 24-cm plate.*

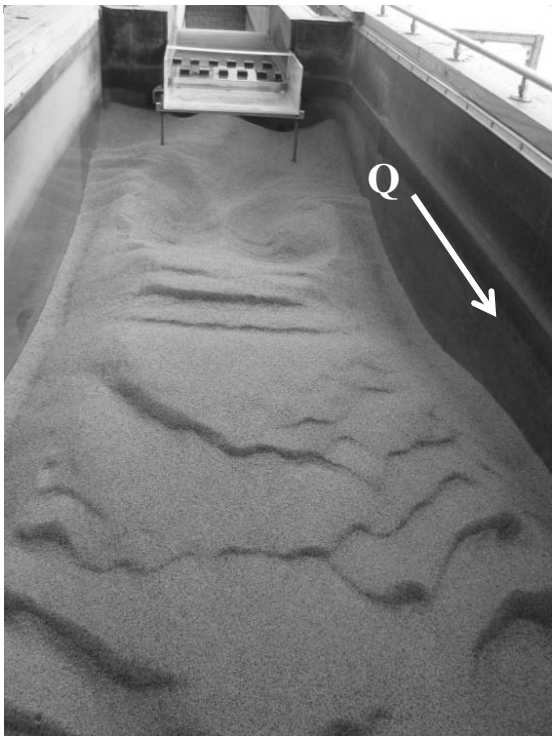

Figure 4.31. *Equilibrium bed photo for 32-cm plate.*

Figure 4.32.*Equilibrium bed photo for 40cm plate.*

Figure 4.33.*Equilibrium bed photo for 48-cm plate.*

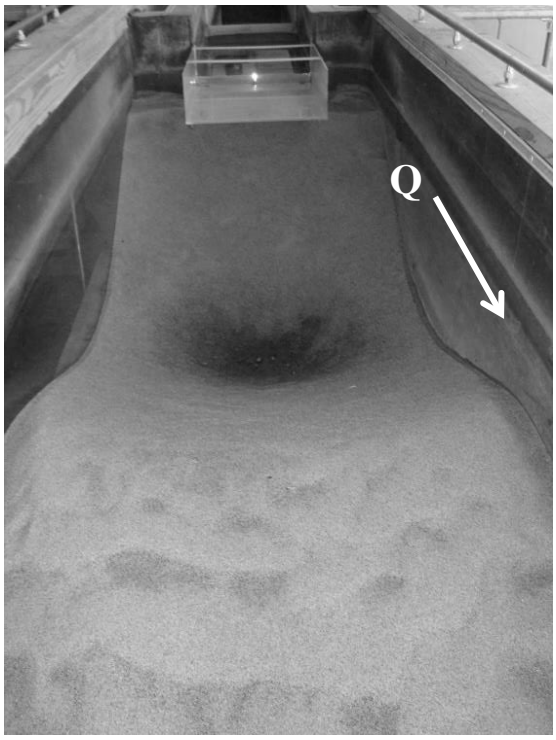

Figure 4.34.*Equilibrium bed photo for 56-cm plate.*

Figure 4.35. *Equilibrium bed photo for 64-cm plate.*

Figure 4.36. *Equilibrium bed photo for 72-cm plate.*

Figures 4.37 and 4.38, respectively, illustrate the elevation of sand remaining after equilibrium had been reached for each plate length and the total scour volume for each plate length.

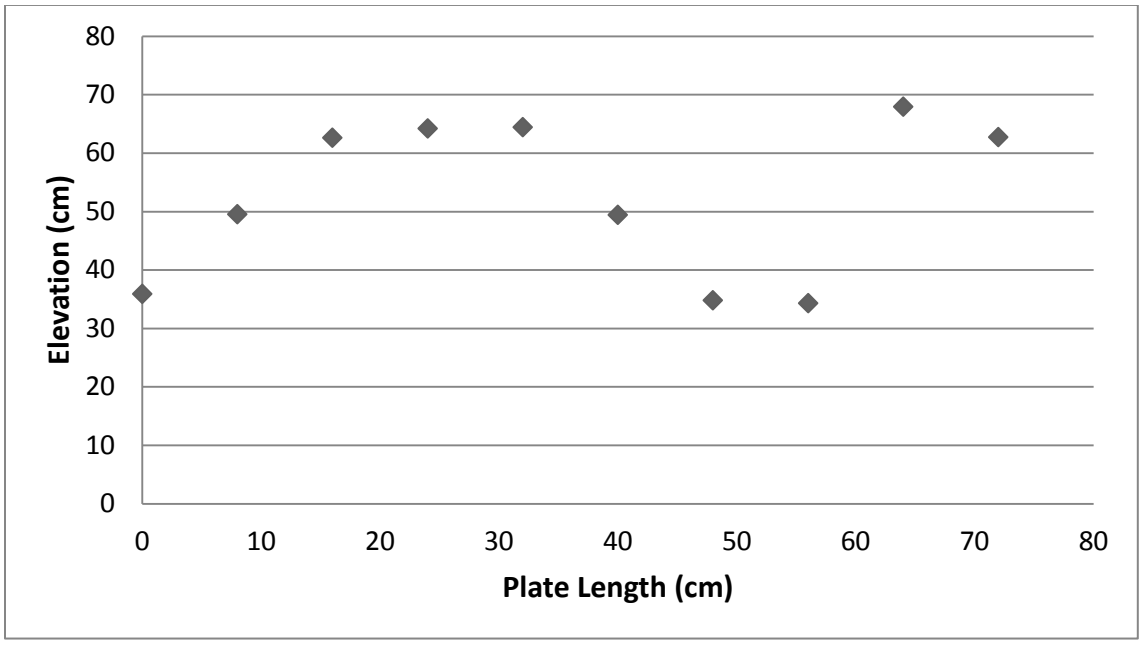

Figure 4.37. *Elevation of deepest scour for each plate length.*

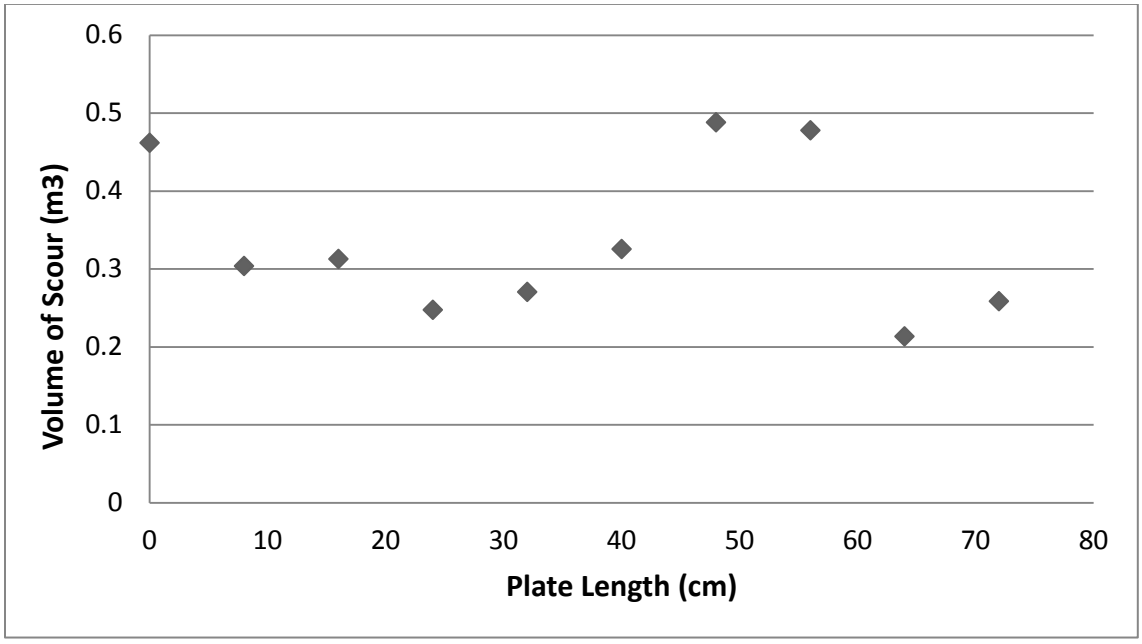

Figure 4.38. *Volume of scoured sediment for each plate length.*

Two types of flow patterns were identified in these experiments. The first was surface recirculation, in which the flow reaches the surface of the water and appears to circulate

upstream. The second pattern observed was flow separation and reattachment. In some areas of the flume, the stream split and flowed in two directions—continuing downstream or back upstream along the bed. These patterns were observed visually in an attempt to understand what flow patterns cause scour. Figure 4.39 shows the two flow patterns identified in the flume.

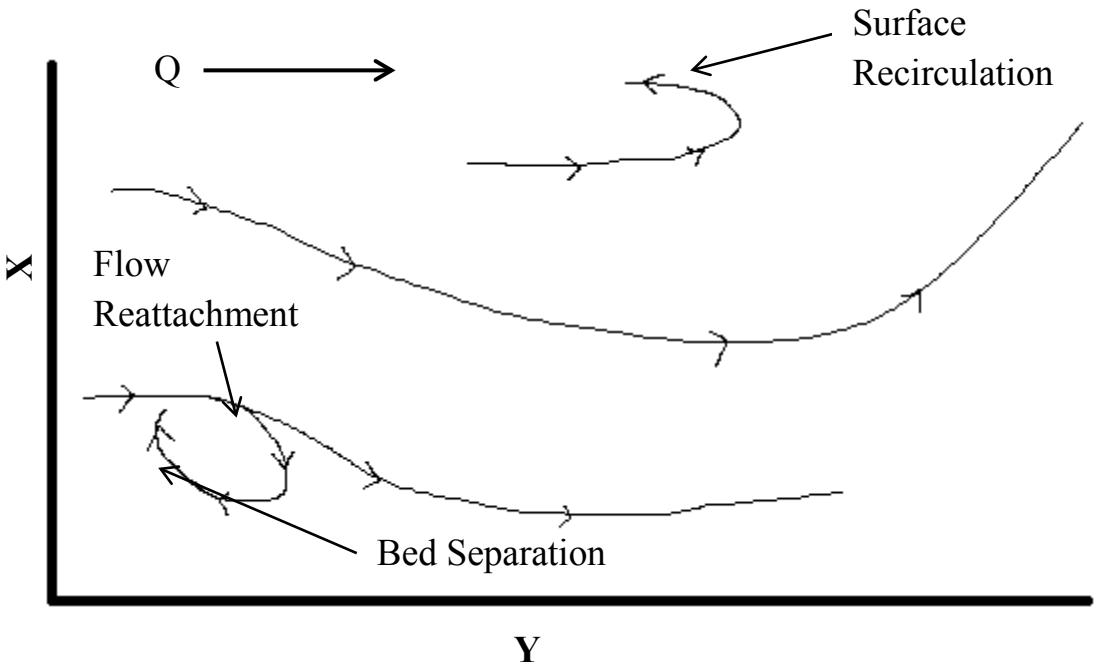

Figure 4.39. *Flow splitting, flow reattacnment, and surface recirculation.*

The location of flow reattachment, $L_{re,}$ and surface recirculation, L_{sre}, were estimated visually and recorded. Those distances are shown in Figures 4.40 and 4.41, below. No surface recirculation was witnessed for the plate lengths of 72 cm and 64 cm.

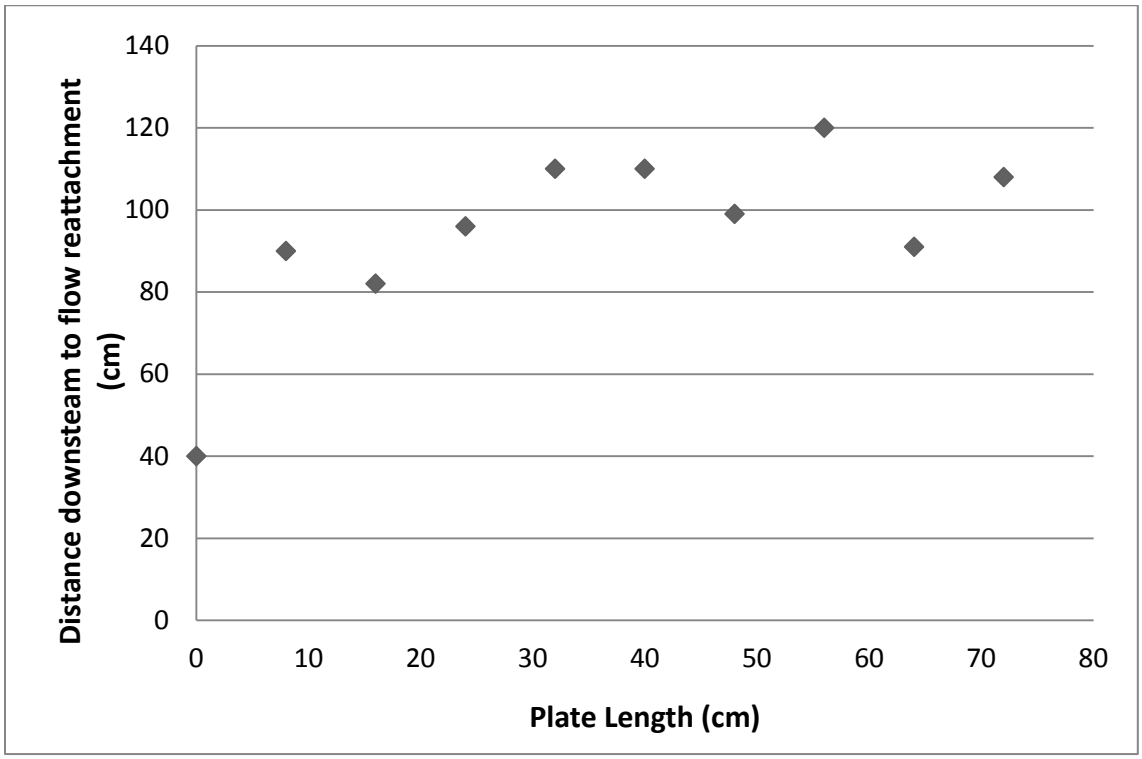

Figure 4.40. *Location of flow reattachment L_{re}, for each plate length.*

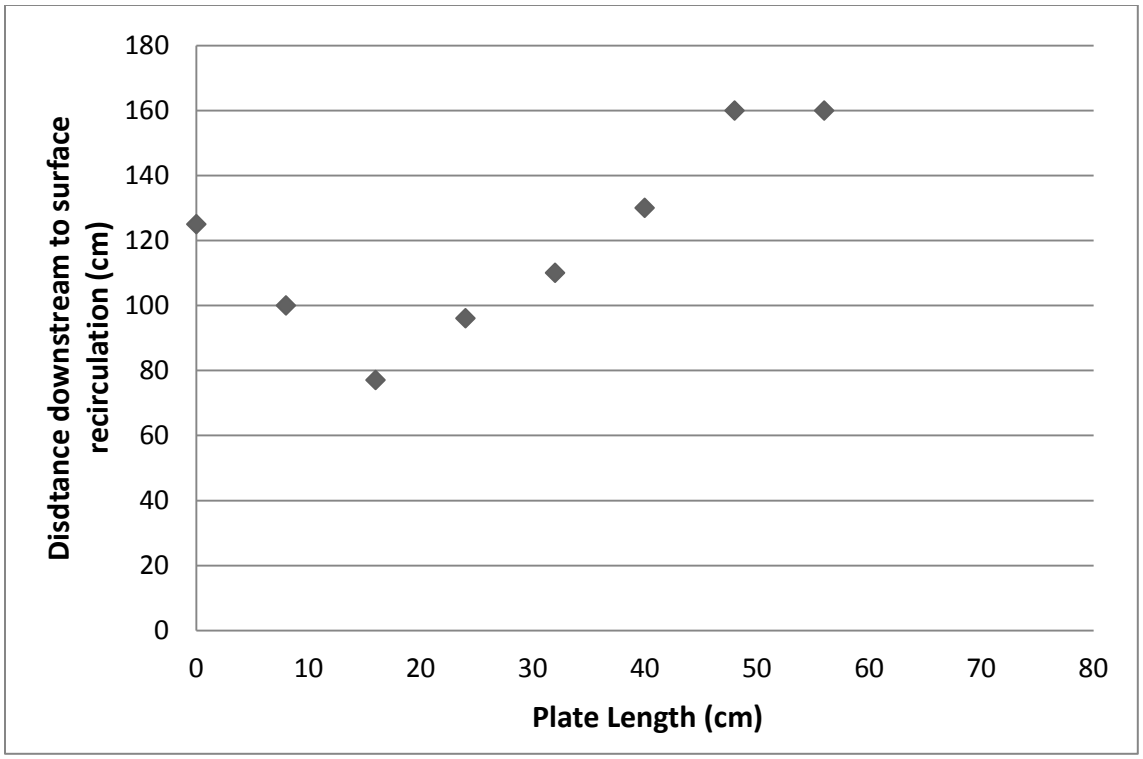

Figure 4.41. *Location of surface recirculation for each plate length. Note: surface recirculation was not witnessed for the 72- and 64-cm plates.*

4.4 Conclusions

The water surface profile measurements show that the location of exiting flow gets further downstream with increasing plate lengths. The increasing plate lengths increase the stilling basin flow depth, but not enough to affect the flow upstream of the stilling basin. The location of deepest scour is then pushed further downstream as plate lengths increase, with the exception of the 32-cm plate, which is slightly closer to the structure than the 24-cm plate.

As plate lengths increases, scour depth is decreased up to the 32-cm plate. The 32- through 56-cm plates then increase the depth of scour, and then the 64- and 72-cm plates decrease scour depth again. However, the 64- and 72-cm plates only marginally decrease scour further, which makes the 32-cm plate the most efficient choice for plate length.

As plate length increases, the location of flow reattachment varies little, but the difference between no plate and any plate length is large. The plate pushes the flow reattachment location downstream, which could potentially cause less scour near the

structure. The first two plate lengths causes the location of surface recirculation to decrease, but the 24-cm plate and increasing plate lengths, push L_{sre} downstream.

Increasing the extension plate length decreases scour, and does not require an accompanying air flow as the diffusers described in Chapter 3 do.

The original hypothesis was that the plate would simply push the deepest point of scour downstream. This was true in all cases tested, but the experiments also showed that for some plate lengths, the volume of scour was reduced, as well. However for the cases with the steeply-sloped scour hole, the volume of scour was not reduced. This is a point of study for future work, as more experiments need to be conducted to find out what causes the steeply-sloped scour pattern in some plate length cases, but causes much less scour in others.

In order to implement this solution on the prototype several steps need to be taken. First of all, the plate size would need to be scaled up to full-scale. Because the model was a 1:30 model, the first attempt at scaling the plate would be to scale it by 30. In the case of the 32-cm plate, the prototype plate would be a 9.6-m plate. Alternatively, the plate length can be scaled up by normalizing by the exiting flow depth. This would result in a plate length to flow depth value of 32cm / 6.7cm = 4.78.

CHAPTER 5: DETAILED VELOCITY MEASUREMENTS

5.1 Experimental Design

A set of experiments was performed in order to determine the water flow pattern and its interaction with the bed for the value of Lp that resulted in the lowest scour depth (Case 5, Lp=32-cm). These experiments were then repeated for the base case with no plate extension. Velocity measurements were taken at hundreds of locations, every five centimeters horizontally along the centerline and every 2.5 cm vertically for each of the two cases.

5.2 Experimental Procedure

For each case, the flume ran at 0.023 cms until the bed reached equilibrium, which was determined using depth measurements taken by the ADV. Equilibrium was reached when the scour depth had changed less than 0.5 percent in a two-hour period. Once it was determined that the bed had reached equilibrium, the flume was drained of water. Several thin layers of cement powder were then applied while the bed was still wet. The cement was allowed to harden for 7-10 days, and the flume was refilled with water and discharge at the same values that created the scour hole. Once the flume was running, the ADV was moved to a specified point along the centerline, and a velocity measurement was taken. Velocity measurements were taken at sampling frequency of 200 Hz, a sampling volume of 4 mm, and a sampling duration range of 4 to 25 minutes depending on the location. For the base case, measurements were taken at 520 locations on the vertical centerline plane in the flow field, and measurements were taken at 147 locations for the 32-cm plate.

Each data file measured with the ADV at a specific point contained hundreds of velocity measurements. The files were run through a Matlab code, also created by Champagne (Champagne 2011) to average them over the measurement time. These average velocity measurements were then sorted and input into Tecplot to create a plot showing a vector for each average velocity point.

In order to visualize the flow patterns, the Tecplot flow fields were plotted against bed profiles that were measured in the original plate extension cases. When the flow fields and bed profiles were plotted together, it appeared as if the flow field was translated downstream; it did not match perfectly with the bed measurements. This could have been due to the thickness of the layer of cement powder, or the bed could have reached equilibrium at a slightly different shape than that of the original case. Regardless of the cause of the inconsistency, the bed profile was estimated based on the shape of the vector field in order to give a visual representation of the bed.

When physically adjusting the ADV, the probe was placed ~5.4cm from the bed surface, which was measured by the ADV's depth function. Because this was done for each measurement along the bed, it was decided that the velocity measurements were in the

right place, and the bed profile from the previous study was not suitable. The bed profile was then estimated to fit the velocity flow field. It is important to realize that the bed profiles are not actual measurements, whereas the bed profiles in previous chapters were actual measurements.

5.3 Results

The vector plots described above are shown in Figures 5.1 and 5.2, below. Each vector represents a time-averaged velocity measurement. The vector lengths are relative to one another to represent their magnitude. The plots also contain streamlines that allow for a visualization of the flow patterns for each of the two cases. It is clear in the plot for no plate extension that flow splitting is occurring. Additionally, surface recirculation is taking place. It would be more evident if surface data points could have been measured, but due to the limitations of the ADV, they were not.

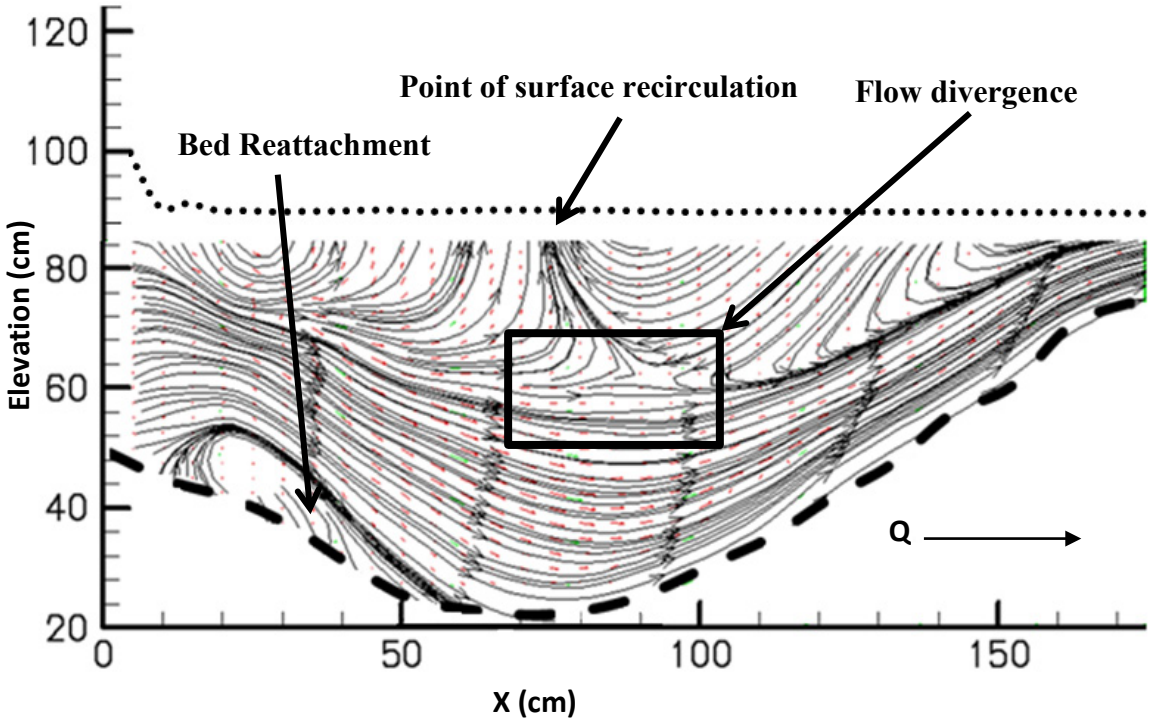

Figure 5.1. *Vector plot with streamlines for no plate extension. Bed profile represented by dashed line and water surface profile represented by dotted line.*

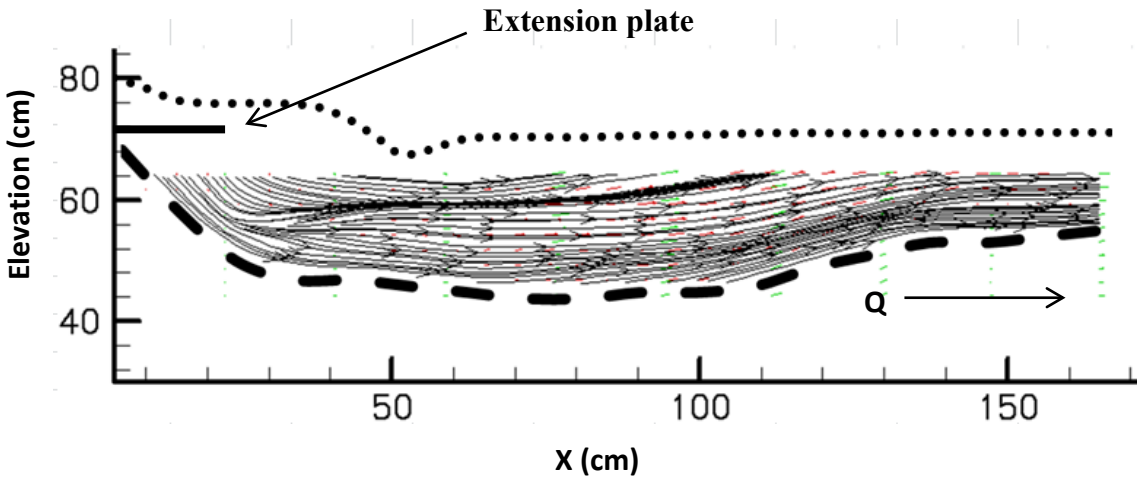

Figure 5.2. *Vector plot with streamlines for Lp=32cm.Bed profile represented by the dashed line and water surface profile represented by dotted line.*

5.4 Conclusions

From the detailed velocity measurements, some understanding of flow pattern is gained. It is clear that with no plate extension, surface recirculation and flow splitting is taking place. Although the bed profiles were estimated, the understanding of the flow pattern still applies, and the bed profile does not affect the accuracy of the velocity measurements.

However, due to limited time, there is not a complete understanding for what causes the flow variations between the base case with no plate extension and the 32-cm plate extension. This is another suggestion for future work: the determination of what causes specific flow patterns in different cases.

CHAPTER 6: OVERALL CONCLUSIONS

6.1 Air Diffusers

Two air diffusers were tested on the 1/30 scale model of SFWMD's S65E gated spillway. The first diffuser, a hollow triangular end sill, allowed compressed air to flow upstream, in the opposite direction of the water flow. The second diffuser, a hollow, rectangular extension from the triangular end sill, allowed air to flow vertically, perpendicular to water flow. Both diffusers were tested with six different cases, ranging from no air injection to five rows of 70 holes, 0.04" in diameter. For each of the diffusers, five rows reduced scour the most. Detailed velocity measurements were taken and analyzed through turbulence statistics. The results of these measurements indicate that increasing the spatial extent (the number of rows of holes for air injection) decreases the exit turbulence, exit velocity, and exit anisotropy.

Although increasing the spatial extent reduces scour, it also requires compressed air flow, which can be energy intensive. Additionally, there is only marginal gain in scour reduction past one row of air injection holes.

From these experiments comes the understanding that air injection causes a backwater effect on the flow exiting the structure. This raises flow depth which dampens the exit velocity, turbulence, and turbulence anisotropy. These variables reduce the energy of the exiting flow, which reduces scour depth. The Vertical-Facing Diffuser Plate intensifies this effect because the location of air injection is in closer proximity to the exiting flow.

These findings meet the first two objectives of this research, listed in Chapter 1, which were to understand why air injection reduces bed scour and to determine the optimal spatial extent of air injection.

6.2 Flat Plate Extension

A set of experiments were performed with various lengths of flat plates extending from the triangular end sill. A plate extension would only require initial construction costs and maintenance, rather than constant air supply. Increasing plate lengths moved the deepest point of scour further downstream. It was determined that the 32-cm plate length was the shortest, and therefore, least expensive plate that decreased scour effectively at the structure. The location of flow reattachment moves downstream slightly with increasing plate length. The location of surface recirculation varies much more and is dependent on plate length. The flow rate was lowered for these experiments so that the limitations of the flume did not interfere with the results. The discharge rate was calculated to be exactly the design discharge of the prototype.

Detailed velocity measurements were taken with the 32-cm plate and again with no plate. This was done to evaluate the flow patterns to better understand why the plate reduces scour. Without a plate, surface recirculation and flow reattachment and splitting takes place, but with the plate, the flow is more streamlined.

The third and fourth objectives listed in Chapter 1 were to determine if a flat plate extension would reduce scour and to understand the flow patterns caused by the extension plate. Those objectives were met.

6.3 Future Research

Due to time constraints with this research, there are some areas of this research that were not further investigated. Four of the cases in the flat plate experiments resulted in steeply-sloped scour holes. The reasoning behind this could not be determined; this is an area that should be studied in future research. Additionally, each of the plate lengths was only tested one time due to time constraints. For a better understanding of what happens with each case, repeatability studies should be conducted to ensure that results found in this study were not anomalies. Flow reattachment and surface recirculation were analyzed visually, so only a basic understanding was gained. Studying these flow patterns in more detail would allow for some explanation as to what patterns cause scour.

Detailed velocity measurements were taken for the 32-cm plate length and the base case with no plate. To determine the correlation between plate length and scour reduction, the flow patterns should continue to be studied.

Additional understanding of flow patterns can be gained from a quadrant analysis of the velocity data collected. While this research did not allow for the time to complete a quadrant analysis, the data can still be analyzed.

This research could also be continued in the direction of implementation. Scaling up the diffusers or the plate could be done. In order to implement either of these solutions, materials would need to be decided upon, operational regimes (for the air diffusers) would need to be worked out, and costs would need to be estimated.

Additionally, all of these experiments were done in clear-water tests. However, in many rivers, suspended sediment is present. Future work could include running similar experiments in the presence of suspended sediment. This could affect the results of the experiments, as suspended sediment increases the density of the water, which could impact the flow pattern.

CHAPTER 7: REFERENCES

Barkdoll, B. and R. Barlock (2011). Erosion Reduction by Air Entrainment Phase IV Task 3-Effect of 2D Diffuser Plate, Michigan Technological University.

Bennett, S. J., C. V. Alonso, et al. (2000). "Experiments on headcut growth and migration in concentrated flows typical of upland areas." Water Resources Research **36**(7): 1911.

Brevik, I. (1977). "Two-dimensional air-bubble plume." Journal of Waterways, Harbors and Coastal Engineering Division **103**(1): 101-115.

Brevik, I. and R. Killie (1996). "Phenomenological Description of the Axisymmetric Air-Bubble Plume." International Journal of Multiphase Flow **22**(3): 535-549.

Brevik, I. and O. Kristiansen (2002). "The flow in and around air-bubble plumes." International Journal of Multiphase Flow **28**: 617-634.

Canepa, S. and W. Hager (2003). "Effect of Jet Air Content on Plunge Pool Scour." Journal of Hydraulic Engineering **129**(5): 358-365.

Champagne, T. M. (2011). Physical Modeling of Air Injection as a Scour Remediation Technique near Gated Weir Stilling Basins. Civil and Environmental Engineering. Houghton, Michigan Technological University. **M.S. Civil Engineering**.

D'Agostino, V. and V. Ferro (2004). "Scour on Alluvial Bed Downstream of Grade-Control Structures." Journal of Hydraulic Engineering **130**(1): 24-37.

Dey, S. and A. Sarkar (2006). "Scour Downstream of an Apron Due to Submerged Horizontal Jets." Journal of Hydraulic Engineering **132**(3): 246-257.

Dey, S. and A. Sarkar (2007). "Effect of Upward Seepage on Scour and Flow Downstream of an Apron due to Submerged Jets." Journal of Hydraulic Engineering **133**(1): 59-69.

Dey, S. and B. Westrich (2003). "Hydraulics of Submerged Jet Subject to Change in Cohesive Bed Geometry." Journal of Hydraulic Engineering **129**(1): 44-53.

Freire, A. P. S., D. D. E. Miranda, et al. (2002). "Bubble plumes and the Coanda effect." International Journal of Multiphase Flow **28**(8): 1293-1310.

Gabillet, C., C. Colin, et al. (2002). "Experimental study of bubble injection in a turbulent boundary layer." International Journal of Multiphase Flow **28**(4): 553-578.

Hager, W. (1998). "Plunge pool scour: early history and hydraulicicians." Journal of Hydraulic Engineering **124**(12): 1185-1187.

Hamid, A., R. Farrant, et al. (1952). "Air entraining devices and their use in correcting flow conditions at weird and can outfalls." Proceedings of the Minnesota International Hydraulics Convention: 519-527.

Jia, Y., T. Kitamura, et al. (2001). "Simulation of Scour Process in Plunging Pool of Loose Bed-Material." Journal of Hydraulic Engineering **127**(3): 219-229.

Liu, P. (2005). "A new method for calculating depth of scour pit caused by overflow water jets." Journal of Hydraulic Research **43**(6): 696-702.

Martínez-Bazán, C., J. L. Montañés, et al. (2002). "Statistical description of the bubble cloud resulting from the injection of air into a turbulent water jet." International Journal of Multiphase Flow **28**(4): 597-615.

Mason, P. (1989). "Effects of Air Entrainment on Plunge Pool Scour." Journal of Hydraulic Engineering **115**(3): 385-399.

Mason, P. and K. Arumugam (1985). "Free Jet Scour Below Dams and Flip Buckets." Journal of Hydraulic Engineering **111**(2): 220-235.

Melville, B. and Y. Chiew (1999). "Time Scale for Local Scour at Bridge Piers." Journal of Hydraulic Engineering **125**(1): 59-65.

Neto, I., D. Zhu, et al. (2008). "Air Injection in Water with Different Nozzles." Journal of Environmental Engineering **134**(4): 283-294.

Nortek (2013). "Products." Retrieved October 17, 2013, from http://www.nortekusa.com/usa/products.

Pagliara, S., W. Hager, et al. (2006). "Hydraulics of Plane Plunge Pool Scour." Journal of Hydraulic Engineering: 450-461.

Schmocker, L., M. Pfister, et al. (2008). "Aeration Characteristics of Ski Jump Jets." Journal of Hydraulic Engineering **134**(1): 90-97.

Simiano, M., R. Zboray, et al. (2006). "Comprehensive experimental investigation of the hydrodynamics of large-scale, 3D, oscillating bubble plumes." International Journal of Multiphase Flow **32**(10–11): 1160-1181.

Stein, O., C. V. Alonso, et al. (1993). "Mechanics of jet scour downstream of a headcut." Journal of Hydraulic Research **31**(6): 723-738.

van Hout, R., A. Gulitski, et al. (2002). "Experimental investigation of the velocity field induced by a Taylor bubble rising in stagnant water." International Journal of Multiphase Flow **28**(4): 579-596.

Xu, W., J. Deng, et al. (2004). "Experimental Investigation on Influence of Aeration on Plane Jet Scour." Journal of Hydraulic Engineering **130**(2): 160-164.

APPENDIX

For access to the files used in analysis of all research described in this thesis, please contact Dr. Brian Barkdoll at barkdoll@mtu.edu.

PERMISSION TO REPUBLISH

The following email correspondence gives permission to use copyrighted materials consisting of the following figures and tables in this thesis: Figure 2.1, Figure 2.2, Figure 2.3, Figure 2.5, Figure 2.8, and Table 2.1.

Rachael Barlock <rrbarloc@mtu.edu> Sep 6

to tedchampagne

Good morning Ted,
I hope all is going well with you. I'm in the final stages of thesis writing for my flume work (@ MTU with Dr. Barkdoll) , and I was wondering if it would be okay if I used some text and figures from your thesis. I am hoping to be able to use them to describe the flume set-up, and I don't know a better or different way to do so without using the figures you used.

Please let me know if this is okay.

Thank you so much!

...

Champagne, Ted - Faculty <tedchampagne@delta.edu> <tedchampagne@delta.edu> Sep 6

to me

Rachael,

I am so excited for you!! I know it takes a tremendous level of dedication to complete the work you have been doing with Dr. Barkdoll. Great job!!!

You may certainly use the material you mentioned from my thesis. I just request that you reference my work. I know you were already planning on doing so...MTU produces great engineers :)

Good luck on the rest of your thesis and whichever path your career takes you!!!

Ted M. Champagne, Instructor
Mathematics Division
Delta College
University Center, MI 48710
tedchampagne@delta.edu